BEITRÄGE ZUR GEOLOGIE DER SCHWEIZ
GEOTECHNISCHE SERIE
herausgegeben von der
Schweizerischen Geotechnischen Kommission
(Organ der Schweizerischen Akademie der Naturwissenschaften)

Lieferung
90

MATERIAUX POUR LA GEOLOGIE DE LA SUISSE
SERIE GEOTECHNIQUE
publiés par la
Commission Géotechnique Suisse
(Organe de l'Académie Suisse des Sciences Naturelles)

The Pb-Zn-As-Tl-Ba-deposit at Lengenbach, Binn Valley, Switzerland

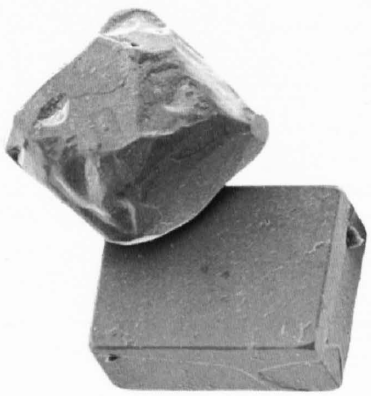

Petrogenesis based on combined geochemical and isotopical (U, Pb, Rb, Sr, S, O, C) investigations

M.D. Knill

1996

Verkauf durch die Schweizerische Geotechnische Kommission, ETH-Zentrum, 8092 Zürich
Publiziert mit Unterstützung der Schweizerischen Akademie der Naturwissenschaften

Dissertationsschrift, Diss ETH Nr. 11296
Eidgenössische Technische Hochschule Zürich, 1996
Referent: Prof. Dr. V. Köppel
Korreferenten: Prof. Dr. C. Heinrich, Prof. Dr. S. Graeser

Redaktion und Satz: Schweizerische Geotechnische Kommission
Lithos und Druck: Druckerei Flawil AG, Flawil
Gedruckt auf chlorfrei gebleichtem Papier

ISBN 3-907997 23 9

VORWORT DER SCHWEIZERISCHEN GEOTECHNISCHEN KOMMISSION

Die vorliegende Arbeit behandelt die Genese der Blei-Zink-Arsen-Thallium-Barium Lagerstätte Lengenbach im Binntal (Kanton Wallis), welche durch die Vielfalt seltener Sulfosalze weit über die Grenzen der Schweiz hinaus bekannt geworden ist.

Während die Mineralparagenesen der Lagerstätte Lengenbach bereits in den vergangenen Jahrzehnten in zahlreichen mineralogischen und kristallographischen Detailstudien eingehend untersucht wurden und viele bisher unbekannte Mineralien, insbesondere Sulfosalze, gefunden werden konnten, fehlte eine geochemische und isotopengeochemische Gesamtbetrachtung.

Die schwierige Aufgabe, die von Herrn Matthias Knill im Rahmen einer Dissertation am Institut für Kristallographie und Petrographie an der ETH-Zürich (heute «Institut für Isotopengeologie und Mineralische Rohstoffe») ausgeführt wurde, bestand darin, mit Hilfe geochemischer und isotopengeochemischer Charakterisierung zahlreicher indikativer Minerale und der alpin-metamorphen Nebengesteine die verschiedenen, möglichen petrogenetischen Prozesse aufzuzeigen, die Bildungsbedingungen der Erzmineralien zu definieren und diese schliesslich geochronologisch einzuordnen.

Die Dissertation von Herrn Knill stellt in diesem Sinne eine exemplarische Studie dar, da sie umfassend sowohl die chemischen Zusammensetzungen der Mineralparagenesen und ihrer benachbarten Gesteine (triadische Metadolomite) als auch die Verhältnisse radiogener (Pb, Sr) und stabiler Isotopen (C, O, S) beinhaltet.

Die geochemischen Daten der As-Pb-Tl reichen Sulfide, Sulfosalze und der Barite, sowie die an Pb, Ag, Tl, Hg, Zn, Ba, Cd, Fe, Cu, Mo, U, V, B, Ga und Cr stark angereicherten Metadolomite deuten auf die Existenz hydrothermaler Lösungen: Metallanreicherung durch Herauslösung (leaching) in zum Teil glasreichen, spätpermischen bis frühtriadischen Vulkaniten mit nachfolgender Ausfällung in den karbonatischen Plattformsedimenten. Allein die signifikante und äusserst komplexe Metall-Elementverteilung ist typisch für viele Entgasungs- (Fumarolen-) und Hydrothermalsysteme in heute aktiven vulkanischen Inselbögen.

Es ist erstaunlich, dass im Bereich der Lagerstätte Lengenbach während der alpinen Metamorphose, die an anderen Orten häufig von einem penetrativen Fluid-Transport begleitet wurde, keine grossräumigere Metalldispersion und Reequilibrierung der Erzparagenesen erfolgte. Während der alpinen Orogenese wurden im Bereich der Lagerstätte unter Drucken von 3–4 kbar (entsprechend einer krustalen Bedeckung von ca. 10–12 Kilometern) und Temperaturen zwischen 300 und 520°C bleireiche Sulfidschmelzen innerhalb der triadisch angelegten Hydrothermalvererzungen gebildet. Alpines fluid führte dann zur Ausfällung der umgebenden Kluftparagenesen. So blieben die ursprünglichen hydrothermalen geochemischen Charakteristika weitgehend erhalten. Die Uran/Blei-Isotopenbestimmungen an den Uraniniten ergaben ein gut definierbares alpines Alter der Metamorphose von 18.5 ± 0.5 Millionen Jahren.

Aufgrund der Mannigfaltigkeit der mineral-, gesteins- und isotopengeochemischen Daten, sowie der generellen mineralogischen Bedeutung der Lagerstätte Lengenbach, war es sinnvoll, diese Arbeit in englischer Sprache zu verfassen, um so die gewonnenen Daten einem internationalen, erdwissenschaftlich interessierten Publikum zugänglich zumachen.

Die Kommission dankt dem Autor für die Möglichkeit, diese Arbeit in ihre Schriftenreihe aufzunehmen, und für die sorgfältige Mitarbeit bei der Drucklegung.

Für den Inhalt von Text und Figuren ist der Autor allein verantwortlich.

Zürich, Oktober 1996

Für die Schweizerische Geotechnische Kommission

V. Dietrich

ACKNOWLEDGMENT

I wish to thank everybody who helped me to carry out this study and gave me support during the field and laboratory work.

I am particularly indebted to Prof. V. Köppel, who offered me the opportunity to work at the Institute for Crystallography and Petrography (or later Institute of Isotope Geology and Mineral Resources) of the Swiss Federal Institute of Technology (ETH) Zürich. His open and positive attitude towards new ideas was always encouraging and I am very grateful for his friendly support and also his constructive criticism during the (mainly rainy) field-days.

Further gratitude is due to Prof. S. Graeser who introduced me to the geology of the Binn Valley. Thanks to his and Prof. V. Köppels initiative, this project was supported by the Swiss National Foundation.

I want to thank Prof. M. Grünenfelder and Prof. C. Heinrich, who were very interested in my subject. Their support, discussions, openness for new ideas, and last but not least their constructive criticism was invaluable for my work.

A prominent support derived from the outstanding collaboration with Dr. B. Hofmann. Several interesting discussions preceded our publications. The Natural History Museum of Bern is thanked for putting several mineral samples at my disposal. Many geochemical analyses were financed by the ESM (Stiftung Entwicklungsfonds Seltene Metalle, Pully, Switzerland). P. Vollenweider carefully made some colour photographs of mineral specimens.

This study would never have been accomplished without the help of many colleagues at the ETH Zürich. For introductory lessons and technical help I am especially grateful to Dr. W. Hansmann (radiogenic isotope analyses and mass spectrometry), Dr. A. von Quadt (computing facilities), Dr. F. Oberli and Dr. M. Meier (high resolution U-Pb geochronology), Dr. D. Grujic (SEM), Dr. P. Ulmer (high-T-melt experiments), Dr. E. Reusser (electron microprobe), Dr. H. A. Gilg (stable isotope analyses) Dr. J. Ridley (reviewing the manuscript) and E. Schärli (preparation of thin and polished sections).

Prof. V. Dietrich and Dr. F. Bianconi are thanked for reading the manuscript. Many thanks to D. Vavrecka-Sidler, who is responsible for the final layout of this work. The «Schweizerische Geotechnische Kommission» facilitated this publication.

The printing-costs of this publication beared the «Schweizerische Geotechnische Kommission», the Institute of Isotope Geology and Mineral Resources (IGMR), the Huber-Kundlich-Stiftung of the ETH Zürich as well as the Natural History Museum of Bern.

The «Arbeitsgemeinschaft Lengenbach» (Lengenbach syndicate) provided access to the mineral quarry. Many thanks to the staff of the Lengenbach deposit, especially T. Imhof and W. Musch. Thank you for the introduction to the science and fine art of «professional rock hunting» and for many unforgettable field days in the mineral quarry and the Wanni region!

The financial support by the Swiss National Foundation (grant No. 21-31286.91) was essential for carrying out this project and is gratefully acknowledged.

Finally, I want to thank my parents and my wife Rägi for their support.

CONTENTS

List of figures

SUMMARY

The Lengenbach Pb-Zn-As-Tl-Ba deposit is located in Triassic metadolostones of the Penninic zone in the Swiss Alps, where Alpine regional metamorphism reached upper greenschist to lower amphibolite grade. The deposit is famous for the large number of rare and well crystallized sulfosalt minerals. Geochemical and isotopical data are presented here to help constrain the origin of this unique occurrence.

Mineral assemblages indicate two metamorphic redox environments: one is controlled by barite-pyrite (with trivalent As) and the other by graphite and/or pyrrhotite-pyrite (with effectively zerovalent As). The As(III)-rich zone is characterized by a mineral assemblage consistent with fO_2 in the stability field of barite + pyrite and an As-(Pb, Tl)-rich sulfide melt at >300°C. The chemical composition of massive sulfosalt accumulations (mainly baumhauerite) document the enrichment of Tl, Ag and Sb during fractional crystallization in a sulfidic melt, and this process explains the high concentration of these elements in the late, hydrothermally precipitated minerals in druses and fissures.

Mineralized metadolostones have anomalous As, Pb, Ag, Tl, Hg, Zn, Ba, Cd, Fe, Cu, Mo, U, V, B, Ga and Cr contents (in decreasing order of enrichment) and possibly slight enrichments in Sn and Au. As, Pb and Zn are present in the 0.1 to 1% range, Tl and Ag reach several hundred ppm. Uraninite is concentrated in silicate-rich bands and yields a late Alpine U-Pb age of 18.5 ± 0.5 Ma. Pb- and S isotopic variations are interpreted to be a result of metamorphic overprinting and re-equilibration within an isochemically metamorphosed ore body. Minerals in Alpine vugs, druses and fissures are more strongly affected by uranogenic Pb released during metamorphism of uraninite precursors than are massive sulfosalt accumulations. The least overprinted stratiform mineralization is characterized by $^{206}Pb/^{204}Pb$ = 18.44–18.56, $^{207}Pb/^{204}Pb$ = 15.60–15.75, $^{208}Pb/^{204}Pb$ = 38.44–38.84 and $\delta^{34}S$ (sulfide) = -25 ± 2‰. S isotopic variations are largely the result of sulfide-sulfate re-equilibration at temperatures of 450 ± 30°C. Arsenopyrite geothermometry and sphalerite geobarometry of fissure minerals indicate conditions of 380–410°C at 3.3 ± 0.6 kbar.

$^{87}Sr/^{86}Sr$ ratios of mineralized samples are lower than or equal to host metadolostones, precluding major infiltration of basement-derived fluids during Alpine metamorphism. The Sr source ($^{87}Sr/^{86}Sr$ close to 0.708) was probably sea water with a radiogenic, detrital mineral component.

Isotopical investigations of minerals in Alpine druses from the carbonate-hosted Lengenbach deposit do not indicate significant interaction with externally derived metamorphic fluids. Isotopic data (C, O, S, Sr, Pb) point to essentially closed system behavior during peak amphibolite facies and retrograde Alpine metamorphism. Well crystallized minerals in fissures and druses formed during the slow cooling, from a hydrothermal fluid which maintained coexistence with a sulfide melt.

The unique mineral assemblage of the Lengenbach deposit is interpreted to be a result of isochemical metamorphic overprinting of a carbonate hosted stratiform sulfide mineralization. The primary mineralization was probably formed at or just below the sea floor and was fed by sulfide-poor hydrothermal fluids. Sulfide was largely derived from sea water by open system bacterial sulfate reduction. The redox sensitive elements U, V and Mo may also be seawater-derived.

To determine the age and the source rock on the stratiform Lengenbach deposit, geochemical and isotopical investigations were performed of rocks from the pre-Mesozoic basement.

The whole rock Pb-isotope compositions of Permian metarhyolites (corrected to 200 Ma) overlap with the composition of stratiform ore minerals from the Lengenbach deposit. The metal source of the mineralizing fluid that formed the carbonate-hosted deposit are therefore thought to be As-rich Permian rhyolites of the basement.

Rb-Sr whole rock analyses of five metarhyolites from the basement define an isochron of 185 ± 17 Ma. The isotopic resetting of this lithology was presumably caused by Mesozoic hydrothermal alteration.

A large number of rare As-rich minerals occur in Alpine fissures and vugs of Permian metarhyolites from the Monte Leone nappe. Cu-As-F mineral occurrences in the basement located 5 km south of the Lengenbach mineralization are related to discordant biotite-epidote rocks, which from structural, geochemical and isotopical evidences are interpreted to represent Alpine metamorphosed shear zones. These pre-Alpine shear zones in the basement of the Monte Leone nappe support the existence of early Mesozoic rifting in the northern Penninic terrain, which was accompanied by hydrothermal activity and the formation of stratiform, carbonate-hosted mineralization.

RÉSUMÉ

Le glisement de Lengenbach est connue pour sa richesse en sulfosels rares. Les minéralisations du Pb-Zn-As-Tl-Ba, entièrement recristallisées durant le métamorphisme alpin, se situent dans la dolomite triassique de la nappe pennique des alpes suisses. Les résultats géochimiques et isotopiques présentés ici apportent divers éléments nouveaux concernant l'origine des minéralisations site unique.

L'association des minéraux indique la formation de deux environnements redox distincts au cours du métamorphisme: le premier environnement est charactérisé par l'association barite-pyrite (avec As trivalent) et le second par le graphite et/ou l'association pyrrhotite-pyrite (avec As zerovalent). La zone riche en As(III) est charactérisée par une paragenèse se situant dans le domaine de stabilité de fO_2 de la barite-pyrite et par un liquide sulfidique riche en As-(Pb, Tl) à des températures >300°C. La composition chimique des accumulations de sulfosels (principalement baumhauerite) reflète un enrichissement en Tl, Ag et Sb durant la cristallisation fractionnée du liquide sulfidique. Ce processus explique la concentration élevée de ces élements dans les minéraux d'origine hydrothermale, précipités dans les veines et druses à la fin de la phase metamorphique alpine.

La minéralisation des métadolomites est charctérisée par un enrichissement significant en As, Pb, Ag, Tl, Hg, Zn, Ba, Cd, Fe, Cu, Mo, U, V, B, Ga et C et par une légère augmentation de la concentration en Sn et Au. La concentration en As, Pb et Zn varie entre 0.1 et 1% alors que celle deTl et Ag atteint plusieurs centaines de ppm. L'uraninite est concentrée dans des zones riches en silicates et sa datation (U-Pb) indique un âge alpine de 18.5 ± 0.5 Ma. Les variations isotopiques du Pb et S s'expliquent par un réequilibrage de la roche métamorphosée isochimiquement. Les minéraux des veines, druses et fissures alpines sont plus fortement affectés par le Pb uranogénique libéré adurant le metamorphisme que les accumulations massives de sulfosels. La minéralisation stratiforme la moins marquée par l'empreinte métamorphique est charactérisée par $^{206}Pb/^{204}Pb$ = 18.44–18.56, $^{207}Pb/^{204}Pb$ = 15.60–15.75, $^{208}Pb/^{204}Pb$ = 38.44–38.84 et $\delta^{34}S$ (sulfide) = -25 ± 2‰. Les variations isotopiques du S correspondent principalement à un réequilibrage des sulfides-sulfates à T = 450 ± 30°C. L'analyse géothermométrique (arsenopyrite) et géobarométrique (zincblende) des minéraux de fissures indiquent des conditions de température et pression de 380 à 400°C et de 3.3 ± 0.6 kbar.

Les rapports $^{87}Sr/^{86}Sr$ de la dolomite et la barite dans les zones minéralisées et non minéralisées de la métadolomite sont similaire. La source de Sr ($^{87}Sr/^{86}Sr$ proche de 0.708) était probablement l'eau de mer avec une composante détritique radiogène.

L'étude des isotopes (C, O, S, Sr, Pb) présents dans les minéraux de fissures du gisement n'indique aucune interaction avec des fluides métamorphes externes. Ces résultats reflètent un système fermé durant la phase rétrograde du métamorphisme alpin. Les minéraux idiomorphes présents dans les fissures se sont formés au cours du lent refroidissement des fluides hydrothermaux qui ont coexistés avec un liquide sulfidique.

L'association unique des minéraux dans le dépôt de Lengenbach est interprété comme le résultat d'un métamorphisme marquée isochimique de la minéralisation sulfidique stratiforme situé dans les carbonates. La minéralisation primaire s'est probablement formé à la surface ou juste audessous du plancher océanique et a été alimentée par des fluides hydrothermaux, pauvres en sulfide. La faible valeur du $\delta^{34}S$ de la minéralisation stratiforme peut s'expliquer par la réduction bactérielle du sulfate. Les éléments sensibles aux conditions rédox, U, V et Mo, semblent également résulter de l'interaction des minérais avec l'eau de mer.

Afin de déterminer l'âge et la source de la minéralisation du dépôt, des études géochimiques et isotopiques ont été effectuées sur des roches du socle pré-mésozoïque. La composition des isotopes du Pb des métarhyolites permiennes (corrigée à 200 Ma) correspond à celle des minéralisations stratiformes du dépôt de Lengenbach. Le socle ryholitique permien, riche en As, semble donc être la source de métal de la minéralisation du site.

L'analyse du Rb-Sr dans cinq métaryholites définit un isochrone de 185 ± 17 Ma. Le rajeunissement de cette lithologie indique que la roche a subit des altérations hydrothermales durant le mésozoïque.

Un nombre important de minéraux rares, riches en As, sont présents dans les fissures alpines des métaryholites permiennes de la nappe du Monte Leone. A proximitée de ces fissures se trouvent des roches discordantes, contenant de la biotite et de l'épidote, et qui, selon des critères structuraux, géochimiques et isotopiques sont interprétée comme une zone de cisaillement, marquée par le métamorphisme alpin. Cette zone de cisaillement pur, pré-alpine, reflète le rift du nord-pennique au début de l'ère mésozoïque, qui a été accompagnéepar une activité hydrothermale et la formation d' une minéralisation stratiforme dans des roches carbonatées.

ZUSAMMENFASSUNG

Die Mineralienfundstelle Lengenbach ist berühmt für eine Vielzahl seltener Sulfosalze. Die Pb-Zn-As-Tl-Ba-Mineralisation, welche während der alpidischen Metamorphose vollständig rekristallisierte, liegt in triadischen Dolomiten des nördlichen Penninikums. Die geochemischen und isotopengeochemischen Ergebnisse dieser Arbeit zeigen verschiedene neue genetische Aspekte dieser einmaligen Minerallagerstätte auf.

Die unterschiedlichen Mineralparagenesen in verschiedenen Zonen der Grube deutet auf verschiedene metamorphe Redoxbedingungen hin. Die As(III)-reiche Zone wird durch eine Mineralparagenese im fo_2-Stabilitätsfeld von Barit + Pyrit und einer As-(Pb, Tl)-reichen Sulfidschmelze charakterisiert. Die chemische Zusammensetzung der massiven Sulfosalzaggregate (hauptsächlich Baumhauerit) dokumentiert die Anreicherung von Tl, Ag und Sb während der fraktionierten Kristallisation der Schmelze und erklärt die starke Anreicherung dieser Elemente in den spätalpinen, hydrothermalen Lösungen.

Die mineralisierten Metadolomite sind signifikant an As, Pb, Ag, Tl, Hg, Zn, Ba, Cd, Fe, Cu, Mo, U, V, B, Ga und Cr angereichert, während Sn und Au nur wenig erhöhte Konzentrationen zeigen. As, Pb und Zn erreichen Gesamtgesteins-Konzentrationen von 0.1 bis 1%, Tl und Ag von mehreren Hundert ppm.

U-Pb Altersbestimmungen an Uraniniten aus silikatreichen Bändern ergaben ein alpidisches Alter von 18.5±0.5 Ma. Pb- und S- Isotopenzusammensetzungen verschieden Mineralien der Grube lassen sich durch metamorphe Reequilibration erklären: Pb- und S-Isotopenverhältnisse von stratiformen, gesteinsbildenden Erzmineralien ($^{206}Pb/^{204}Pb$ = 18.44–18.56, $^{207}Pb/^{204}Pb$ = 15.60–15.75, $^{208}Pb/^{204}Pb$ = 38.44–38.84 und $\delta^{34}S$ (sulfide) = -25 ± 2‰) sind gegenüber Kluftmineralien homogen und weniger angereichert an uranogenem Pb. Der Unterschied in der S- Isotopenzusammensetzung in verschiedenen Zonen der Grube und in verschiedenen Mineralien lässt sich durch Reequilibration von Sulfid- und Sulfatschwefel während der Metamorphose erklären (T = 450 ± 30°C). Arsenopyrit-Geothermometer und Zinkblende-Geobarometer von Kluftmineralien deuten auf Temperatur- und Druckverhältnisse von 380–410°C und 3.3 ± 0.6 kbar.

Die $^{87}Sr/^{86}Sr$- Verhältnisse von Dolomit und Barit der Erzzone sind gegenüber von unmineralisiertem Dolomit nicht erhöht. Das Meerwasser muss als wahrscheinlichste Sr-Quelle angenommen werden.

C, O, S, Sr und Pb- Isotopenuntersuchungen an Kluftmineralien zeigen keinen Einfluss externer, metamorpher Lösungen. Die neuen Daten deuten auf ein alpidisch geschlossenes System während der retrograden Metamorphose. Idiomorph auskristallisierte Mineralien in Hohlräumen bildeten sich aus einer hydrothermalen Lösung, welche mit einer Sulfidschmelze koexistierte.

Die primäre Mineralisation bildete sich vermutlich auf oder nahe dem Meeresboden, wobei die erzbildenden Lösungen sulfidarm waren. Die niedrigen $\delta^{34}S$-Werte der stratiformen Vererzung lassen sich am besten durch bakterielle Reduktion von Sulfat erklären. Die redoxsensitiven Elemente U, V, und Mo wurden vermutlich durch Interaktion des Erzes mit dem Meerwasser angereichert.

Prämesozoische Gesteine wurden auf ihre geochemische und isotopengeochemische Zusammensetzung untersucht, um neue Erkenntnisse über die Quelle und das Alter der Mineralisationen im Binntal zu gewinnen.

Die Pb-Isotopenzusammensetzung permischer Rhyolite (korrigiert für 200 Ma) stimmt mit der Isotopensignatur stratiformer Erzmineralien des Lengenbaches überein. Die As-reichen Rhyolite des kristallinen Sockels werden deshalb als Metallquelle für die erzbildenden Lösungen vorgeschlagen. Die gleichen Gesteine definieren eine Rb-Sr Isochron mit einem Alter von 185 ± 17 Ma. Die Verjüngung dieser Einheit wurde durch hydrothermale Aktivität während des frühen Mesozoikums verursacht.

In alpinen Klüften der Metarhyolite wurden verschiede seltene Arsenate gefunden. In unmittelbarer Nähe solcher Kluftparagenesen tritt ein Biotit-Epidot-Gestein auf, welches anhand von strukturellen, geochemischen und isotopengeochemischen Kriterien als metamorph überprägte Scherzone interpretiert wird. Diese präalpinen Scherzonen dokumentieren das frühmesozoische Rifting im Nordpenninikum, welches von hydrothermaler Aktivität und polymetallischer Erzbildung begleitet wurden.

INTRODUCTION

Regional geology

The Lengenbach deposit is located in a Triassic (LEU, 1986a and 1986b) metadolostone at the northern front of the Monte Leone nappe in the Pennine realm of the Alps (fig. 1). Conditions of Tertiary metamorphism were transitional between upper greenschist and lower amphibolite facies (FREY et al., 1974; VANCE & O'NIONS, 1992). Biotite-garnet geothermometry in Monte Leone gneisses yielded maximum temperatures of 500 to 520°C (HÜGI, 1988), in agreement with results from the Steinental 12 km SE of Lengenbach where maximum temperatures of 520°C were reached about 28 Ma ago according to Sm/Nd and U/Pb data of garnets (VANCE & O'NIONS, 1992).

The metadolostone is 240 m thick at Lengenbach, shows isoclinal folding in nearby outcrops and dips 80 to 85° south, with slight overturning. The mineralization is stratigraphically 180 to 200 m above the base of the metadolostone, close to overlying Mesozoic Bündnerschiefer.

The Triassic platform metadolostones forming the sedimentary cover of the Monte Leone nappe were deposited at the early stages of regional extension. Synsedimentary faults have been identified in the depositional realm of the Monte Leone nappe (LEU, 1986a and 1986b).

The overlying Jurassic-Cretaceous Bündnerschiefer series consist of carbonate-rich schists with a primary thickness of several km, deposited in the strongly extensional regime of the Penninic zone. Several intercalations of metabasalts (see part III) are interpreted as synsedimentary extrusions (LEU, 1986a and 1986b).

The crystalline core of the Monte Leone nappe consists of orthogneisses of a pre-Permian basement, Permian metavolcanics and paragneisses. The paragneisses partially represent metamorphosed Permian sediments (KRAMERS, 1970; HÜGI, 1988). At Mt. Cervandone, 4 km SW of the Lengenbach site, a metarhyolite-hosted Cu-As-F occurrence is known (GRAESER, 1965), close to which Alpine fissures contain several unusual As-rich minerals such as
asbecasite [$Ca_3(Ti,Sn)(As_6Si_2Be_6)O_{20}$],
cafarsite [$Ca_{5.9}Mn_{1.7}Fe_3Ti_3(AsO_3)_{12} \cdot 4\text{-}5H_2O$],
chernovite [$(Y,La)AsO_4$],
cervandonite [$(Ce,La)(Fe,Ti,Al)_3SiAs(Si,As)O_{13}$],
fetiasite, gasparite-(Ce) [$(Ce,La)AsO_4$] and
tilasite [$CaMg(F/AsO_4)$] (GRAESER, 1966; GRAESER & ROGGIANI, 1976; GRAESER et al., 1973). A similar association of As-rich fissure minerals occurs in gneisses 1 km E of Lengenbach at Gorb (fig. 1) and in the Mättital area (KRZEMNICKI, 1992).

The mineralizations of the Binn Valley are part of an extensive district of Pb-Zn-mineralization in Triassic rocks of Europe and northern Africa (AMSTUTZ & FONTBOTÉ, 1985), both within the Eastern Alps, e.g. Bleiberg, Raibl, Salafossa, Mezica (BRIGO et al., 1977), the Swiss Alps, e.g. Davos, Hondrich near Spiez (OBERHÄNSLI et al., 1985) as well as in non-Alpine areas, e.g. «Bleiglanzbänke» of Germany (HOFMANN & v. GEHLEN, 1993), Wiesloch, Germany (SEELIGER, 1963), Upper Silesia, Poland (GALKIEWICZ, 1967). In the Binn Valley, the Lengenbach is the most intensely mineralized locality in the Triassic metadolostones; less intense mineralization is widespread along a strike of about 15 km of the metadolostones (GRAESER, 1965). Besides sulfide mineralization, a small magnetite orebody occurs in the Triassic metadolostones in the Feldbach Valley (fig. 1).

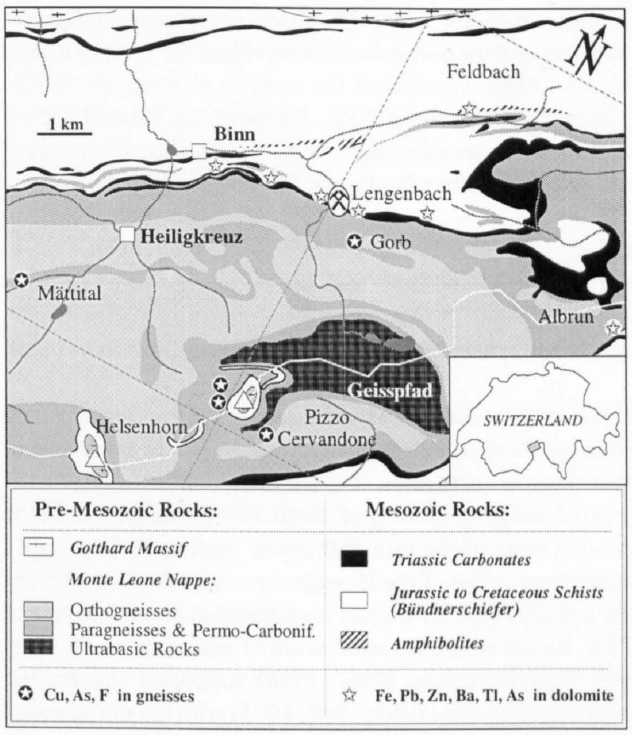

Figure 1: Schematic geological map of the Binn Valley with the locations of the main mineralizations (modified after BADER, 1934).

Petrogenesis of the Lengenbach deposit: metamorphogenic versus metamorphosed mineralization

The concept that regional metamorphic processes may have been responsible for the generation of ore forming hydrothermal solutions has been proposed by several geoscientists working on Au-mineralization. NESBITT (1988) refers to these deposits, in which Au is the chief economic metal as «mesothermal lode gold deposits». In the literature they are also referred to as metamorphogenic (for reference see PIRAJNO, 1992). Such hydrothermal mineralization is hosted in rocks metamorphosed to greenschist and lower amphibolite facies. In most cases, the mineralizing event post-dated peak metamorphism. Within this broad category are included the quartz veins of the Monte Rosa terrain from the Swiss Alps (CURTI, 1987; DIAMOND, 1990; LATTANZI et al., 1989). These mesothermal gold veins probably best illustrate ore forming processes during regional metamorphism in the Alps.

On the other hand mineralization may be metamorphosed, in the sense that it predates the metamorphism and has therefore been affected by a considerable change in pressure-temperature conditions that may have modified textures, mineralogy, grade and shape.

The genesis of the Lengenbach deposit has been the subject of investigations by GIUSCA (1930), BADER (1934), GRAESER (1965; 1968; 1969; 1975), HOEFS & GRAESER (1968) and HÜGI (1988): a pre-Alpine origin of the stratiform Fe-Pb-Zn-mineralization has been advocated for a long time (GIUSCA, 1930; BADER, 1934) and was supported by HOEFS & GRAESER (1968) on the basis of the light S isotopic composition of common sulfides. Although Alpine overprinting and recrystallization of the mineralization is evident, GIUSCA (1930) and BADER (1934) considered the system as relatively closed during Alpine metamorphism. Furthermore, they related the occurrence of neighboring volcanic rocks to the formation of the stratiform mineralization in the Triassic metadolostones.

GRAESER (1965; 1968; 1975) assumed an open system during late Alpine time with an metamorphically induced addition of As, Tl, Ag, Sb and Cu into pre-existing pyrite, galena and sphalerite mineralization during late Alpine times.

HÜGI (1988) studied fluid inclusions of Alpine fissure quartz from the Lengenbach deposit. He distinguished three different types of inclusions. Type I, CO_2-rich inclusions were formed under conditions of about 400°C and 2 kbar. In the As-rich zone of the mineralization, such inclusions partly bear arsenic glass. Type II- inclusions are salt-rich, whereas the aqueous type III-inclusions formed at about 250°C and 1 kb. Based on the determination of arsenic glass in CO_2-rich fluid inclusions HÜGI (1988) supported the genetic model of GRAESER (1965; 1968; 1975) with the introduction of As-rich solutions in the dolostones during retrograde Alpine metamorphism.

This work investigates the influence of the regional Tertiary metamorphism on the Lengenbach deposit to scrutinize the model of a two stage mineralization by combined geochemical and isotopical (O, C, S, Rb-Sr, Pb-Pb, U-Pb) methods.

Although the mineral assemblage of the Lengenbach deposit appears to be unique, its geochemistry shows similarities with stratiform base metal deposits. The purpose of the first part of this study is to provide a database to allow the testing of different genetic hypotheses, particularly whether As, Tl and some other elements were introduced during Alpine times or whether the concentrations of these elements are of Pre-Alpine origin.

Purpose and organization of the project

The aims of this investigation were:

1st to present new arguments for or against the metamorphogenic addition of As, Tl, Ag, Sb and Cu from external sources into the Lengenbach deposit (Part I), and

2nd to determine the source rock of the mineralizing fluids and to investigate the Cu-As-F mineralization located in the basement-gneisses of the Monte Leone nappe and to clarify their relations with the neighboring stratiform Pb-Zn-As-Tl-Ba-mineralization of the Lengenbach (Part II), and

3rd to clarify the genetic relation of Mesozoic amphibolites to the carbonate-hosted mineralization in their footwall (Part III).

This work is divided into three parts: The first section focuses on the geochemistry and genesis of the Lengenbach deposit, whereas investigations of mineralization in neighboring gneisses will be discussed in the second part. The geochemistry of the Mesozoic amphibolites will be discussed in the third section.

The project was supported by the Swiss National Science foundation (grant No. 21-31286.91). A complementary investigation of the whole rock and mineral chemistry as well as S-isotope geochemistry was simultaneously initiated by B. Hofmann from the Natural History Museum of Bern, who carried out the electron microprobe analyses of uraninites, the S isotope measurements as well as the geochemical bulk rock analyses. Already at an early stage of the project a close and fruitful cooperation was established resulting in a publication in Mineralium Deposita: Geochemistry and genesis of the Lengenbach Pb-Zn-As-Tl-Ba-mineralization, Binn Valley, Switzerland (HOFMANN & KNILL, in press). Geochemical whole rock analyses of samples from the Lengenbach deposit were financed by ESM (Stiftung Entwicklungsfonds Seltene Metalle, Pully, Switzerland).

PART I:
GEOCHEMISTRY OF THE PB-ZN-AS-TL-BA-DEPOSIT AT LENGENBACH

I.1 Zoning of the mineralization

The Lengenbach mineral occurrence in the Binn Valley, Valais, Switzerland, has been famous for its wealth of rare and well crystallized Pb-As-Tl sulfosalt minerals since the early 19th century. Early mineral collecting took place between 1835 and 1900. Since 1958, the quarry has operated every summer for the recovery of mineral specimens: 50 to 100 m^3 of rock are quarried annually.

The mineralogical and crystallographical aspects of the hydrothermal mineral assemblage of the Lengenbach are subjects of numerous publications and will only be dealt briefly in this work. In metadolostone, well crystallized minerals constitute a small volume fraction of the rock and are restricted to druses and fissures, whereas stratiform layers of pyrite and minor galena, sphalerite and xenomorphic sulfosalts dominate the bulk of the mineralization.

Within the Lengenbach deposit, several geochemical zones characterized by different mineral assemblages (see fig. I.1) and As/Pb ratios are present and have been described previously (GRAESER, 1965; STALDER et al., 1969; HOFMANN et al., 1993). In this work, based on As/Pb ratios and As valency, the following geochemical zones are distinguished:

As(III)-rich zone with pyrite, barite, As(III)-sulfides and low-Fe sphalerite. Main As-phases are baumhauerite, sartorite, orpiment and realgar. Textural evidence indicates the former existence of a Pb-Tl-As-S-melt phase above±300°C in this zone. Nonsulfide minerals include dolomite, calcite, quartz, hyalophane, phlogopite, K-Ba micas, rutile and uraninite. In silicate-rich bands (approximately 25% SiO_2), uraninite and rutile are found in direct contact without signs of brannerite formation, while a single brannerite crystal was found in a druse associated with sartorite (GRAESER & GUGGENHEIM, 1990). Graphite is absent and Ba-concentrations are high. Barium silicates, quartz, rutile and uraninite are concentrated in stratiform bands of a few cm thickness. Barium silicates most likely are the result of barite-silicate reactions as observed in other metamorphosed barite-rich deposits such as Kipushi, Zaïre (CHABU & BOULÈGE, 1992).

Intermediate redox zone (includes As-poor zone of GRAESER, 1965; GRAESER, 1975; HOFMANN et al., 1993): pyrite, barite, As-poor sulfosalts (e.g. jordanite), galena, sphalerite with variable Fe-content, arsenopyrite in druses. This zone is found stratigraphically above the As-rich zone and is characterized by sulfosalts with lower As/Pb. Pure As sulfides are absent. As occurs in minerals in trivalent (sulfosalts) as well as zerovalent (arsenopyrite) form, probably a result of the irregular distribution of the redox buffers barite and graphite. The variable color of the metadolostones is caused by the irregular distribution of graphite.

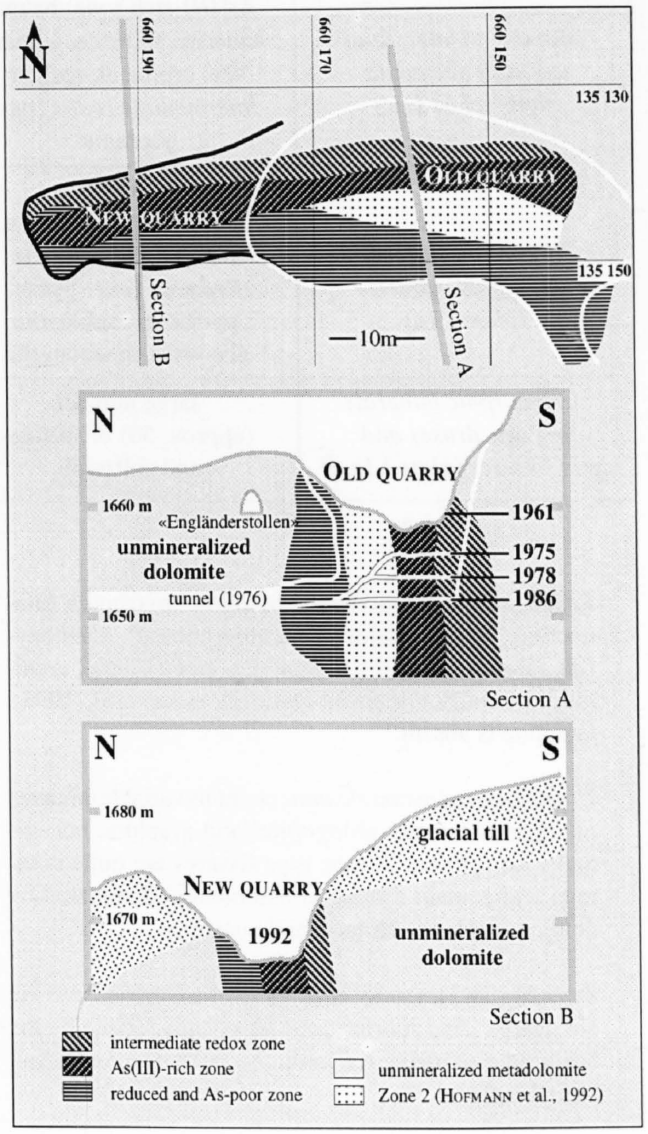

Figure I.1: Schematic map of the Lengenbach deposit (after HOFMANN et al., 1993).

Table I.1: Major geometric types of mineralization in the Lengenbach deposit.

geometric type of mineralization	**sulfid minerals**	**nonsulfid minerals**	**importance for bulk composition**
Stratiform mineralization (plate I.1a, b)	pyrite, galena, sphalerite	barite, quartz, K-Ba-micas, Ba-feldspar, tourmaline, uraninite	major host of Fe, S, Ba, Sr, U important for Zn, Pb
Massive to interstitial sulfosalt accumulations (plate I.1c)	*As(III)-rich zone:* baumhauerite, sartorite, tennantite, orpiment, realgar. *Intermediate redox zone:* jordanite	dolomite-, calcite and barite porphyroclasts, quartz	major host of As, Pb, Tl, Ag, Sb important for Cu, S
Discordant sulfosalt or sulfide veinlets (plate I.1d)	*As(III)-rich zone:* baumhauerite, sartorite, realgar, dufrenoysite *Reduced zone:* pyrite, pyrrhotite, sphalerite (Fe-rich), arsenopyrite	barite	minor host of Pb, As, Tl, Ag, S
Idiomorphic minerals in vugs, druses and open fissures (plate I.1e, f)	large number (approx. 50) of sulfides and sulfosalts	barite, Ba-K-feldspar, K-Ba-micas, quartz, goyazite, tourmaline	minor host of Pb, As, Tl, Ag, Cu, Ba

Reduced zone characterized by pyrite, pyrrhotite (monoclinic, low temperature paramorphosed), arsenopyrite, Fe-rich sphalerite, magnetite, green biotite, uraninite, rare coulsonite and nolanite (HOFMANN et al., 1993). Graphite is absent.

Unmineralized metadolostone contains variable amounts of silicates (mostly phlogopite) and graphite, but virtually no sulfides. Alpine type fissures are quite common and contain a mineral assemblage dominated by dolomite, calcite, adularia and quartz.

Zone 2 (after HOFMANN et al. 1993) was restricted to the old quarry. This As-rich zone was characterized by the occurrence of native As, jordanite and dufrenoysite and lacked realgar.

I.2 Geology and geometric types of the mineralization

The known extent of the Lengenbach sulfide occurrence is confined to several stratiform mineralized zones in a volume of rock about 70 m long, 30 m wide and 40 m high. The original outcrop in the Lengenbach stream has been removed during quarrying operations. In the present quarry, the metadolostone was covered by 5 to 10 m of Quarternary glacial till.

The host rock of the stratiform mineralization is a white to gray (graphite bearing) sugary dolomite. Coarse grained dolomite porphyroclasts occur within the mineralized zone of the dolostone. Alpine, idiomorphic dolomite crystals coexist in druses together with sulfides, sulfosalts, silicates, sulfates, phosphates and oxides.

Four major geometric types of mineralization can be recognized (tab. I.1):

- *Stratiform layers*, in which the most dominant ore mineral is pyrite, vary in thickness from a few cm to 50 cm and contain up to 80% pyrite by volume (plate I.1a). Similar layers of lesser thickness are formed by galena and sphalerite and rarely by magnetite (plate I.1b). The As-rich sulfosalt mineralization is stratabound, occurs usually close to the pyrite layers and is often most intense in pressure shadows of coarse dolomite nodules restricted to this zone (plate I.1c).

- *Massive to interstitial sulfosalt accumulations* (dominantly baumhauerite) associated with realgar and orpiment are found in irregular pockets of up to 20 cm diameter.

- Cracks filled with massive and partly idiomorphic sulfides fan out from massive ore pockets (*discordant sulfosalt veinlets*, plate I.1d). The host metadolostone contains variable amounts of phlogopite but is poor in other silicates. It is «sugary», i.e. individual isometric dolomite grains of 0.1 to 0.3 mm diameter are loosely held together. Both white (graphite free) and gray (graphitic) metadolostone varieties are encountered, the gray varieties being restricted to areas of less-intense As-mineralization. Stratiform silicate-rich (barian microcline, barian muscovite, quartz) layers of a few cm thickness are rare but can occasionally be followed over up to 15 m along strike. These layers with up to 124 ppm bulk U contain accessory uraninite.

– Well-crystallized sulfides, oxides, silicates, sulfates, carbonates and phosphates occur as *idiomorphic minerals in vugs, druses* (plate I.1e) and *open fissures* (plate I.1f). In isolated patches, an assemblage with magnetite, arsenopyrite and pyrrhotite is found (plate I.1b).

Ductile and brittle deformation structures can be distinguished in the Lengenbach quarry. Porphyroclasts (coarse grained crystals) of dolomite, calcite, barite, quartz and tourmaline within sugary dolomite indicate that their formation predates the end of ductile dolostone deformation. The formation of druses is most prominent in pressure shadows of large dolomite porphyroclasts and is most likely a result of combined deformation and dissolution processes. Brittle deformation structures within the mineralized metadolostone occur as thin fissures perpendicular to the bedding and are filled with either sulfosalts or an assemblage of pyrite-pyrrhotite-arsenopyrite-sphalerite.

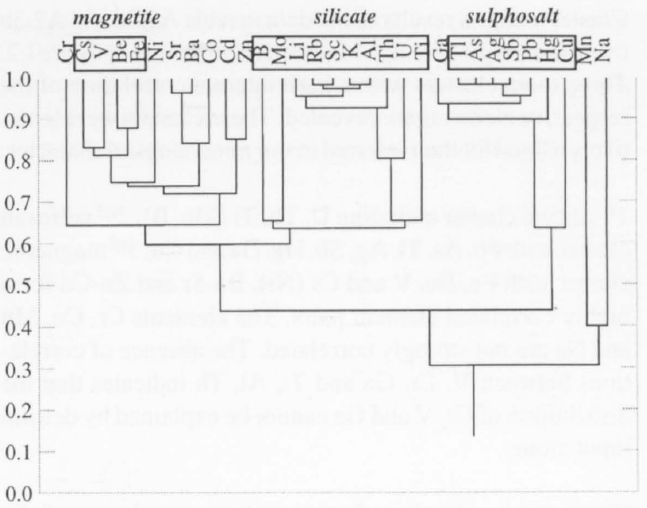

Figure I.2: Dendrogram cluster analysis (nearest neighbor, Program Cluster by SYSTAT) for 34 whole rock samples from the Lengenbach deposit based on inverse distance similarity of Pearson-correlated data. The tree diagram was calculated by a single linkage method.

I.3 Whole-rock geochemistry

I.3.1 Samples and methods

Samples of the Lengenbach mineralization were either selected in the quarry or obtained from the collections of the Natural History Museum of Bern.

For whole-rock geochemical analyses, samples of 1 to 5 kg (sample LB17: 50 kg) were crushed, split and ground in a tungsten carbide disc mill. Analyses of Na, Sc, Fe, Co, Ni, Zn, As, Se, Rb, Sr, Mo, Ag, Sb, Cs, Ba, La, Ce, Sm, Eu, Tb, Yb, Lu, Sm, Au, Th and U were performed by INAA (Instrumental Neutron Activation Analysis) by Bondar-Clegg and Company Ltd., Ottawa; Li, Na, Al, K, Ti, Cr, Mn, Fe, Co, Ni, Cu, Zn, As, Sr, Y, Zr, Nb, Mo, Ag, Cd, Ba, Pb, Bi by ICP-OES (Inductively Coupled Plasma-Optical Emission Spectroscopy), Hg by cold vapor AAS (Atomic Absorption Spectroscopy), Tl by AAS, In, Sn and Fe>10% by XRF (X-ray fluorescence), all at the same laboratory. Be, B, Ga and V (fusion-ICP-OES) and REE (ICP-Mass-Spectroscopy) were analyzed by XRAL Laboratories, Toronto. Some samples were analyzed for Sn by KBr fusion-hydride-AAS and for Au using a wet chemical method by Omac laboratories, Ireland. Samples with high concentrations of Pb, Tl, Ba and As were reanalyzed by XRF using synthetic standards with a similar matrix at the University of Bern. Mean values were tabulated where element concentrations consistent within error were obtained by different methods. Acid-dissolution ICP-OES analyses of Ba and Sr yielded low values due to incomplete decomposition of barite and were omitted in favor of INAA and XRF data.

I.3.2 Results

Whole rock geochemical data for 33 elements in 29 representative whole rock samples from distinct zones from the Lengenbach deposit and 5 reference samples of unmineralized metadolostone from nearby occurrences are presented in table A2.3a and A2.3b. For most elements the five unmineralized metadolostone samples (LB30, 31, 32, 33, HB209) show concentrations similar to average carbonate (TUREKIAN & WEDEPOHL, 1961) but with significant enrichments of Li, Rb and Cs. Compared with white metadolostone, the graphite bearing unmineralized samples (LB31, 33) are slightly enriched in As (enrichment factor 3.8), Sb (3.0), U (2.8) and Zn (2.0). Barium is slightly depleted (0.6).

Compared with the unmineralized metadolostone, mineralized samples show enrichments of a large number of elements (in decreasing order, with range of enrichment): >1000-fold enriched: As, Pb; 1000–100-fold: Ag, Tl, Sb, Hg, Zn, Ba, Cd; 100–10-fold: Fe, Cu; <10-fold: U, Mo, V, B, Ga and Cr. Low concentrations close to the detection limit were found for In (<1 ppm), Sn (<2–5 ppm), Ge (<10 ppm), Se (<5 ppm). Au was analyzed in 8 additional samples yielding a range of <2 to 24 ppb with the highest values occurring in sulfosalt-rich samples and in a sample containing fuchsite. Overall, Ba values are high, averaging 1.1%, this element ranks second in mass enrichment after Fe in the bulk of the mineralization. The As(III)-rich zone has a high atomic As/Pb ratio of 1.6, reflecting the abundance of As-rich minerals such as sartorite (As/Pb = 2), baumhauerite (As/Pb = 1.33) and pure As sulfides.

Although the analyzed samples may be biased towards high concentrations of Pb-As-Zn-Cu and low Fe values due to the use of «ore-grade» samples, visual estimates of pyrite/sulfosalt volume ratios by other Lengenbach investigators (GRAESER, S., IMHOF, T. , OBERHOLZER, W., STALDER, H.A., pers. comm., 1992) yielded a value of about 10, indicating that no severe error in element ratios is introduced during sampling (pyrite/Pb ratio calculated from As-rich samples assuming all Fe is pyrite-bound: 7.4).

Cluster analysis results of the data in table A2.3a and A2.3b using the Single Linkage Method are presented in figure I.2. Three main clusters with a high internal correlation of the respective elements are revealed. These clusters were tentatively named for their inferred major mineralogical character:

1st silicate cluster including U, Th, Ti (Mo, B); 2nd sulfosalt cluster with Pb, As, Tl, Ag, Sb, Hg, Ga and Cu; 3rd magnetite cluster with Fe, Be, V and Cs (Ni). Ba-Sr and Zn-Cd form highly correlated element pairs. The elements Cr, Co, Mn and Na are not strongly correlated. The absence of correlations between V, Cr, Ga and Ti, Al, Th indicates that the distribution of Cr, V and Ga cannot be explained by detrital input alone.

These results clearly reflect the close association of the sulfosalt-forming elements As-Tl-Ag-Ga-Sb-Pb-Hg-Cu. The association of Th and U with silicates and of Cs, V and Be with magnetite is established. Zn, Cd, Co, Ni are associated with mostly As-poor samples of variable affinity. The limited data available for Au and Sn indicate that these elements are most likely associated with the sulfosalt cluster. The association of Ga with sulfosalts and not with Zn is unusual, but can probably be explained by metamorphic redistribution (partitioning into melt phase?).

The results of rare earth element (REE) analysis of five mineralized (including three magnetite-rich) and two unmineralized metadolostones from the Lengenbach and one magnetite-rich sample from the Feldbach iron deposit are presented on table A2.4. Figure I.3 shows REE patterns of mineralized samples normalized to unmineralized metadolostone from the Binn Valley. This procedure best illustrates the rather slight differences between mineralized and unmineralized samples. Heavy rare earth elements (HREE) tend to be enriched in the mineralized samples (SGd-Yb/SLa-Sm 0.14–0.21 compared to 0.11 in barren metadolostone), but most prominent is a positive Eu-anomaly in all mineralized samples (Eu/Eu* 1.14–1.89). In contrast to the Lengenbach deposit, the Feldbach magnetite sample shows distinctly different characteristics with a stronger HREE enrichment (SGd-Yb/SLa-Sm 0.37) and no positive Eu anomaly (Eu* 0.85). I conclude that HREE and particularly Eu have been added to the mineralized metadolostones at Lengenbach. Therefore, based on REE data, the Feldbach magnetite occurrence is not genetically related to the Lengenbach deposit.

Higher Ti and Th concentrations, Ti/Al, Th/Al as well as Si/Al ratios of the silicate rich layers (compare samples LB8, LB23, LB19 in tab. A2.3 and A2.4) indicate an origin from pelitic sediments or from insoluble residues of the host metadolostone. REE's of sample LB8 are depleted by a factor of about 5 relative to the immobile elements Al, Th and Ti, however. I tentatively interpret silicate rich layers as hydrothermally leached (REE-depleted) insoluble residues within the host carbonates.

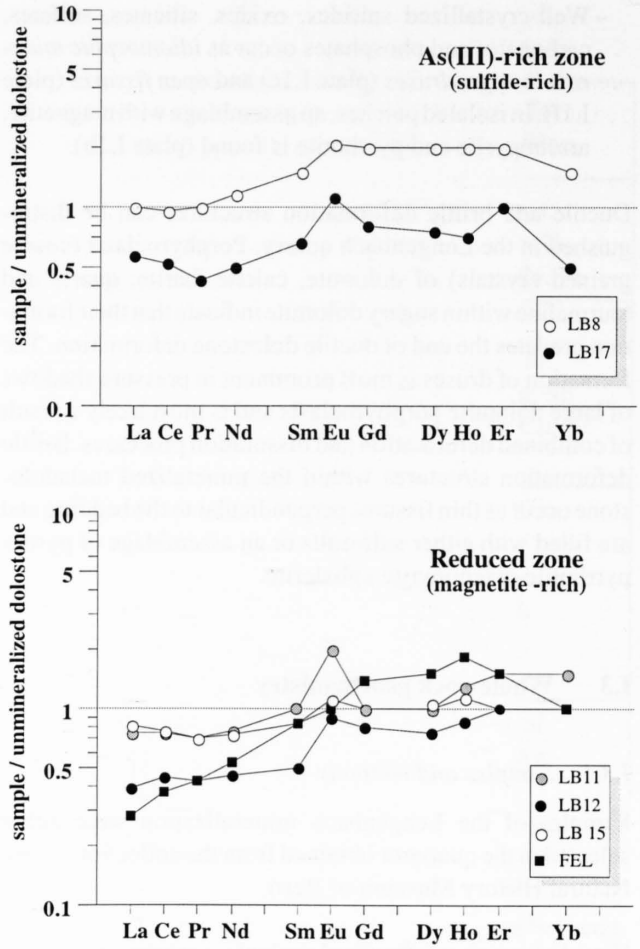

Figure I.3: REE-pattern for mineralized samples from the Lengenbach and Feldbach mineralizations. The data are normalized to the average of the unmineralized metadolostone samples LB30 and LB31.

I.4 The sulfidic melt of the Lengenbach deposit

I.4.1 Introduction

Different mechanisms have been proposed to explain mobilization of sulfide deposits during regional metamorphism. Mobilization by partial metamorphic melting of sulfidic ores has been advanced by Lawrence (1967) to explain «sulfide metapegmatites» in the Broken Hill deposit, Australia. Vokes (1971) took into account that melting can also take place in common sulfide systems at temperatures regarded as prevailing in medium grade metamorphic facies: «Metamorphic heating of Kieslagerstätten type ores containing Fe, Cu, Zn, Pb and S together with minor amounts of As, Pb, Ag, etc. to temperatures over 500°C would lead to a differential melting of the ores with a formation of melts relatively rich in Cu, Pb, As, Sb, Ag and S. These melts would presumably remain in the general vicinity of the parental ore body in the absence of tectonically controlled migration». Up to the recent investigations concerning the petrogenesis of the Lengenbach deposit, this prediction has not been confirmed by field observations.

Evidence of the former existence of a metamorphogenic, As-rich sulfide melt in the Lengenbach mineralization was presented by HOFMANN (1994). *Sulfosalt inclusions* arranged along healed fractures in quartz are an excellent confirmation of the formation of a sulfidic melt in the Lengenbach deposit. This recent study showed that a sulfidic melt was trapped simultaneously with an aqueous fluid. The interaction of the melt with hydrothermal fluids is evident from *As-S daughter minerals in fluid inclusions* (HÜGI, 1988), indicating that this fluid in equilibrium with the mineralization was extremely As-rich (hundreds of ppm). Microprobe analyses of homogenized sulfide inclusions (T = 500°C) showed that Tl was strongly enriched in the melt compared with bulk As-rich ore (HOFMANN, 1994). For a comparison with massive sulfosalt accumulations B. Hofmann provided the detailed geochemical data of homogenized melt inclusions (tab. A2.2 and fig. I.4). Melt inclusions formed of sulfosalt are characterized by relatively low Pb/As and elevated Tl/Pb, Sb/Pb and Ag/Pb, indicating a late stage trapping of a Pb-poor, residual melt.

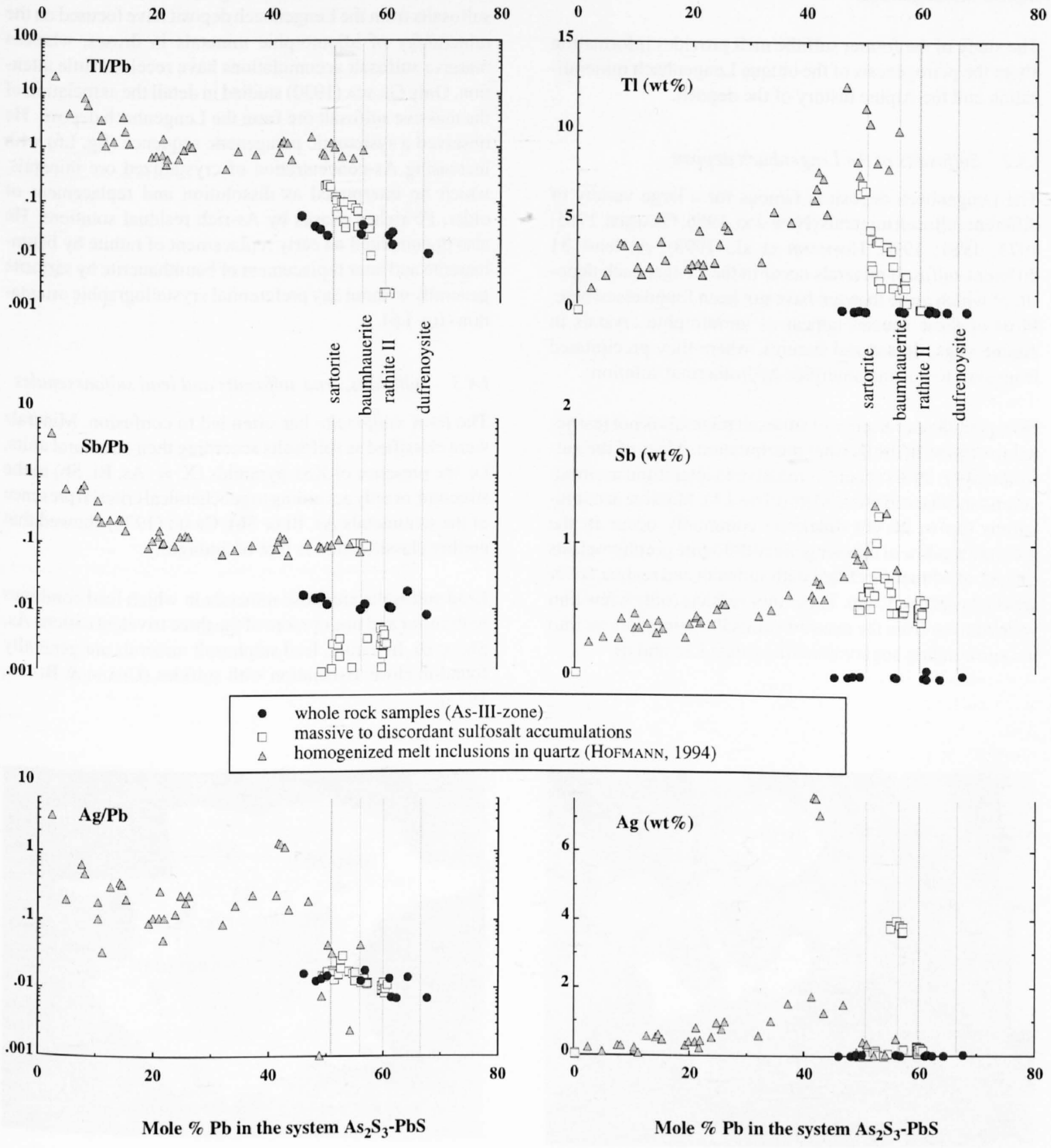

Figure I.4: Geochemical composition of whole rock samples, sulfosalt accumulations and melt inclusions from the Lengenbach deposit. The Pb/As-ratio of the main lead-sulfoarsenides are shown as reference-lines.

The present study shows that the ore paragenesis of the As(III)-rich zone of the Lengenbach deposit is compatible with a restricted ore mobilization by the formation of a sulfidic melt on a macroscale (mm to dm) during metamorphism. Massive sulfosalt accumulations in the carbonate-hosted, polymetallic mineralization from the Binn Valley can be best explained by the formation of a sulfidic melt during Alpine metamorphism. This interpretation is based on the phase relations of lead sulfoarsenides, micro- and macroscopic observations as well as geochemical and isotopical investigations.

The study of the former sulfidic melt provides information about the petrogenesis of the unique Lengenbach mineralization and the Alpine history of the deposit.

I.4.2 Sulfosalts of the Lengenbach deposit

The Lengenbach deposit is famous for a large variety of different sulfosalt minerals (Nowacki, 1965; Graeser, 1965; 1975; 1981; 1990; Hofmann et al., 1993). At least 31 different sulfosalt minerals occur in the Lengenbach deposit, of which more than ten have not been found elsewhere. Most of these species appear as idiomorphic crystals in Alpine vugs, druses and fissures, where they precipitated from syn- to postmetamorphic hydrothermal solutions.

However, the occurrence of sulfosalt minerals is not restricted to Alpine hydrothermal precipitation. Most of the sulfosalt (appr. 99%) occurs as massive to interstitial accumulations and discordant veinlets (plate I.1). Massive accumulations (up to 20 cm diameter) commonly occur in the pressure shadow of coarser grained dolomite porphyroclasts (plate I.1c). Fractures filled with sulfosalt and realgar cover areas up to 50 by 50 cm. These thin veinlets (only a few mm wide) fan out from the massive sulfosalt accumulations into the surrounding sugary dolomite (plate I.1c and d).

Microprobe analyses of massive sulfosalt ore indicate a relatively restricted range of chemical composition of minerals in massive accumulations in contrast to a large variety of idiomorphic sulfosalt minerals in druses and fissures (fig. I.5 and tab. A2.1). Several X-ray diffraction analyses confirmed little mineralogical variety of massive to interstitial sulfosalts (Oberholzer & Vogler, pers. com.). Xenomorphic sulfosalt consists predominantly of jordanite ($Pb_{26}As_{12}S_{46}$), rathite II ($Pb_{19}As_{25}S_{56}$), baumhauerite ($Pb_{12}As_{16}S_{36}$), baumhauerite-2a ($[Pb,Ag]_{11}[As,Sb]_{17}S_{36}$), sartorite ($PbAs_2S_4$) as well as realgar ($As_4S_4$). Most studies of sulfosalts from the Lengenbach deposit have focused on the mineralogy of idiomorphic minerals in druses, whereas massive sulfosalt accumulations have received little attention. Only Giusca (1930) studied in detail the association of the massive sulfosalt ore from the Lengenbach deposit. He observed a systematic paragenetic sequence (fig. I.6) with increasing As-concentration of crystallized ore minerals, which he interpreted as dissolution and replacement of older, Pb-richer phases by As-rich residual solutions. He also documented an early replacement of rathite by baumhauerite and later replacement of baumhauerite by sartorite generally without any preferential crystallographic orientation (fig. I.6).

I.4.3 Sulfosalts, lead sulfosalts and lead sulfoarsenides

The term «*sulfosalt*» has often led to confusion. Minerals were classified as sulfosalts according their structural units, i.e. the presence of XS_3-pyramids (X = As, Bi, Sb) in the structure, or only according to geochemical criteria (presence of the semimetals As, Bi or Sb). Craig (1974) showed that neither classification is free of ambiguity.

Lead sulfosalts are those minerals in which lead combines with sulfur and one or more of the three trivalent cations As, Sb, or Bi. In nature, lead sulphosalt minerals are generally found in close association with sulfides (Chang & Bever, 1973).

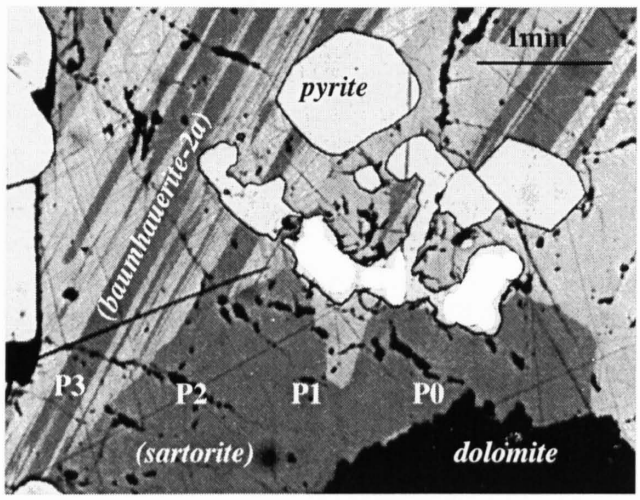

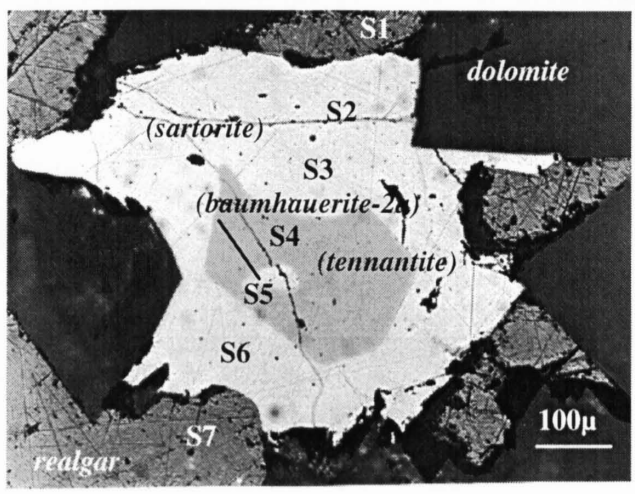

Figure I.5: Polished section of massive sulfosalt ore from the Lengenbach deposit with the localization of microprobe analyses. The identification of the sulfosalt minerals (in brackets) is based on the chemical composition only.

ROSCH & HELLNER (1959) synthesized six lead sulfoarsenides (sartorite, baumhauerite, rathite(I), rathite(II), dufrenoysite and jordanite) under hydrothermal conditions in the temperature range of 150°C to 600°C. Unfortunately no attempt was made to study the stability relations among the phases. The relatively high temperatures of some experiments make a pure hydrothermal formation doubtful.

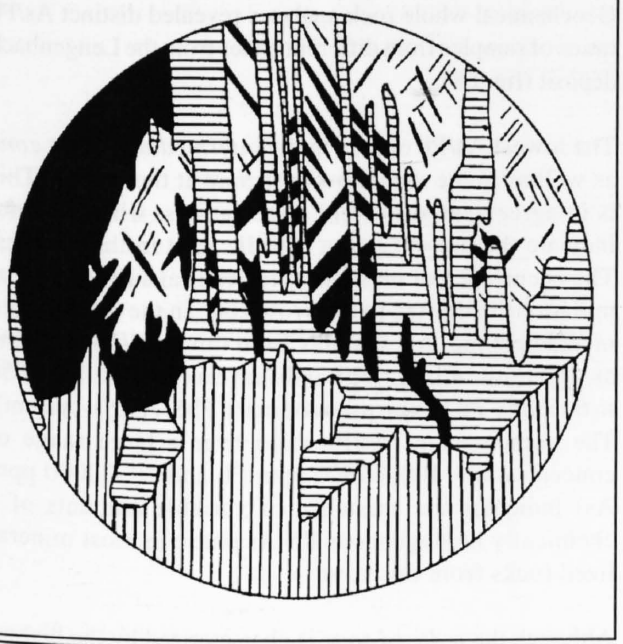

TABLE OF THE OBSERVED REPLACEMENTS

? → seligmanninte
jordanite → dufrénoysite
jordanite → baumhauerite

baumhauerite → skleroklase
liveingite → skleroklase → hutchinsonite
baumhauerite → hutchinsonite

rathite → skleroklase → realgare

hutchinsonite → realgare
realgare

Figure I.6: Early microscopic observations of massive sulfosalt ore from the Lengenbach deposit (from GIUSCA (1930), the table is translated form german). The paragenetic sequence was interpreted as dissolution and replacement of Pb-rich phases by As-rich residual solutions. The figure on the top shows the mineral paragenesis of massive sulfosalt accumulations: white = rathite, black = baumhauerite, horizontal striped = sartorite, vertical striped = dolomite. The table on the bottom shows the observed replacements.

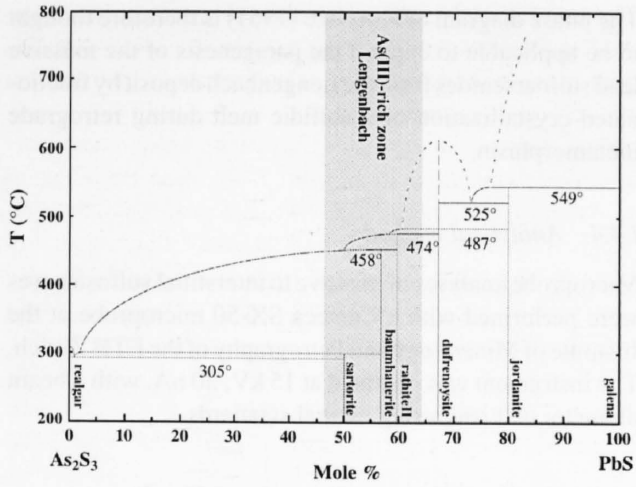

Figure I.7: Phase relation in the system PbS-As2S3 (after KUTOGLU, 1961) and range of As(III)-rich zone of the Lengenbach deposit. The figure illustrates the incongruent melting of the lead sulfoarsenides.

Many sulfosalts are suitable thermochemical indicators (CRAIG, 1974). KUTOGLU (1961) proposed a phase diagram for the system PbS-As2S3, whereas five lead sulphoarsenides are present in the system (fig. I.7). All phases except dufrenoysite show incongruent melting, producing a PbS-richer phase plus liquid. Based on the pseudobinary system PbS-As2S3, CHANG & BEVER (1973) presented a generalized paragenetic sequence of the lead sulfoarsenides, the metal (lead)-rich forming early, those rich in both the semi-metal and sulfur subsequently. A similar history would also be the case for lead sulfoantimonides and lead sulfobismuthides, which however crystallize at distinctly higher temperatures. Therefore, only lead sulfoarsenides melt under medium-grade metamorphism.

Phase transition temperatures of natural lead sulfoarsenides can be influenced by the concentrations of metals other than Pb, the presence of volatiles as well as the pressure conditions. Massive to interstitial baumhauerite and sartorite from the Lengenbach deposit contain significant concentrations of Sb (<1.2 wt%), Tl (<7.0 wt%) and Ag (<3.81 wt%) (tab. A2.1). Heating experiments with a standard U.S.G.S flinc-stage of several fractions of baumhauerite (sample L92-009 with 0.5 to 0.8 wt% Sb, 1 to 3.6 wt% Tl, 0 to 4 wt% Ag) indicate initial and final melting temperatures between 465 and 485°C. The agreement of these experimental results with the temperatures from the phase relation diagram of KUTOGLU (1961), point to a negligible influence of Sb, Tl or Ag-contamination on the transition temperatures of the PbS-As2S3-system. BRETT & KULLERUD (1967) investigated the Fe-Pb-S system and concluded that melting of sphalerite-galena-pyrite-assemblages may begin below 700°C. They concluded that water and other volatiles such as H_2O or CO_2 have negligible effects on the subsolidus relations in sulfide-type systems and that they may influence melting temperatures only significantly if they are soluble in the liquid. Gold-tube pressure experiments demonstrated that pressure has essentially no effect on the melting temperature of jordanite (ROLAND, 1968).

The phase diagram of KUTOGLU (1961) is therefore thought to be applicable to explain the paragenesis of the massive lead sulfoarsenides from the Lengenbach deposit by fractionated crystallization of a sulfidic melt during retrograde metamorphism.

I.4.4 Analytical method

Microprobe analyses of massive to interstitial sulfosalt ores were performed with a Cameca SX-50 microprobe at the Institute of Mineralogy and Petrography of the ETH Zürich. The instrument was operated at 15 kV, 20 nA, with a beam diameter of 1 µm, using natural standards.

I.4.5 Mineral chemistry of massive sulfosalt accumulations

Microprobe analyses along profiles of massive sulfosalt accumulations (fig. I.5) confirmed the microscopic observations of GIUSCA (1930): accumulations of sulfosalts show decreasing Pb/As ratios from the center to the margin, whereas the Tl-concentration increases.

A positive correlation of the Tl-concentration with decreasing Pb-As-ratio was also observed in sulfosalt samples from different sites (fig. I.4). The analyses showed that Tl, Sb and Ag are concentrated in different mineralogical phases. The highest concentration of Tl (up to 12 wt%) were measured in minerals with a Pb/As ratio close to sartorite (appr. 50 wt% Pb), whereas Sb (up to 1.3 wt%) is enriched in a more Pb-rich phase. Ag (appr. 4 wt%) is concentrated in a phase with a distinct Pb/As ratio and 57 wt% Pb (presumably baumhauerite-2a).

I.4.6 Phase relations: bulk compositional constraints on partial melting in the As_2S_3-PbS- system

The phase diagram of KUTOGLU (1961) shows that melts of lead sulfoarsenides can form in natural As-rich sulfide systems (e.g. Pb-Zn-mineralization) during medium grade metamorphism, whereby the temperature of the solid-melt transition significantly depends on the bulk As/Pb ratio of the system (fig. I.7).

Geochemical whole rock analyses revealed distinct As/Pb ratios of samples from different zones from the Lengenbach deposit (fig. I.8).

The lowest As/Pb occurs in the *intermediate redox zone* as well as in the *unmineralized zone* at the quarry. This is in agreement with field observations, which did not indicate the presence of a sulfidic melt in these zones. The occurrence of massive to interstitial sulfosalt accumulations is limited to a narrow zone in the mineralized metadolostone. All samples from this *As(III)-rich zone* as well as the silica-rich bands have a composition of 50 to 62 mol% Pb (in the pseudobinary PbS-As_2S_3-system). The homogeneous As/Pb ratio over a large range of concentration (100–60000 ppm Pb and 30–20000 ppm As) indicates the existence of variable amounts of a chemically homogeneous Pb-As phase in most mineralized rocks from this zone.

Although the *reduced zone* is characterized by the highest As/Pb ratio, no field observation indicates the formation of a melt in this zone.

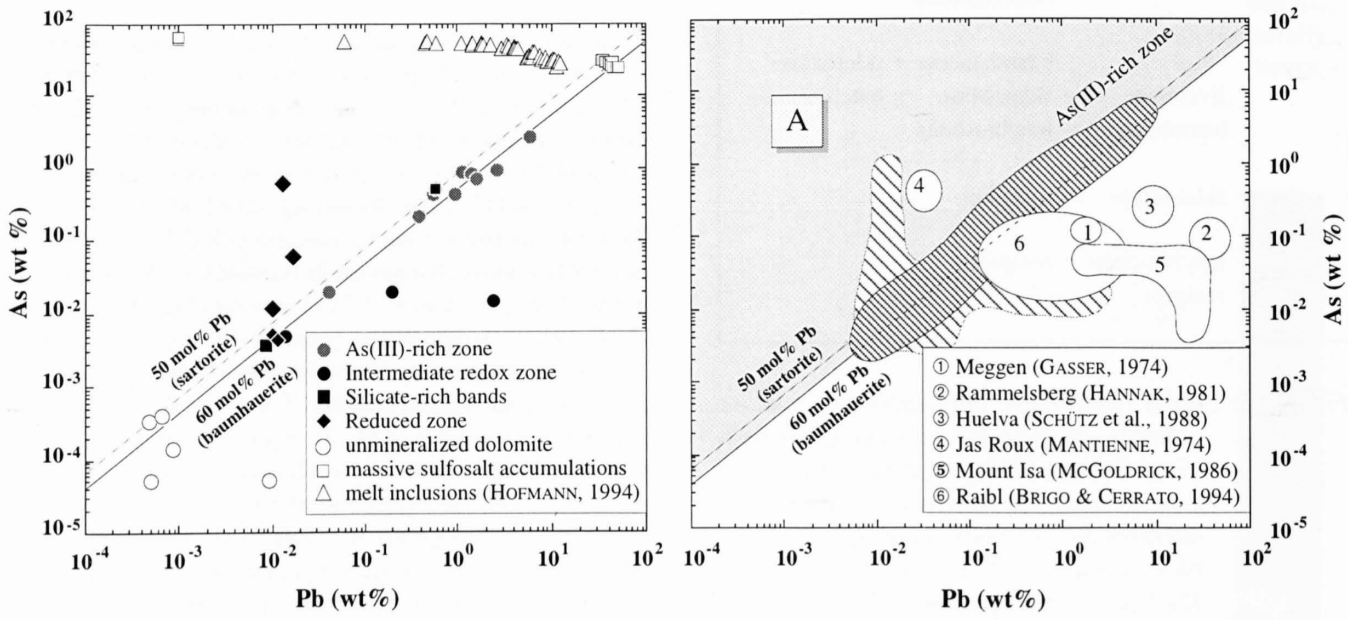

Figure I.8: Left: Pb-As composition of whole rock samples, massive sulfosalt accumulations and melt inclusions from the Lengenbach deposit. The composition of baumhauerite and sartorite are shown as reference lines. Right: comparison of bulk rock composition from the Lengenbach deposit with other stratiform sulfide deposits. A defines the field of a possible sulfidic melt at temperatures < 475 °C (KUTOGLU, 1961).

I.4.7 *Experiments of sulfidic melts in carbonates*

To clarify the influence of the host rock on the texture of a crystallizing sulfidic melt, experiments of natural sulfosalt were performed in carbonates. The melt experiments of lead-sulfoarsenides were carried out in a Johannes-Piston-cylinder equipment (SCHMIDT, 1992) at the Institute of Mineralogy and Petrography of the ETH Zürich. 0.15 g of baumhauerite from the Lengenbach deposit (sample L22012) were filled into Pt-capsules between two layers of 0.3 g calcite or dolomite (grain size: 300 µm). The dry samples were heated during 120h at 510°C and 3 kbar. Temperature and pressure were chosen similar to the peak metamorphic, lower amphibolite facies conditions of the terrain (HÜGI, 1988; VANCE & O'NIONS, 1992). Standard polished-section techniques (the section mounts were prepared from cold-setting resins) were prepared of the quenched samples to investigate the newly generated textures.

The melt-experiments produced distinct textures of recrystallized sulfosalt ore: in the dolomitic matrix the baumhauerite melt crystallized in the former layered fabric, whereas calcite was impregnated by the sulfidic melt (fig. I.9). Similar textures were observed in the field: Several calcitic veins with an average thickness of about 3 cm occur in the sugary metadolostone from the Binn Valley. Plastic deformation is often evident in these. Where such calcitic veins are in contact with massive sulfosalt ore, their color varies from dark yellow to brown due to finely dispersed sulfosalts.

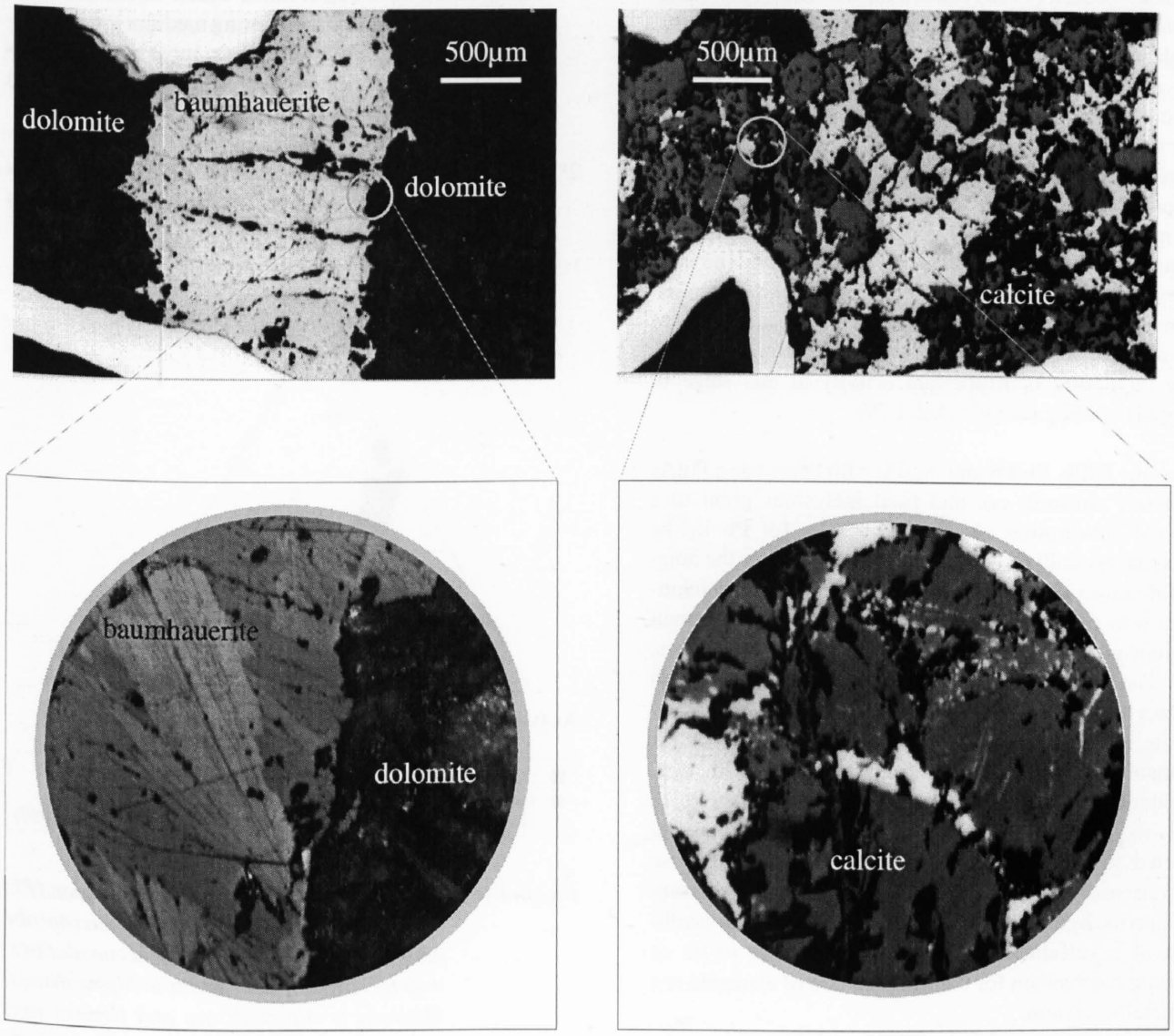

Figure I.9: Polished section of recrystallized baumhauerite (sample L22012 from the Lengenbach deposit). The experiment showed different textures of laboratory-crystallized sulfosalt-melt in dolomitic and calcitic host rock. The sulfidic melt was produced in Pt-capsules in a piston-cylinder at 510°C.

I.4.8 Discussion and conclusions

The paragenetic sequence of the massive sulfosalt ore from the Lengenbach deposit can be explained by a fractional crystallization from a sulfidic melt. The thermal stability of sulfoarsenides explains the occurrence of rathite, baumhauerite, sartorite and realgar in massive form, representing solidified melt pockets.

CHANG & BEVER (1973) postulated that lead sulfoarsenides are essentially restricted to mesothermal and epithermal deposits. The formation of a sulfidic melt during amphibolite facies metamorphism indicates that this assumption should not be generalized.

The occurrence of sulfosalt as massive accumulations as well as discordant melt injections raises the question of the mechanisms causing different deformation fabrics of the host rock. VOGLER (1986) studied the deformation of metadolostone and concluded that the transition between brittle and plastic deformation mainly depends on the deviatoric stress and the temperature. The coexistence of brittle and plastic deformation fabrics of the dolomitic host rock can either be explained by variable rates of deformation or by a change of the pressure conditions. I favor the process of fluid pressure shift during retrograde cooling from lithostatic to more hydrostatic condition at about 400°C to explain the transition from ductile to brittle deformation. The transition was contemporaneous with the formation of the first minerals in Alpine vugs (HÜGI, 1988), the crystallization of uraninites as well as the sulfide-sulfate equilibration, indicating increasing hydrothermal activity at this stage of retrograde cooling (see also fig. I.29).

Increasing Tl/Pb, Sb/Pb and Ag/Pb with decreasing Pb/As of massive sulfosalt ore and melt inclusions point to a restricted substitution of Tl, Sb and Ag for Pb in the successive crystallizing phases. At the contact to the adjacent dolomite a Tl-rich mineral phase (presumably hutchinsonite) was detected in several discordant sulfosalt melt injections as the last crystallizing phase (HOFMANN, pers. com.). The enrichment of Tl, Sb and Ag is in agreement with the observation that minerals rich in these elements (edenharterite, imhofite, lorandite, smithite, stephanite, proustite, trechmannite and others) are restricted to hydrothermal precipitations in Alpine vugs (fig. I.10). HOFMANN et al. (1993) showed that Tl-rich sulfosalts in Alpine druses are restricted to the As-rich zone of the deposit. All these observations suggest that Tl, Sb and Ag partition preferentially into the hydrothermal phase. The retrograde crystallization of a sulfidic melt is therefore thought to be an important mechanism for the fractionation of elements in a polymetallic system.

Metamorphic massive sulfide deposits have generally a simple mineral assemblage comprising pyrite, pyrrhotite, sphalerite, galena and arsenopyrite (e.g. Swedish Caledonides, SUNDBLAD et al., 1984). Oxygen fugacity is close to the pyrite/pyrrhotite buffer and most As is present in arsenopyrite as a formally zerovalent element (HEINRICH & EADINGTON, 1986). In the Lengenbach deposit, such conditions prevailed in the reduced zone. In the As(III)-rich zone, abundant pyrite and barite buffered oxygen fugacity at a higher level and precluded the reduction of As(III) and arsenopyrite formation. This preservation of As(III) enabled the formation of thioarsenates in melt form during metamorphism and in sulfosalt minerals during retrograde cooling.

There are three major prerequisites for the formation of sulfidic melt aggregations under medium grade metamorphic conditions:

1st Based on the phase diagram of lead-sulfoarsenides, the Pb/As of a system must be relatively low (fig. I.7). There are other stratiform sulfide deposits, e.g. Huelva or Raibl which have Pb/As ratios which would allow the formation of a sulfidic melt during medium grade metamorphic conditions. Nevertheless, most stratiform Pb-Zn deposits seem to be too poor in As (or too rich in Pb) for the formation of a sulfidic melt.

2nd Thermodynamic calculations of HEINRICH & EADINGTON (1986) proved that As^{3+} (which is the valency state of As

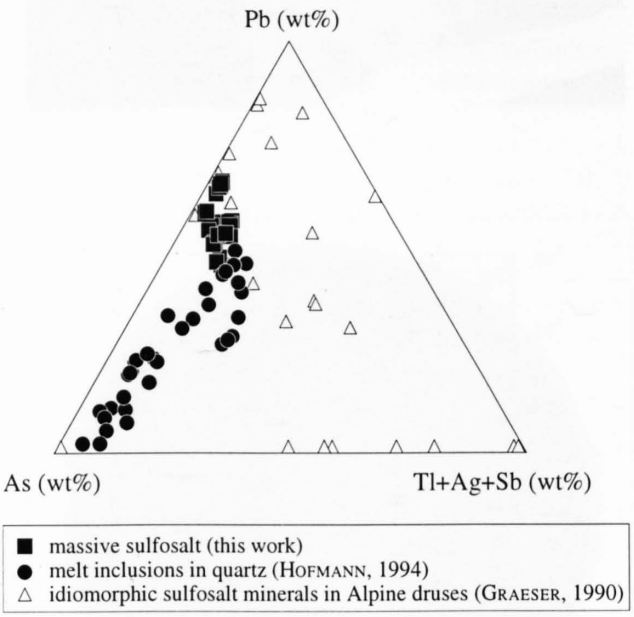

Figure I.10: Ternary plot of the chemical composition (Pb, As and Tl+Ag+Sb) determined by microprobe analyses of massive sulfosalt accumulations, melt inclusions and sulfosalts in Alpine druses. Minerals in Alpine druses and fissures are: dufrenoysite, rathite, baumhauerite, sartorite, realgar, hutchinsonite, liveingite, jordanite, edenharterite, geokronite, hatchite, imhofite, lorandite, marrite, proustite, pyrargite, stephanite, trechmannite, xanthokon, wallisite, stalderite, lengenbachite, bournouite, seligmannite.

in sulfosalts) is stable at 250°C in hydrothermal systems under relatively oxidizing conditions ($fO_2 > 10^{-40}$ bar). At lower oxygen-fugacity, arsenopyrite and loellingite are the stable solid phases in coexistence with a sulfur-bearing aqueous fluid with excess Fe. In the As(III)-zone, sulfate in the form of baryte was certainly the dominant S-bearing mineral, buffering by coexistence with pyrite the system during recrystallization. The lack of sulfate as well as the existence of arsenopyrite explain the absence of a sulfidic melt in the reduced zone.

3rd Field observations as well as melt experiments showed that the host rock of a sulfidic melt influences the texture of the ore (e.g. formation of accumulations or impregnation). The reason for the divergent behavior of the melt in different carbonates is unclear; a possible explanation could be distinct surface effect of the host minerals.

The homogeneous As/Pb-ratio of the whole rocks samples from the As-rich zone of the Lengenbach deposit can be best explained by the existence of variable amounts of a sulfidic melt with a constant As/Pb-ratio.

The O- and C- isotope compositions of sugary dolomite around Alpine druses in the Lengenbach deposit is slightly lighter than the composition of dolomite porphyroclasts. This difference indicates the influence of external fluids only in vuggy metadolostones (see section I.9.3). Homogeneous O and C- isotopic composition of dolomite close to sulfidic melt pockets as well as discordant melt injections point to a aqueous-poor environment of the sulfidic melt.

The existence of a sulfidic melt at peak metamorphism and during retrograde metamorphism is inconsistent with late Alpine hydrothermal influx of As into preexisting Pb-Zn-ores. The presence of high As-concentration close to peak metamorphic conditions is confirmed by arsenopyrite geothermometry indicating temperatures of 400°C during arsenopyrite formation in more reducing environments and the presence of As-S-phases in high-temperature fluid inclusions in quartz (HÜGI, 1988).

I.5 Pb isotopes

I.5.1 Pb isotopes of the stratiform mineralization

Nine separates of minerals occurring as stratiform layers (massive pyrite, galena, tourmaline) of the Lengenbach deposit conform to the growth curve for average crustal Pb (tab. A2.3c and fig. I.13). Model ages of about 200 Ma correspond to the stratigraphic age of the host rock.

Figure I.11 illustrates that many Pb-Zn deposits in Triassic host rocks of Europe have an anomalous Pb isotopic composition, characterized by model ages of 300 to 400 Ma and relatively high μ-values (KÖPPEL, 1983; BREVART et al., 1982; LE GUEN et al., 1991, ARRIBAS & TOSDAL, 1994). All these deposits from Eastern and Southern Alps, Massif Central and Betic Cordillera are related to the Vendée-Cévennes-Drosendorf-terrane. The main lithologic unit within this zone is a thick sequence of uppermost Proterozoic through Devonian metasedimentary (chiefly pelites and quartzites) and metavolcanic rocks (MATTE, 1991; ARRIBAS & TOSDAL, 1994).

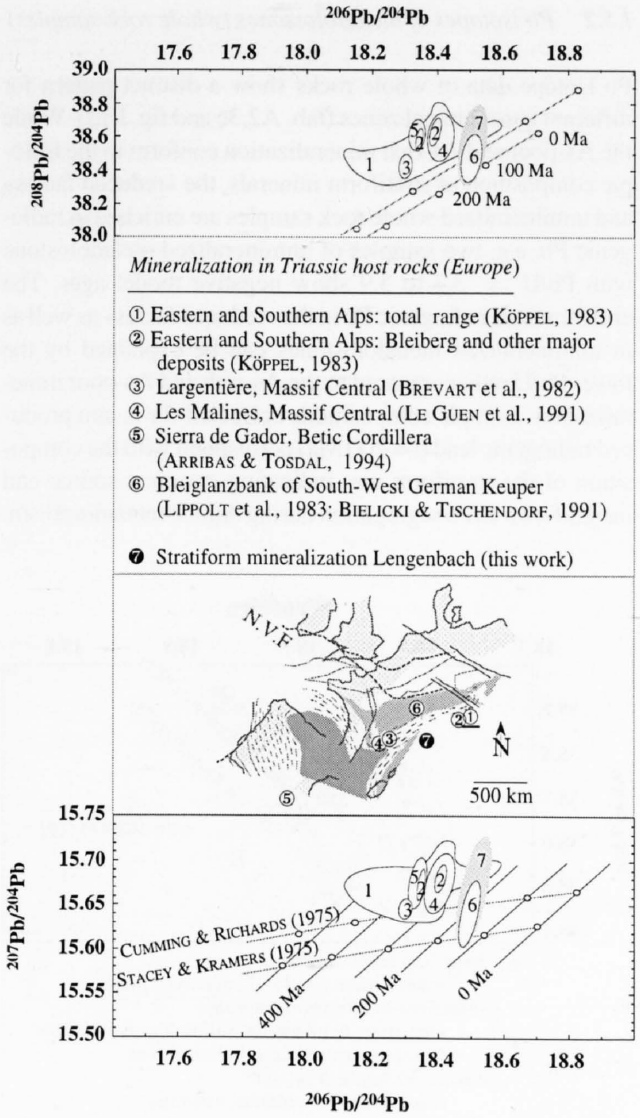

Figure I.11: Pb-Pb diagrams for mineralization of the Binn Valley in comparison to Pb-Zn deposits from various regions in Europe. The diagrams show the growth curves for average continental crustal Pb as defined by STACEY & KRAMERS (1975) with μ = 9.74 and W = 38.63 (μ and W are the $^{238}U/^{204}Pb$, respectively $^{232}Th/^{204}Pb$ ratios of the second evolution stage) and by CUMMING & RICHARDS (1975).

Mineralization from Bleiglanzbänke from southern Germany is characterized by model ages close to the age of the host rock (LIPPOLT et al., 1983; BIELICKI & TISCHENDORF, 1991).

I.5.2 Pb isotopes of metadolostones (whole rock samples)

Pb isotope data of whole rocks show a distinct pattern for different geochemical zones (tab. A2.3c and fig. I.12). While the As-poor and As-rich mineralization conform to the isotopic composition of stratiform minerals, the «reduced facies» and unmineralized whole rock samples are enriched in radiogenic Pb, e.g. two samples of unmineralized metadolostone with Pb/U = 3.3 to 3.9 show negative model ages. The enrichment in radiogenic Pb in the «reduced facies» as well as in unmineralized metadolostones can be explained by the lower Pb/U ratio compared to the As-rich and As-poor mineralization. Isotopic compositions corrected for in situ produced radiogenic lead (t = 200 Ma) correspond with the composition of the stratiform ore, indicating common source and insignificant U/Pb segregation during Alpine metamorphism.

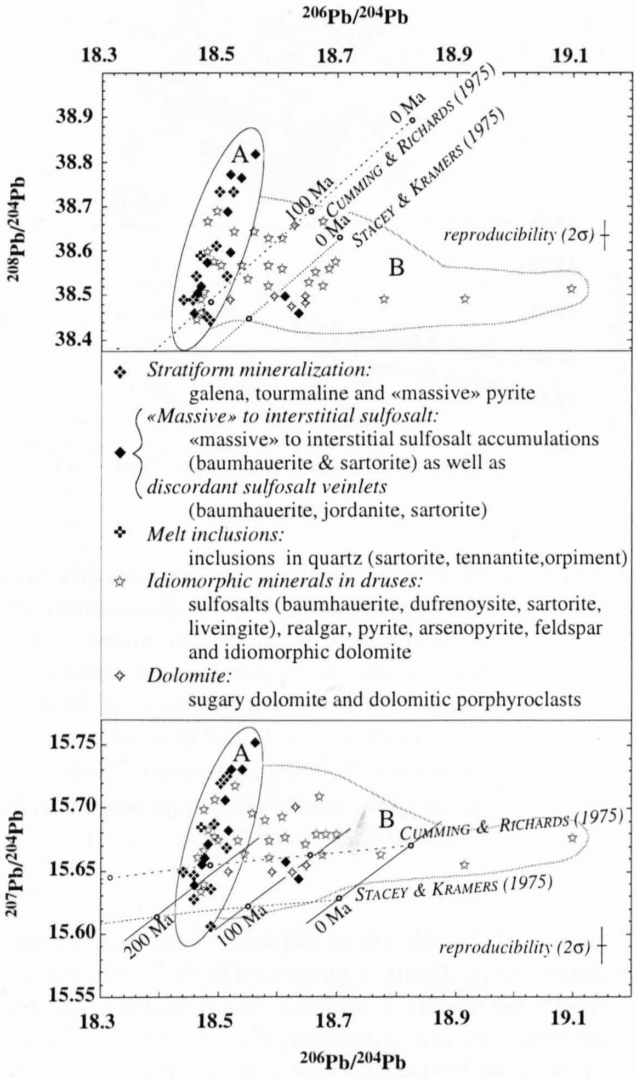

Figure I.13: Pb isotope diagrams for minerals of the Lengenbach deposit with growth curves for average crustal Pb according to STACEY & KRAMERS (1975) (μ = 9.74, W = 37.19 and isochrons) and according to CUMMING & RICHARDS (1975). Field A: Stratiform mineralization and massive sulfosalts; field B: minerals in druses, fissures and vugs and rock forming dolomite.

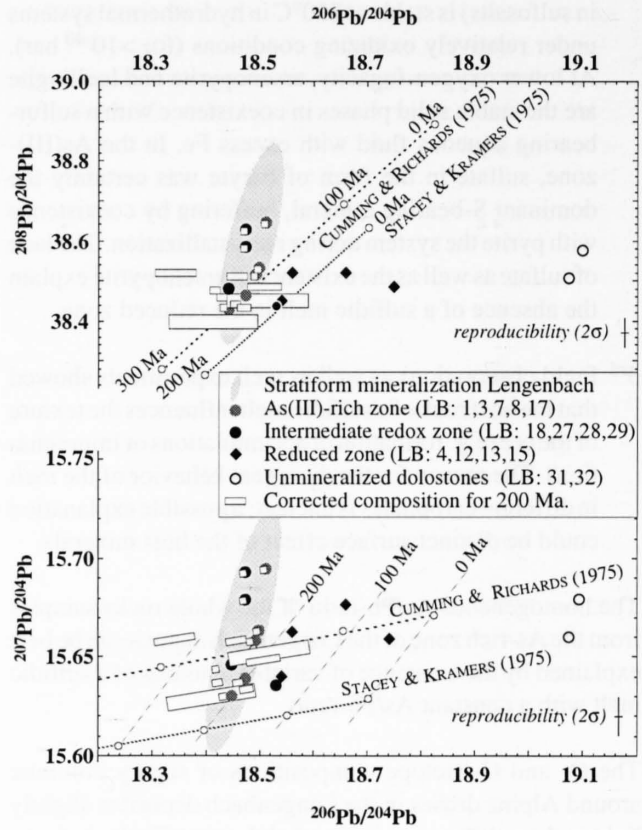

Figure I.12: Pb-isotope evolution diagrams for whole-rock samples of the Lengenbach deposit. The gray field defines the composition of the stratiform mineralization. The errors of the corrected compositions (rectangles) were calculated assuming an uncertainty at the given concentration levels of 4% for U and Th (INAA) and 8% for Pb (ICP-ES).

I.5.3 Pb isotope data of minerals

Massive to interstitial sulfosalts and discordant sulfosalt veinlets have a similar isotopic signature to the stratiform mineralization. Two samples of disseminated sulfosalts, which are in contact to the sugary dolomite, are enriched in radiogenic Pb. Melt inclusions of sulfosalts in quartz (sample B6281, tab. A2.5) have an isotopic composition corresponding to the stratiform mineralization.

Data from single minerals in druses define a field partly overlapping with data of stratiform galena, tourmaline and massive, banded pyrite (tab. A2.5 and fig. I.13). Many of the idiomorphic minerals in druses (sulfosalt, pyrite, arsenopyrite, realgar, feldspar) and all types of dolomite (sugary dolomite, dolomite porphyroclasts and idiomorphic dolomites in druses) are enriched in uranogenic, but not in thorogenic Pb (fig. I.13). Minerals in druses with an isotope signature similar to the stratiform mineralization are mainly associated with the Pb-rich mineralization. The most radiogenic minerals, with negative model ages, are idiomorphic dolomite crystals and stratiform pyrites of the reduced zone coexisting with magnetite ($^{206}Pb/^{204}Pb$: 19.3–22.3).

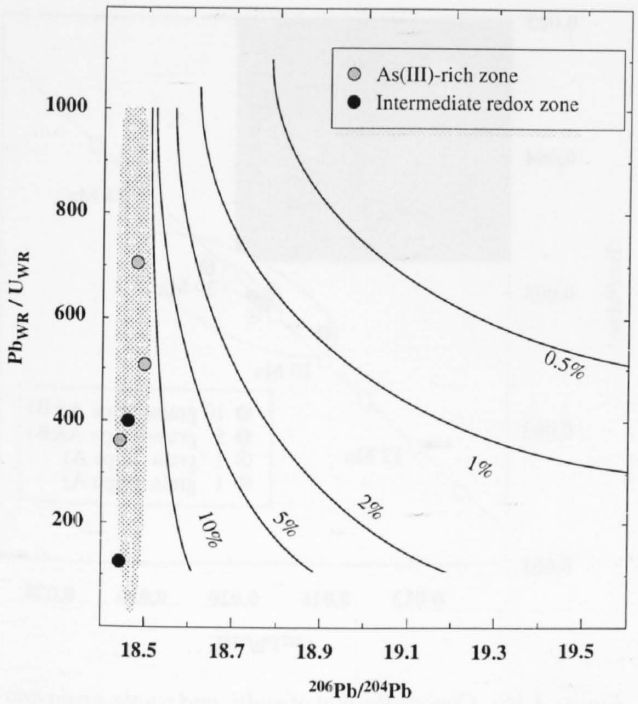

Figure I.14: Mixing model for common Pb ($^{206}Pb/^{204}Pb$ = 18.5) with radiogenic Pb that evolved in an U-bearing system since 180 Ma to produce the observed isotopic ratios.

Correction for in situ produced radiogenic Pb of all analyzed minerals reduces the $^{206}Pb/^{204}Pb$ by less than 1‰ because of the analytically determined low $^{238}U/^{204}Pb$ ratio (<<1) and the Alpine age (<20 Ma) of the minerals.

I.5.4 Discussion of Pb isotope data

Sulfosalt minerals from the Lengenbach deposit are characterized by a distinct variation of μ-values (e.g. stratiform minerals range from μ = 9.7 to 10.2, see tab. A2.5). This variation can best be explained by fractionation during the analytical procedure (section 6.1.4).

Pb isotope data of minerals from the Lengenbach deposit indicate a preferential enrichment of uranogenic Pb in Alpine druses. Possible source rocks of this uranogenic Pb would have had U/Th ratios >5, assuming no fractionation of uranogenic and thorogenic Pb occurred during the mobilization of Pb. Gneisses (U/Th = 0.1–0.7) as well as Bündnerschiefer (U/Th<0.3) can be ruled out as possible source rocks. On the other hand a potential source with high U/Th ratios are unmineralized Triassic dolostones (U/Th = 3.2–25, average 5). An input of radiogenic Pb from outside the dolostone during the formation of Alpine minerals in druses is therefore unlikely.

If the radiogenic and common Pb of the mineralized metadolostones had been homogenized during Alpine metamorphism, only an insignificant increase of the $^{206}Pb/^{204}Pb$ ratio would have resulted, because of the high Pb/U ratio (approx. 500) of the bulk rocks.

However, in the case of incomplete mixing, a significant increase of $^{206}Pb/^{204}Pb$ may be expected. Assuming an average mineralized whole rock with a primary Pb/U ratio of e.g. 400 is isotopically opened after 180 Ma and the released radiogenic Pb is mixed with 1% of the common Pb of the rock, the crystallized minerals would be enriched in $^{206}Pb/^{204}Pb$ by 2.4% (fig. I.14). I therefore postulate that mixing of Pb isotopes was incomplete due to limited exchange between coexisting sulfide melt and hydrothermal fluid. While the Pb-As-Tl-S-melt was the main reservoir for common Pb, radiogenic Pb was preferentially released from nonsulfide-associated U bearing phases to the hydrothermal fluid. The isotope data suggest limited fluid-melt exchange of about 1% which is in agreement with the estimated proportion of Pb-minerals in druses compared to the bulk Pb in the deposit.

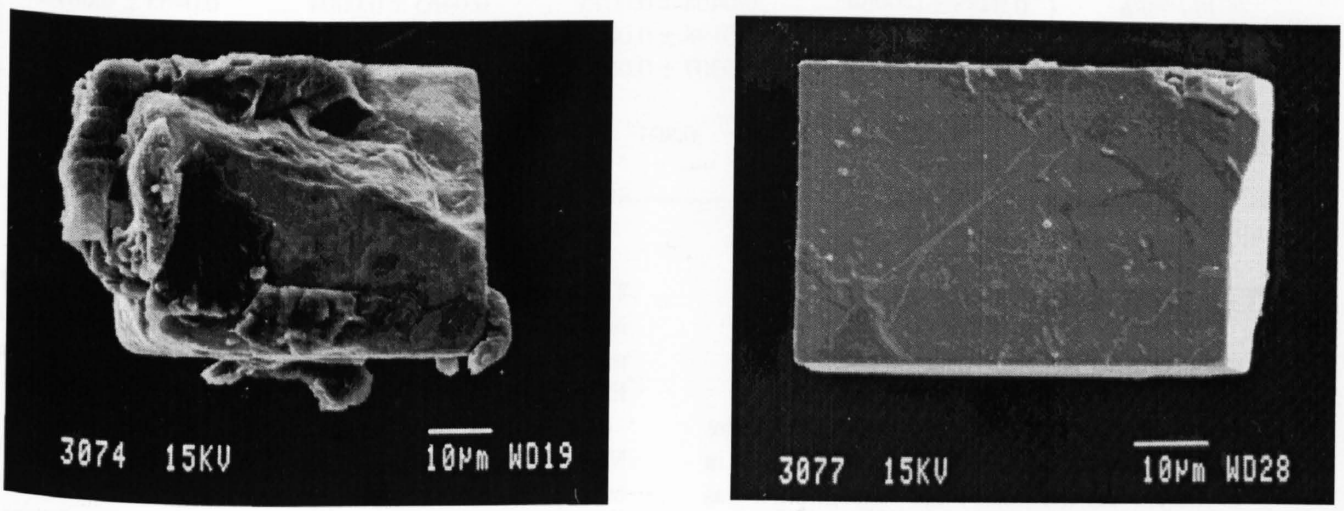

Figure I.15: SEM-picture of uraninite crystals from the Lengenbach deposit before and after ultrasonic treatment.

Table I.2: Microprobe analysis of Lengenbach uraninites (average of 70 spot analyses).

	wt%	at%
U	82.94	30.54
Th	3.64	1.37
Pb	0.26	0.11
Ca	0.08	0.18
Si	0.10	0.2:
Fe	0.50	0.92
Ti	0.03	0.05
As	0.27	0.32
O (calc.)	12.00	66.21
Total	100.01	100.00
Pb/U	0.0036 ± 8	
Th/U	0.045 ± 4	
U-Pb-Th-age (Ma)	25 ± 5	

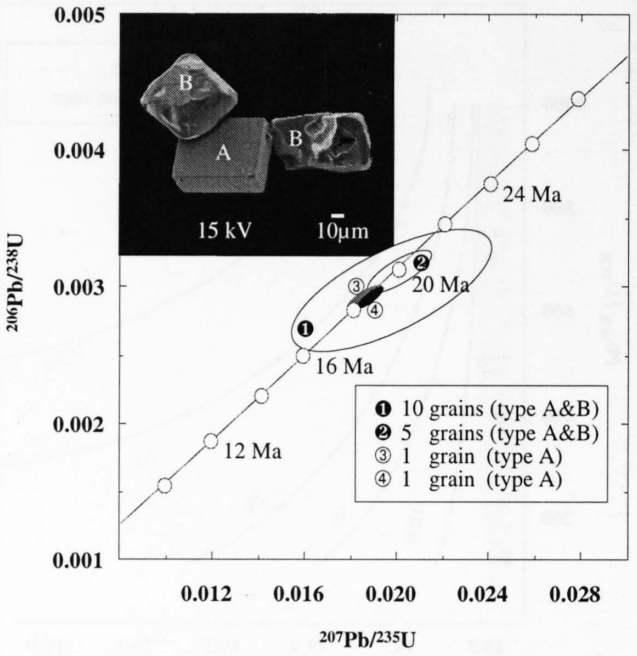

Figure I.16: Concordia-plot of multi- and single-grain analysis of uraninites from the Lengenbach deposit.

Table 2.3: U-Pb analytical data for uraninites of the Lengenbach deposit. The assumed common Pb composition is 18.43, 15.61 and 38.30 for $^{206}Pb/^{204}Pb$, $^{207}Pb/^{204}Pb$ and $^{207}Pb/^{204}Pb$ respectively. All within run statistical errors are given at a 2 sigma level.

sample	UO_2-0	UO_2-3	UO_2-1	UO_2-2 a
crystals (diameter)	10	5	1 (55µm)	1 (25µm)
type	A&B	A&B	A	A
multi grain	multi grain	single grain	single grain	
U (ng)	84940	10234	12828	1298
Pb (ng)	1576	41	35	4
% Pb c	85	33	2	23
$^{206}Pb/^{204}Pb$	30.065 ± 0.002	185.415 ± 0.099	2967.50 ± 22.3	266.05 ± 0.42
$^{207}Pb/^{204}Pb$	16.178 ± 0.001	23.438 ± 0.091	152.85 ± 16.18	27.070 ± 0.041
$^{208}Pb/^{204}Pb$	38.645 ± 0.002	41.354 ± 0.036	85.431 ± 0.666	41.205 ± 0.065
$^{207}Pb/^{206}Pb$	0.0485 ± 0.0064	0.0468 ± 0.0013	0.0465 ± 0.0004	0.0463 ± 0.0010
$^{207}Pb/^{235}U$	0.0195 ± 0.0035	0.0198 ± 0.0009	0.0186 ± 0.0003	0.0183 ± 0.0005
$^{206}Pb/^{238}U$	0.00291 ± 0.00037	0.00307 ± 0.00011	0.00290 ± 0.00005	0.00287 ± 0.00006
Correlation coefficient	0.666	0.801	0.914	0.689

I.6 U-Pb dating of uraninites

I.6.1 Samples and methods

Uraninite was extracted from 50 kg of the crushed bulk ore sample LB17 by heavy mineral separation (panning in water) of different size fractions. Final concentration was performed by hand picking from the most radioactive fraction.

The morphology of uraninite crystals and the nature of intergrown minerals were analyzed by SEM on a JSM-840 microscope at the Laboratory of Solid-state Physics of the ETH Zürich.

Microprobe analyses were performed with a Cameca SX-50 microprobe at the University of Bern. The instruments were operated at 15 kV, 20 nA, with a beam diameter of 1µm, using synthetic as well as natural standards.

Table I.4: Pb isotopic composition of minerals intergrown with uraninite from the Lengenbach deposit.

probe	B 3760 D2	B 3760 GL	B 3760 M2 L	B 7153 L
mineral	dolomite	biotite	magnetite (leach)	magnetite
$^{206}Pb/^{204}Pb$	18.631 ± 0.002	19.043 ± 0.028	18.591 ± 0.003	18.561 ± 0.009
$^{207}Pb/^{204}Pb$	15.702 ± 0.001	15.702 ± 0.023	15.722 ± 0.003	15.686 ± 0.007
$^{208}Pb/^{204}Pb$	38.658 ± 0.003	38.600 ± 0.058	38.725 ± 0.011	38.604 ± 0.018
Model-t	208	-98	277	226
μ	10.07	9.98	10.17	10.02
W	38.99	35.82	40.06	38.88
$k\ (= W/\mu)$	3.9	3.6	3.9	3.9

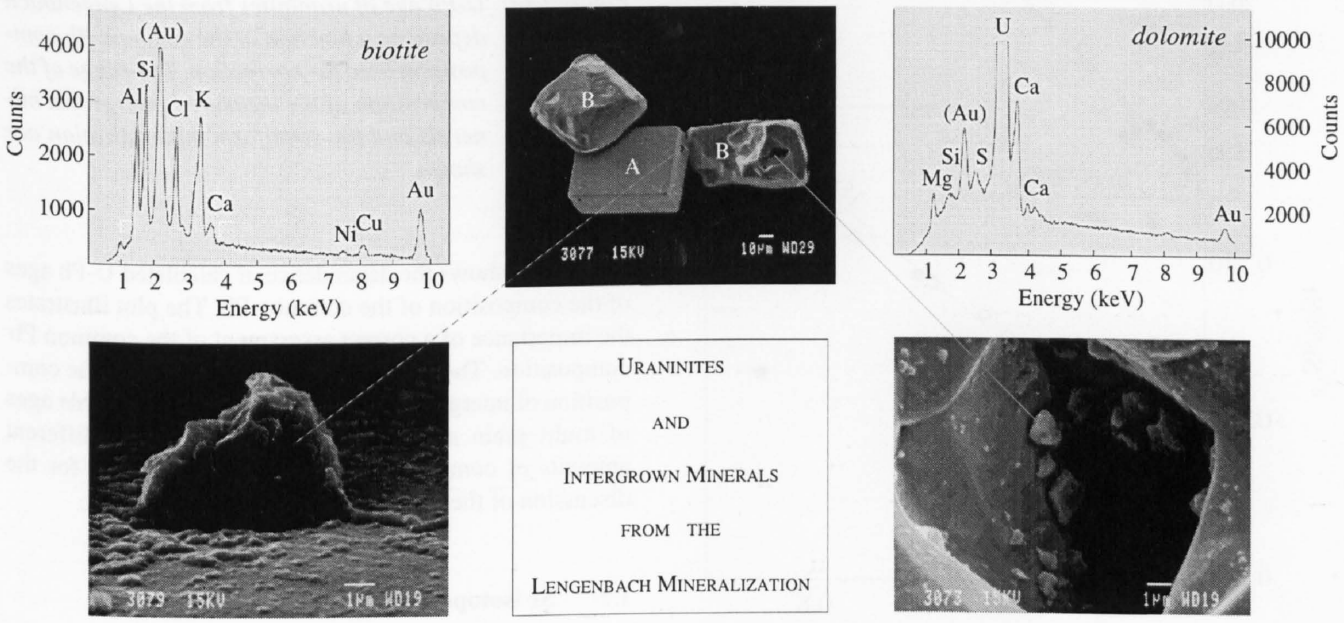

Figure I.17: Scanning electron microscopic picture of uraninites (two different morphologies A and B) and intergrown minerals from the Lengenbach deposit. Dolomite, biotite and minor magnetite could be identified by energy-spectrums.

The isotopic measurements of uraninite crystals were carried out on a Varian MAT Tandem mass spectrometer at ETH Zürich. The analytical procedure is described in detail by OBERLI et al. (1981).

I.6.2 Results

U-Pb dating of uraninite was carried out on two multi- and two single-grain samples. Electron microprobe analyses (tab. I.2) show that uraninite from the Lengenbach deposit is very pure, unoxidized $(U_{0.96}Th_{0.04})O_{2.00}$ and yields a chemical U(Th)-Pb age of 25 ± 5 Ma. Scanning electron microscopy revealed two different morphological types of uraninite (A and B). Type A uraninites are idiomorphic grains (cubes with small octahedron faces) whereas type B uraninite is idio- to xenomorphic and intergrown with dolomite, dark green biotite and minor magnetite. To reduce the common Pb contribution, single grain analyses were performed on two hand-picked, ultrasonically cleaned (fig. I.15) crystals of type A.

Data are presented in table I.3 and figure I.16. The most precise ages were obtained on single grains yielding U-Pb ages of 18.5 ± 0.5 Ma. The ^{207}Pb-^{206}Pb age of the uraninite single grain UO_2-1 is 25.4 ± 9 Ma (1 Sigma). Loss of radiogenic Pb appears unlikely in the view of the difference in size of the two crystals, and their identical age. The results agree with those of the multi-grain analyses which have, however, a larger uncertainty due to the high common Pb component.

I.6.3 The composition of common Pb of uraninites

The isotopic analyses of uraninite crystals yield significant amount of common Pb (2–85%). Two sources are responsible for the contamination of the radiogenic U-Pb-system with common ^{204}Pb:

1st common Pb derived from chemical treatment: the compositions and concentrations of blanks were measured to correct for this component. Total blank amounted 150 to 170 pg with following composition: $^{206}Pb/^{204}Pb$ = 18.57, $^{207}Pb/^{204}Pb$ = 15.76 and $^{208}Pb/^{204}Pb$ = 38.57.

2nd More significant amount of common Pb derived from intergrown minerals such as dolomite, biotite and magnetite (fig. I.17 and tab. I.4).

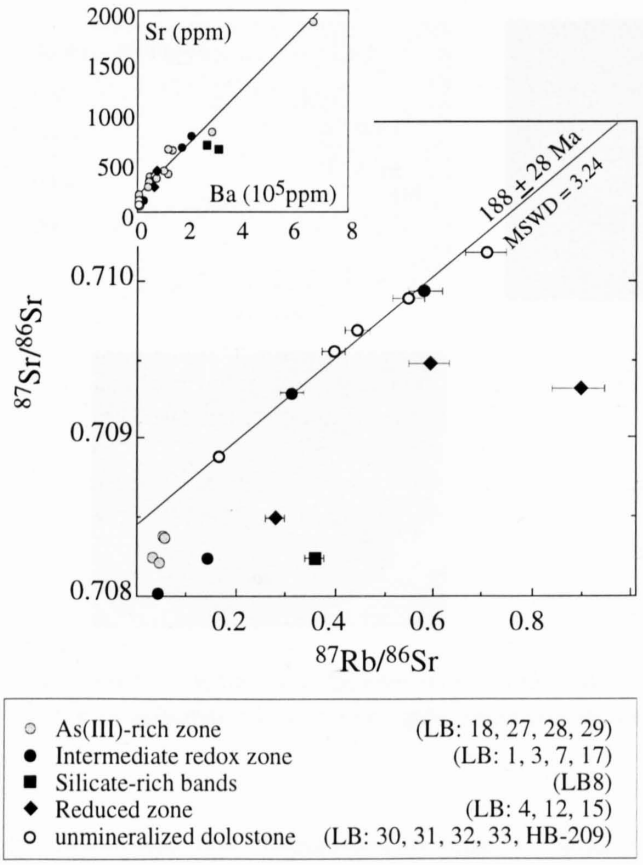

Figure I.19: Rb-Sr evolution diagram of whole rock samples (n = 17) and Ba-Sr correlation (n = 29) of the Lengenbach deposit. The isochron was calculated by the York-fit model with $l = 1.42 \cdot 10^{-11} a^{-1}$. The fit for the unmineralized metadolostones yields an age of 188 ± 28 Ma and initial $^{87}Sr/^{86}Sr$ = 0.70844 ± 4 with MSWD = 3.24 (mean standard weighted deviation). The errors of the $^{87}Sr/^{86}Sr$ were calculated assuming an uncertainity of 4% for Rb (ICP-ES) and 2% for Sr (XRF) at the given concentration level.

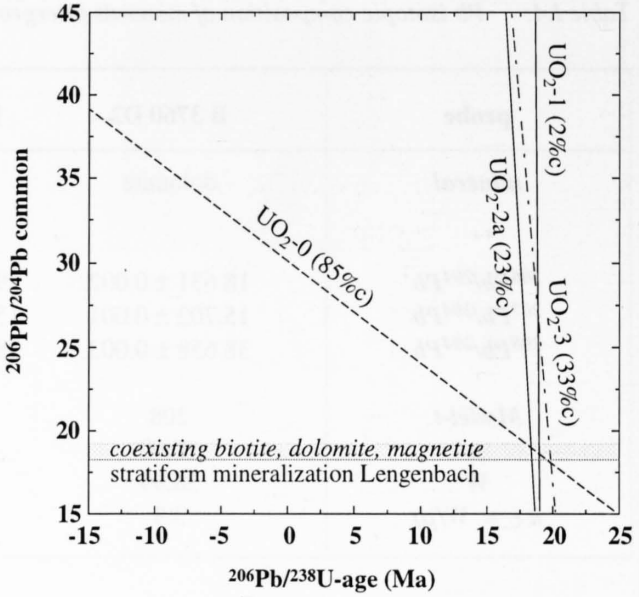

Figure I.18: U-Pb age of uraninites from the Lengenbach deposit as a function of the common Pb composition used for correction. The range of the composition of the measured intergrown minerals and the stratiform mineralization are shown.

Figure I.18 shows the dependence of calculated U-Pb ages of the composition of the common Pb. The plot illustrates the importance of a correct assessment of the common Pb composition. The correction of common Pb with the composition of intergrown minerals produces comparable ages of multi grain and single grain analyses with different amounts of common Pb. See also section I.10.3 for the discussion of the geochronological data.

I.7 Sr isotopes

I.7.1 Sr isotopes of metadolostones (whole rock samples)

Seventeen whole rock Sr isotopic analyses were performed on samples from different zones of the deposit (tab. A2.3c and fig. I.19). All samples are enriched in radiogenic Sr as compared to Triassic sea water composition ($^{87}Sr/^{86}Sr$ = 0.7070 to 0.7078, Koepnick et al., 1990). The lowest $^{87}Sr/^{86}Sr$ ratio (0.70801) was determined in a fuchsitic sample of the As-poor zone. A graphitic, unmineralized sample yielded the highest $^{87}Sr/^{86}Sr$ ratio (0.71018).

Unmineralized bulk rocks define an isochron of 188 ± 28 Ma. Its initial ratio (0.70844 ± 4) is slightly higher than the $^{87}Sr/^{86}Sr$ ratios of four samples from the As-rich mineralization ($^{87}Sr/^{86}Sr$ = 0.7083 ± 1). Samples of the «reduced facies» as well as one sample from the silicate rich zone differ in their isotopic composition from unmineralized or As(III)-rich samples. This can be explained by a loss of Sr in sulfate-poor zones during metamorphism. The anomalous Ba/Sr-ratio in silicate rich zones indicates a depletion

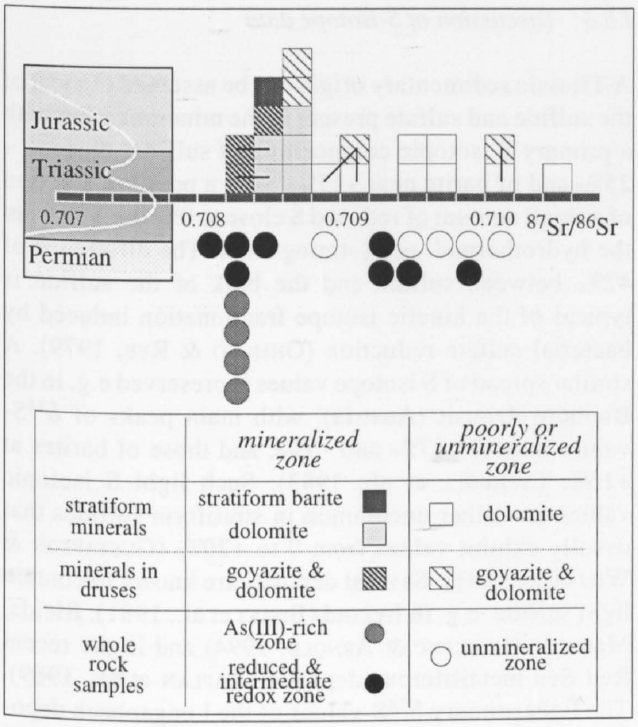

Figure I.20: $^{87}Sr/^{86}Sr$ composition of minerals and whole rocks of the Lengenbach deposit. The curve shows the seawater composition vs. time after KOEPNICK *et al. (1990). Lines indicate pairs of adjacent druse and host rock minerals.*

of Sr as a result of the metamorphic formation of Ba-silicates. The loss of Sr to a fluid phase may also explain the predominance of goyazite (Sr-Al-phosphate) over its Ba-analogue gorceixite in druses.

The contents of K (0.32 to 0.78%), Al (0.44 to 0.82%) and Rb (5–26 ppm) in positive correlation with radiogenic Sr indicates a detrital component and explains the relatively high $^{87}Rb/^{86}Sr$ of several unmineralized metadolostones from the Binn Valley.

I.7.2 Sr isotopes of mineral separates

Sr-isotope analyses were also performed on separated and handpicked, pure dolomites, goyazites (Sr-Al-phosphates) and barites (tab. A2.6 and fig. I.20). The data of mineral separates are compared with whole-rock analyses of mineralized and unmineralized samples from the Lengenbach deposit. Mineral separates as well as whole rock samples are enriched in radiogenic Sr compared to Triassic sea water ($^{87}Sr/^{86}Sr$ = 0.7070 to 0.7078, KOEPNICK et al., 1990).

Unmineralized, phlogopite-bearing, sugary dolomite separates yield the highest present-day $^{87}Sr/^{86}Sr$ ratios (0.7092–0.7102). The enrichment of radiogenic Sr in unmineralized, Sr-poor zones can be explained by the relatively high content of Rb in the dolomitic metasediments. Idiomorphic minerals (dolomites and goyazites) in Alpine druses show similar Sr isotope ratios as the adjacent sugary dolomite.

I.7.3 Discussion of Sr-isotope data

The slightly lower $^{87}Sr/^{86}Sr$ ratios of the As-rich mineralization compared to the initial composition of unmineralized metadolostones indicates that the amount of basement-derived Sr involved in the mineralizing process was insignificant. The most probable less-radiogenic Sr source was sea water or diagenetic Sr liberated from carbonates during dolomitization.

Whole rock samples, mineral concentrates and minerals in druses of the mineralized zone from the Lengenbach deposit have the lowest $^{87}Sr/^{86}Sr$ ratios (0.7083–7084). Considering the high present-day $^{87}Sr/^{86}Sr$ ratios of the gneisses, significant mass transfer from the basement to the Pb-Zn-mineralization of the Lengenbach during the Alpine metamorphism can be ruled out. Minerals in druses of the Lengenbach deposit match the isotopic composition of the host rock and indicate an almost closed system for Sr during late stage metamorphism. This makes a major transfer of As, Tl and Cu from the gneisses during retrograde Alpine metamorphism, as suggested by GRAESER (1965) very unlikely.

I.8 S isotopes

I.8.1 Analytical methods

Pure mineral fractions for all isotopic analyses were obtained by selection of optically pure crystals from hand specimens or hand-picking from heavy mineral concentrates.

S isotopes were measured at Göttingen University using standard methods (SO_2 gas) explained elsewhere (RICKE 1964).

I.8.2 Results

The results of S isotopic analyses on 60 samples are presented in table A2.7 and figure I.21. Compared with the total spread of $\delta^{34}S$ from –21.8 to –7.1‰ (total variation 14.7‰) observed by HOEFS & GRAESER (1968), the variation observed in this study is much larger with values ranging from –25.7 to +12.4‰ (total variation 38.1‰). Massive stratiform pyrite layers have consistently low $\delta^{34}S$ values ranging from –18.5 to –24.5‰ (tab. A2.7). Stratiform sphalerite isolated from other sulfides has similar low values (–20 to –24‰). Within the stratiform mineralization, no zoning of $\delta^{34}S$ values is discernible. Zones showing different redox states of S and As are characterized by significantly different S isotope values of S minerals in druses and fissures, however.

All minerals in the As(III)-rich zone are ^{34}S depleted, (stratiform pyrite –21.9 ± 2.2‰, sulfosalts –19.7 ± 1.2‰, stratiform barite –7.6 ± 1.5). The difference in $\delta^{34}S$ between coexisting barite and pyrite of 11.4 to 13.9‰ is indicative of equilibrium at temperatures of 420 to 500°C, calculated according to OHMOTO & LASAGA (1982). The lowest $\delta^{34}S$ -

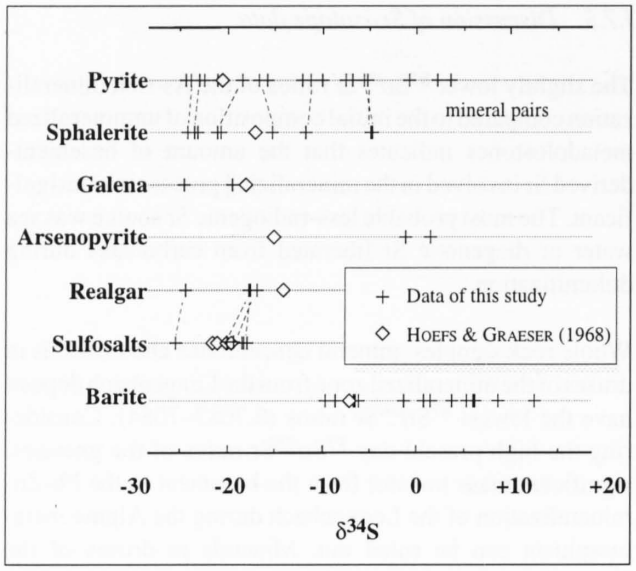

Figure I.21: Range of S isotope values in different minerals from the Lengenbach deposit. Coexisting mineral pairs are linked.

value (–25.7‰) was measured on samples from discordant fissures with realgar and sartorite. The average $\delta^{34}S$ of all sulfide samples from the As-rich zone is –16.1‰ that of As(III)-rich minerals –19.7‰.

In the intermediate redox zone, sulfides in druses show a large variation in $\delta^{34}S$ from –7 to –24.7‰. $\delta^{34}S$ of massive barite ranges from +0.7 to +5.3‰ which is lighter than barite in druses (5.9 to +12.4‰). A mineral pair consisting of a small pyrite cube ($\delta^{34}S$ = –10.0‰) in massive barite ($\delta^{34}S$ = +5.3‰) shows a difference in $\delta^{34}S$ of 15.3‰, indicative of an equilibrium fractionation temperature of 390°C.

In the reduced zone, the isotopic composition of S is throughout heavy, averaging –1.8‰ (range –5.5 to +3.4‰), indicative of thermochemical sulfate reduction or externally derived sulfide.

Pairs of cogenetic sulfides and sulfosalts show very similar $\delta^{34}S$ -values close to isotopic equilibrium at 400–500 °C. The often significant deviations are interpreted to indicate variable post-equilibration isotope exchange in one or both phases of the pair due to interaction with hydrothermal fluids. Evidence of local isotopic equilibrium strongly contrasts with the heterogeneity of the S isotope data at the deposit scale, indicating that isotopic equilibration only occurred on scales of cm to dm.

There is no systematic correlation between As-concentrations and $\delta^{34}S$ values, i.e. galena from As-poor zones and realgar from the As(III)-rich zone show similar S isotope values.

I.8.3 Discussion of S-isotope data

A Triassic sedimentary origin can be assumed of most of the sulfide and sulfate present in the mineralization with a primary S isotopic composition of sulfides close to –25‰ and of barite near +17‰, with a possible addition of a small amount of reduced S close to 0‰ derived from the hydrothermal, ore forming fluid. The difference of 42‰ between sulfate and the bulk of the sulfide is typical of the kinetic isotope fractionation induced by bacterial sulfate reduction (Ohmoto & Rye, 1979). A similar spread of S isotope values is preserved e.g. in the Bleiberg deposit (Austria), with main peaks of $\delta^{34}S$-values around –27‰ and –7‰, and those of barites at +15‰ (Schroll et al., 1983). Such light S isotopic values are rather uncommon in stratiform sulfides that usually exhibit values from 0 to +20‰ (Gustafson & Williams, 1981). Several deposits are known to contain light sulfide, e.g. in Ireland (Boast et al., 1981), Bleïda, Marocco (Leblanc & Arnold, 1994) and in the recent Red Sea metalliferous deposits (Kaplan et al., 1969). The light primary $\delta^{34}S$-values of the Lengenbach deposit indicates that the sulfide concentration in the metal transporting fluid was low and did not contribute significantly to the deposition of sulfides.

The S isotope variations within the mineralization exhibit characteristics that can best be interpreted by assuming the deposition of primary (sedimentary) sulfides and barite followed by closed system metamorphism:

- Stratiform sulfides have low $\delta^{34}S$-values, the least overprinted samples probably indicating a primary sedimentary value of –24 to –25‰.

- Massive barite has isotopically equilibrated with coexisting pyrite at temperatures of 390 to 500°C. High modal pyrite/barite ratios resulted in large shift of $\delta^{34}S$ of barite from probable primary Triassic values near +17 to +21‰ (Muschelkalk values, Pearson et al., 1991) to pyrite-buffered metamorphic values of –6 to –10‰. Due to its high abundance, pyrite suffered only a minor isotopic shift from –25 to –22 ± 2‰.

- As-rich minerals (massive, in discordant fissures and in druses) are isotopically light and similar to stratiform sulfides.

- Druse minerals exhibit large variations indicating sulfide-sulfate-interactions at variable ratios and temperatures.

- Late druse barite is isotopically heavier than massive barite by up to 20‰, indicating a late introduction of heavy sulfate into the system. This event may be correlated with incursion of a later metamorphic fluid, low in CO_2 (Hügi, 1988).

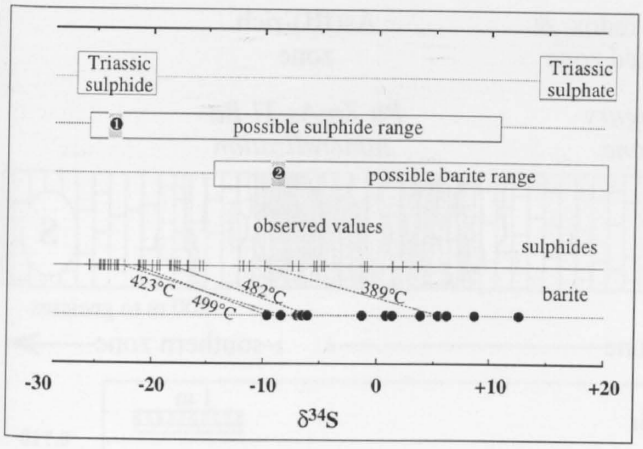

Figure I.22: Diagram showing the possible ranges of S isotopic compositions in sulfides and barite assuming closed system metamorphic equilibration at 500° C of pre-metamorphic pyrite ($\delta^{34}S$ close to -25‰) and of barite ($\delta^{34}S$ +19±2‰). 1 and 2 are the bulk $\delta^{34}S$ values calculated for the As(III)-rich zone based on average composition and equilibration at 400°C.

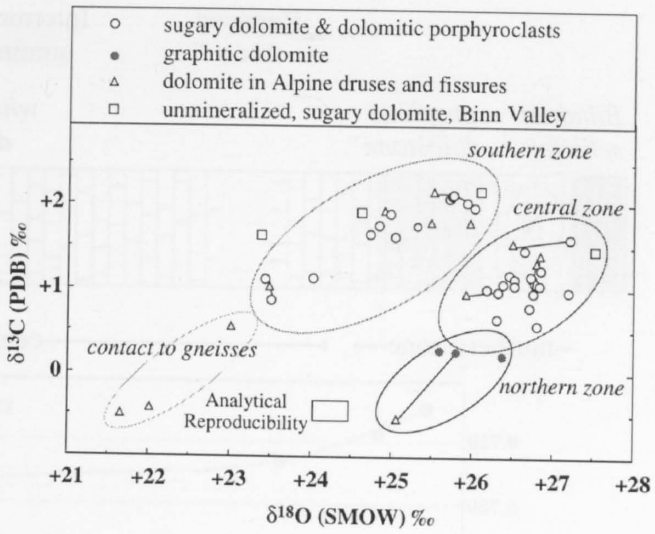

Figure I.23: Plot of $\delta^{13}C$ vs. $\delta^{18}O$ values of dolomite separates from the Lengenbach deposit and unmineralized metadolostones from the Binn Valley. The zones refer to the quarry in summer 1991. Lines indicate pairs of druse and host rock minerals.

During metamorphism at 500°C, sulfide-sulfate equilibrium fractionation would be about 12‰, which resulted on re-equilibration of $\delta^{34}S$ to between –25.0 to +5.6 in sulfides and $\delta^{34}S$ of –13.6 to +17.0 in barites depending on initial sulfide/sulfate ratios. Thermochemical sulfate reduction induced by graphite is another possible source of isotopically heavy sulfide. The observed values fall well within the range possible by either of these processes.

The primary sulfide/barite ratio can be estimated from bulk concentrations of Fe, Pb, Zn and Ba. It is then possible to obtain a mass balance for S isotopes. Mass balance assuming closed system metamorphism indicates that prior to metamorphism, 84% of S in the As(III)-rich zone is bound to pyrite, 6.7% to As, 3.4% to Pb, 0.9% to Zn and 4.6% to barite. Due to the high sulfide/sulfate ratio, metamorphic re-equilibration affected the isotopic composition of sulfate much more than that of sulfide. The evolution of S isotopic composition during metamorphism of the Lengenbach deposit is schematically represented in figure I.22.

I.9 O and C isotopes

I.9.1 Samples and methods

Samples from the Lengenbach quarry and other localities from the Binn Valley were used for analyses (tab. A2.8). Pure (sulfide and graphite-free), handpicked dolomite was analyzed to exclude the influence of organic matter during dissolution (CHAREF & SHEPPARD, 1984). CO_2 was extracted from dolomites by 100% phosphoric acid treatment at 25°C (reaction time: 3 days) at the Geological Institute, ETH Zürich. Correction factors are from FRIEDMAN & O'NEIL (1977). The CO_2 released from these extraction lines was analyzed on a VG micromass 903 triple-collector mass spectrometer. Analytical reproducibility was better than ±0.2‰ for O and C isotope ratios.

I.9.2 O and C isotope variations of dolomite separates

The $\delta^{18}O$ and $\delta^{13}C$ values of all types of dolomite separates from the Lengenbach deposit range from $\delta^{18}O$ (SMOW) = +21.5 to +27.5‰ and $\delta^{13}C$ (PDB) = –0.5 to +2.2‰ (tab. A2.8 and fig. I.23). The values of unmineralized dolomites from various localities of the Binn Valley show a similar spread as the dolomite samples from the Lengenbach quarry. Graphitic dolomite has the lowest $\delta^{13}C$ ratios of all rock-forming dolomites, indicating metamorphic graphite-dolomite equilibration in these samples ($\delta^{13}C$ (PDB) of graphite = –13.2; GRAESER, 1968). The $\delta^{18}O$ and $\delta^{13}C$ values of rock-forming, sugary dolomite separates are similar to those of unmetamorphosed Triassic marine dolostones (fig. I.25).

A profile through the Lengenbach quarry shows the variation of the isotopic composition of sugary dolomite separates (fig. I.24). The correlation of $\delta^{13}C$ values with the stratigraphic position can be explained by a primary variation caused by variable biogenic activity.

Alpine dolomites in druses of the Lengenbach deposit (appr. 200 m above the gneiss contact) reflect the isotopic composition of the adjacent sugary dolomite. Only Alpine dolomite crystals in druses close (<1m) to the contact with basement gneisses document a lowering of the isotopic ratios by interaction with an «external», metamorphic fluid (fig. I.23).

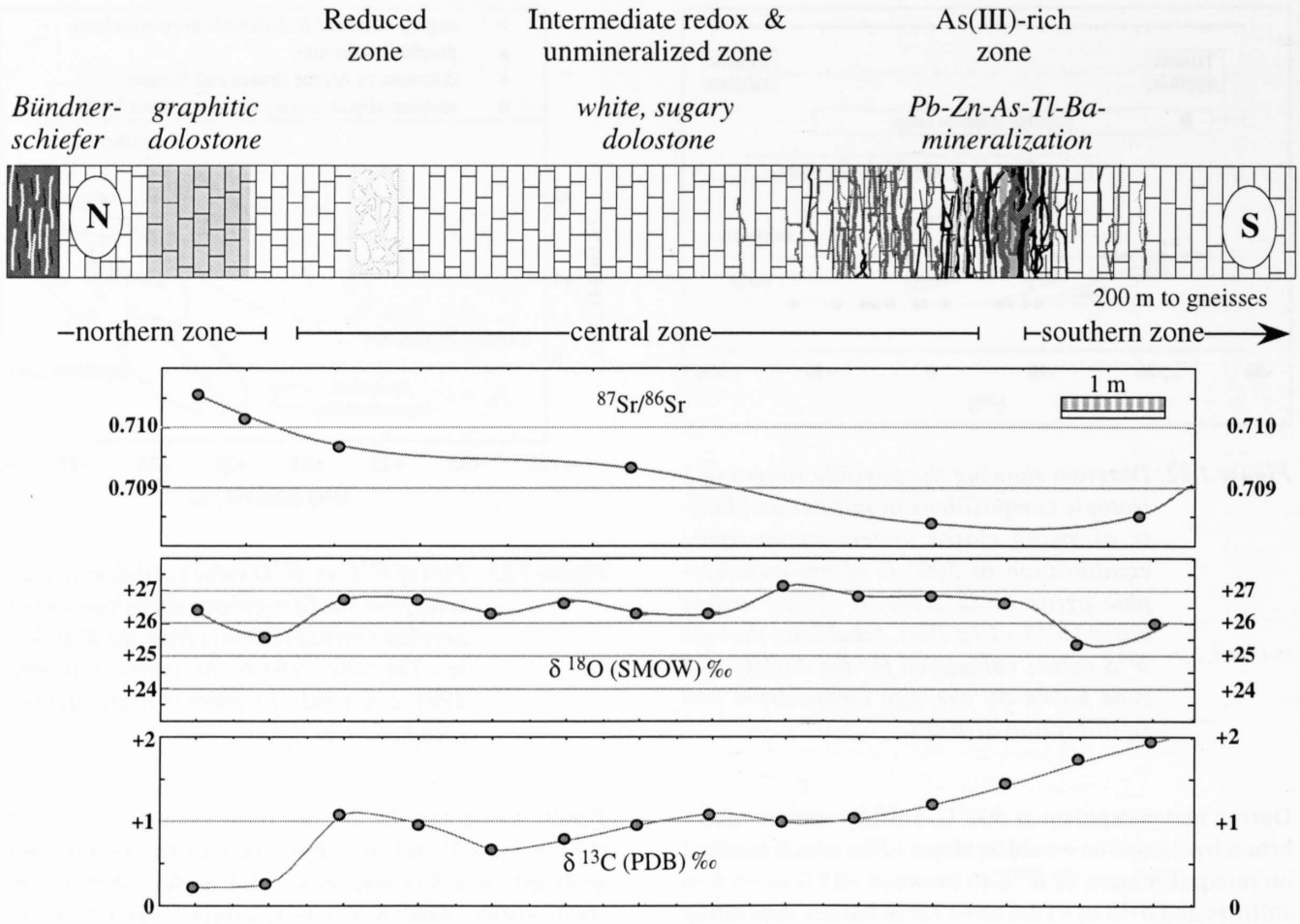

Figure I.24: Sr, O and C- isotopic composition of sugary dolomite separates along a profile in the quarry. The sampling was performed at the Lengenbach deposit in summer 1991.

I.9.3 O-C variation of dolomite adjacent to sulfosalt accumulations and Alpine druses

O and C isotopes were measured of dolomites (sugary dolomite, dolomite porphyroclasts and dolomites in Alpine druses) close (<5 cm) to massive sulfosalt accumulations as well as along a profile into a Alpine druse with coexisting idiomorphic sulfosalt and dolomite crystals. Plate I.2 illustrates different isotopic signatures of dolomite adjacent to massive sulfosalt and dolomite adjacent to vugs: The average isotopic compositions of the samples from the distinct localities are significantly different and probably reflect primary variations of the sediments (section I.9.2). The main difference of the two samples lies in the homogeneity of the isotopic composition in a sample: measurements of sugary dolomite and a dolomite porphyroclast close to massive and interstitial sulfosalt accumulations yield a homogeneous isotopic composition, whereas the sugary dolomite around an Alpine druse varies significantly. Idiomorphic dolomite crystals coexisting with idiomorphic baumhauerite in Alpine druses as well as sugary dolomite around vugs tend to slightly lighter isotopic compositions.

I.9.4 Discussion of O- and C-isotope data

The $\delta^{18}O$ and $\delta^{13}C$ values of sugary dolomite, dolomite porphyroclasts as well as idiomorphic dolomites in druses from the Lengenbach deposit are similar to those of unmetamorphosed, Triassic marine dolostones. In contrast to the Binn Valley, metacarbonates of the Simplon-area (15 km east of the Lengenbach) are significantly depleted in heavy O- and C-isotopes (fig. I.25). The trend suggests exchange during interaction of unmetamorphosed, marine limestone with metamorphic, gneiss-derived fluid in this area. The isotopic composition of this metamorphic fluid was calculated on the basis of data from fluid inclusions ($\delta^{13}C$ of CO_2) and fissure-quartz ($\delta^{18}O$ for T = 150 to 400°C) of the Monte Leone gneisses (Hoefs & Stalder, 1977). The isotope trend of metadolostones from the Central Alps may be attributed to continuous isotopic exchange reactions between the metamorphic fluid evolving from basement gneisses and carbonates at different fluid-rock ratios (F/R, atomic%) and temperatures. The isotopic composition of the hydrothermally altered rock was calculated according to the equation of Fu et al. (1991). Metacarbonates (F/R<2) as well as calcites and dolomites in fissures in basement-gneisses (F/R>1) of the Simplon-area indicate the influence of a

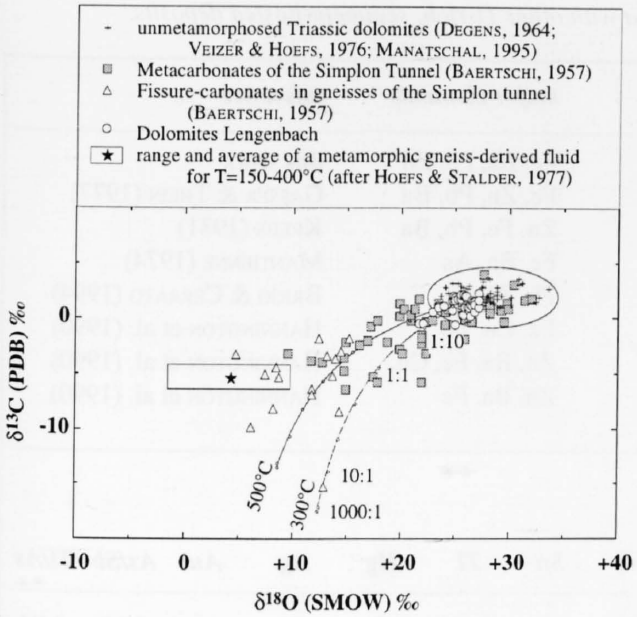

Figure I.25: Plot of $\delta^{13}C$ vs. $\delta^{18}O$ values of dolomite separates from the Lengenbach deposit in comparison to unmetamorphosed Triassic metadolostones, metacarbonates and carbonates in Alpine fissures. Curves represent a lowering of $\delta^{13}C$ and $\delta^{18}O$ values resulting from the interaction of an unmetamorphosed metadolostone ($\delta^{13}C$ = +1.9‰, $\delta^{18}O$ = +28.0‰) and a metamorphic, gneiss-derived fluid ($\delta^{13}C$ = -6.0‰, $\delta^{18}O$ = +3.9‰, X_{CO_2} = 0.1) at 300°C and 500°C. The marks of the curves denote increments of increasing fluid-rock-ratios (atomic percent). The calculations are based on equilibrium C and O isotope fractionation data of equations by O'NEIL et al. (1969) and BOTTINGA (1968).

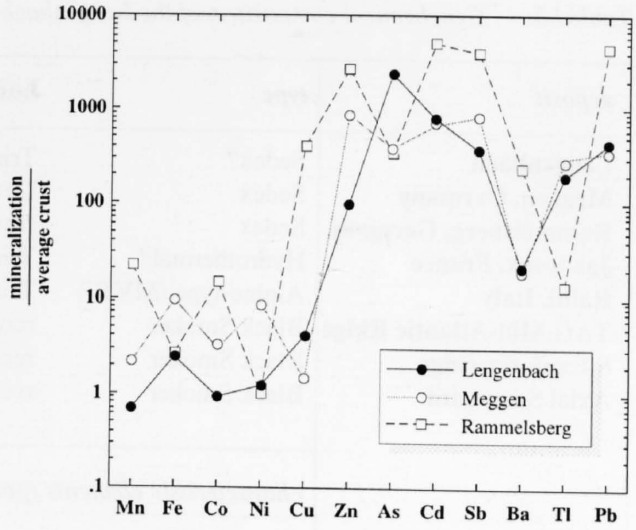

Figure I.26: Geochemical patterns of the Lengenbach deposit in comparison to Meggen (GASSER, 1974) and Rammelsberg (HANNAK, 1981). The data are based on an average composition of the mineralization and normalized to an average crustal composition (TAYLOR & MCLENNAN, 1985).

metamorphic fluid. However, all dolomites of the Lengenbach deposit (F/R<0.1) still retain a diagenetic signature of marine limestone. The similar isotopic composition of rock-forming, sugary dolomite and idiomorphic dolomite crystals in fissures from the Lengenbach deposit indicate the equilibration of the late Alpine fluid with the dolomitic host rock under rock-dominated conditions.

I.10 Discussion and conclusion of part I

I.10.1 Element inventory of the Lengenbach deposit compared with other ore deposits

Although the mineralogy of the Lengenbach deposit is unique, the geochemistry shows many similarities with other types of ore deposits. The association of Pb-As-Tl-Cu-Hg-Sb-Ba is typical of hydrothermal fluids derived from evolved continental crust and is found in Kuroko-type and sediment-hosted massive sulfides, in epithermal systems and high-temperature fluids such as the Salton Sea and Cheleken geothermal systems (WHITE, 1981). In magmatism-related hydrothermal systems covering a large range of temperatures with comparatively low thermal gradients, the base metals Cu, Zn and Pb are often separated from Tl, Hg, Au, Sb and As by sequential precipitation from the fluid. The association of Pb, Cu and Zn with Tl and Hg can be the result of very high thermal gradients such as realized by the discharge of hydrothermal fluids on the sea floor, or the association of low-temperature Tl, Hg-rich Fe-sulfides with base metals. Not surprisingly, all types of massive sulfide deposits are enriched in Tl, although to variable extents.

The Meggen sediment hosted massive sulfide deposit in Germany (GASSER, 1974; GASSER & THEIN, 1977) demonstrates well, that high Pb and Tl concentrations can be present in pyrite-rich, unmetamorphosed stratiform deposits (tab. I.5 and fig. I.26). Many Alpine type Pb-Zn-occurrences are characterized by elevated concentrations of As and Tl (e.g. SCHROLL, 1983; BRIGO & CERRATO, 1994). Both Wiesloch, Germany (SEELIGER, 1963) and the Silesian Pb-Zn-deposits of the MVT type are As, Tl-rich but typically lack Cu. The Tl-rich mineralization of Jas Roux, French Alps (MANTIENNE, 1974) is mineralogically similar to the Lengenbach deposit but almost completely lacks Pb.

The Hemlo gold deposit in Ontario shows some similarities with the Lengenbach deposit (HARRIS, 1989): anomalous Mo, V, As, Sb, Hg, Tl and Ba and the occurrence of some rare minerals typical of the Binn Valley (baumhauerite, seligmannite, dufrenoysite, cafarsite). In contrast to the Lengenbach deposit, the Hemlo deposit is however an Au-rich deposit with low concentrations of Pb, Zn and Cu.

Table I.5: Geochemical comparison of the Lengenbach deposit with other Tl-rich, sediment-hosted deposits.

deposit	*type*	*host age*	*major elements*	*reference*
Lengenbach	Sedex?	Triassic	Fe, Ba, Pb, Zn	this work
Meggen, Germany	Sedex	Devonian	Fe, Zn, Pb, Ba	GASSER & THEIN (1977)
Rammelsberg, Germany	Sedex	Devonian	Zn, Fe, Pb, Ba	KREBS (1981)
Jas Roux, France	Hydrothermal?	Triassic	Fe, Ba, As	MANTIENNE (1974)
Raibl, Italy	Alpine-type (MVT?)	Triassic	Pb, Zn, Fe	BRIGO & CERRATO (1994)
TAG,Mid-Atlantic Ridge	Black Smoker	recent	Fe, Cu, Zn	HANNINGTON et al. (1990)
S Explorer ridge	Black Smoker	recent	Zn, Ba, Fe, Cu	HANNINGTON et al. (1990)
Axial Seamount	Black Smoker	recent	Zn, Ba, Fe	HANNINGTON et al. (1990)

	characteristic elements (ppm)											
	Pb	*Cu*	*Cd*	*As*	*Sb*	*Sn*	*Tl*	*Hg*	*Ag*	*Au*	*As/Sb*	*Tl/As*
Lengenbach	8300	102	70	3600	95	7	140	2	78	tr.	37.9	0.04
Meggen, Germany	7000	35	66	574	163	60	227	n.d.	3	tr.	3.5	0.40
Rammelsberg, Germany	90000	10000	500	500	800	50	10	40	160	1.2	0.6	0.02
Jas Roux, France	255	8	n.d.	1140	408	n.d.	136	n.d.	9	n.d.	2.8	0.12
Raibl, Italy	50000	n.d.	800	800	n.d.	80	600	n.d.	n.d.	n.d.	10.0	0.75
TAG,Mid-Atlantic Ridge	500	92000	300	73	17	2	27	16	72	2.1	4.3	0.37
S Explorer ridge	1100	32000	200	544	27	10	43	11	97	0.6	20.1	0.08
Axial Seamount	3500	4000	522	570	350	7	100	20	190	4.9	1.6	0.18

In summary, the closest geochemical affinity exists with sediment-hosted, exhalative massive sulfide deposits that typically exhibit high Ag and low Au concentrations. The absence of a Mn anomaly is atypical of exhalative deposits and poses an unexplained problem. The Lengenbach deposit is unusual in its predominance of As expressed by very high As/Sb ratios (tab. I.5).

Recent metalliferous exhalites are known from a variety of geological settings and show some general similarities with the Lengenbach deposit such as elevated concentrations of Tl, As, Mo, Ag, Hg and Cd (HANNINGTON et al., 1990). Of particular interest are the Fe-rich metalliferous sediments of the Red Sea, which show U-enrichments (up to 31 ppm) similar to the magnetite-rich samples from the Lengenbach deposit (6–15 ppm U), possibly due to adsorption from sea water (KU, 1969). U-enriched metalliferous sediments are also known from the mid-Atlantic ridge (MILLS et al. 1994). An interpretation of the Lengenbach magnetite as formed originally as iron hydroxide sediment is also consistent with the observed elevated Cs contents, an element readily sorbed onto Fe-hydroxides. Alternatively, the magnetite-pyrrhotite assemblage can also be interpreted as a relict of reactions between hydrothermal fluids and metadolostone wall rocks. The enrichment of redox-sensitive elements may then be due to reactions between oxidizing porewaters and carbonates. The occurrence of isotopically relatively heavy sulfide in such a S-deficient paragenesis might indicate a strong influence of a relatively S-poor hydrothermal fluid.

Positive Eu anomalies are indicative of plagioclase alteration in the source area of the fluids, as is the case in oceanic hydrothermal alteration (CAMPBELL et al., 1988; HERZIG et al., 1991; COCHERIE et al., 1994; MITRA et al., 1994). Evidence of Eu depletion in hydrothermal alteration zones in the gneissic basement of the Monte Leone nappe, that may be related to the Lengenbach mineralizing event is presented in part II of this work.

Table I.6: Inferred primary modal composition of the Lengenbach deposit.

element	**wt%**	**modal composition**	**host mineral**
Fe	9.83	*21.10*	*pyrite*
As	0.36		1.7% As in pyrite
Tl	0.014		0.07% Tl in pyrite
Zn	0.78	*1.16*	*sphalerite*
Cd	0.007		0.6% Cd in sphalerite (+Ag)
Pb	0.83	*0.96*	*galena*
Ag	0.008		0.8% Ag in galena (+Tl)
Cu	0.01	*0.03*	*chalcopyrite*
Ba	1.14	*1.94*	*baryte*
Sr	0.03		1.55% Sr in barite

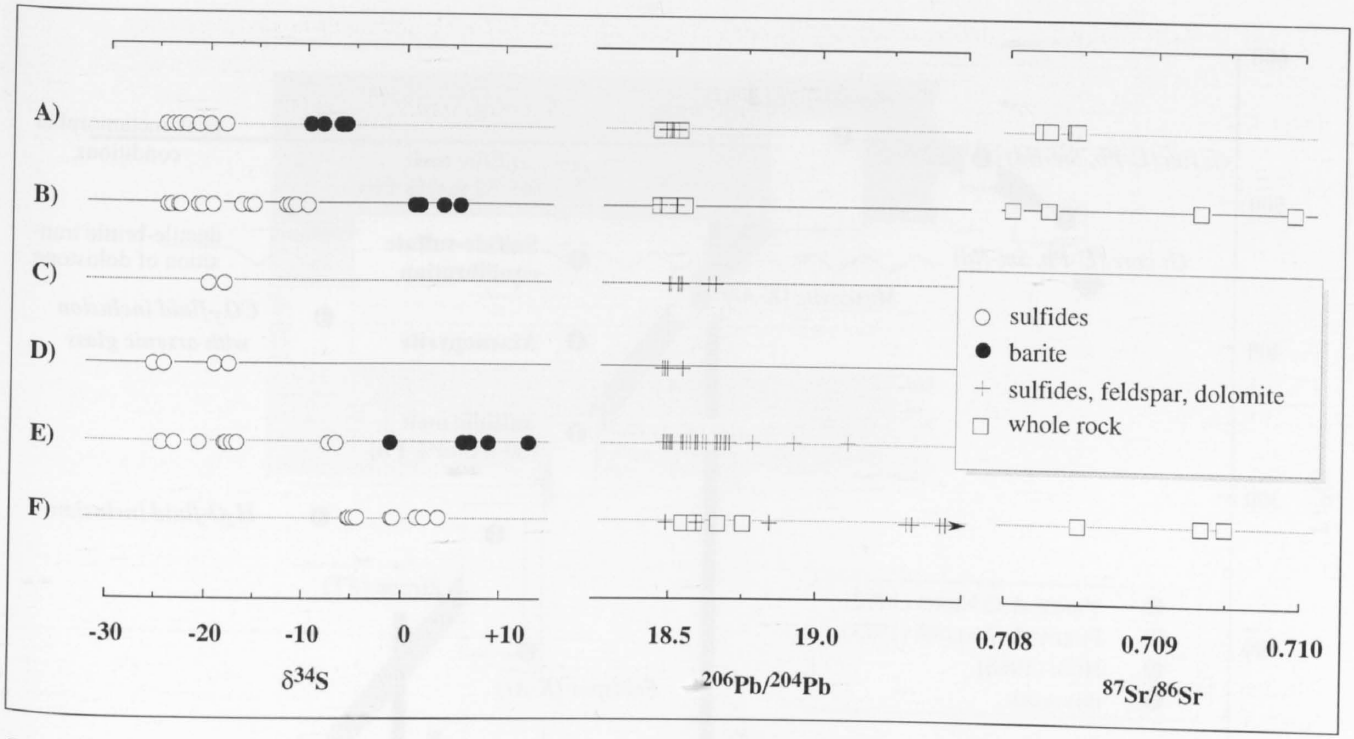

Figure I.27: Overview of isotopic data from the Lengenbach deposit:
A) Stratiform mineralization (As-rich), B) Stratiform mineralization (As-poor), C) Massive to interstitial sulfosalts, D) Discordant sulfosalt veinlets, E) Idiomorphic druse minerals, F) Reduced zone: low fo_2 mineral assemblage.

High Tl and As concentrations of some Pb-Zn deposits of the Eastern Alps (Bleiberg, Raibl) are related to Tl-bearing jordanite inclusions in dolomite and sphalerite (Brigo & Cerrato, 1994). In the model of closed system metamorphism, it is also possible to explain the present element inventory of the Lengenbach deposit in terms of a low-temperature mineral assemblage of As-Tl-rich pyrite (21 vol%), Ag-bearing galena (1.0 vol%), Cd-bearing sphalerite (1.2 vol%), Sr-bearing barite (2 vol%) and small amounts of Cu-sulfides which can accommodate the existing element inventory (tab. I.6).

The required primary minor element concentrations in pyrite (1.7% As, 0.07% Tl), galena (0.8% Ag) and sphalerite (0.6% Cd) are well within the range of low-T deposits (e.g. Kucha & Viaene, 1993). A pyrite host for Tl and As would explain the general association of As-Tl-rich assemblages with massive stratiform pyrite bands. The present concentrations of Tl in pyrite are 0.12 ppm and less (Dillen et al., 1984), demonstrating that Tl is not easily incorporated into the lattice at metamorphic conditions.

I.10.2 Combined interpretation of isotope data

A summary of isotope data from the different structural types of mineralization and geochemical zones is presented in figure I.27. The figure illustrates the dependence of the isotopic composition on the zone and geometric type of mineralization. See chapter I.8, I.9 and I.10 for a detailed discussion of the results.

I.10.3 Alpine thermal history of the Lengenbach deposit

This section combines the chronological and thermometrical data from the Lengenbach deposit with results of previous studies of the terrain. The aim of this section is to reconstruct the retrograde Alpine history of the stratiform mineralization in the Binn Valley. According to U-Pb-ages of garnets, K-Ar-ages of hornblende, muscovite and biotite as well as zircon and apatite fission-track-ages Vance & O'Nions (1992) proposed a cooling path for the Steinental 12 km SE of the Lengenbach deposit, where metamorphic conditions of 500 to 520°C were reached about 28 Ma ago. The assemblage arsenopyrite-pyrrhotite-pyrite-sphalerite in veinlets within the reduced zone of the deposit allow the application of the sphalerite geobarometer and the arsenopyrite geothermometer (Scott, 1983). The FeS content of the sphalerite is 16.26 ± 0.78 mole% (32 microprobe point analyses), yielding a pressure of 3.3 ± 0.6 kbar. Arsenopyrite of this paragenesis contains 31.47 to 31.74 at% As (XRD and microprobe data) corresponding to a temperature of 395 to 410 °C. Arsenopyrite in druses (31.1–31.3 at% As) and as a rock-forming mineral (30.7 to 30.9 at% As) of the intermediate redox zone contains less As, probably due to higher S activity in this environment.

U-Pb ages of uraninites from the Lengenbach deposit (18.5 ± 0.5 Ma) point to a crystallization during retrograde metamorphism at about 400°C (fig. I.28). At the same stage, sulfides and sulfates equilibrated and the first, CO_2-rich fluid inclusions formed in quartz. All these data indicate increasing hydrothermal activity during this period. The

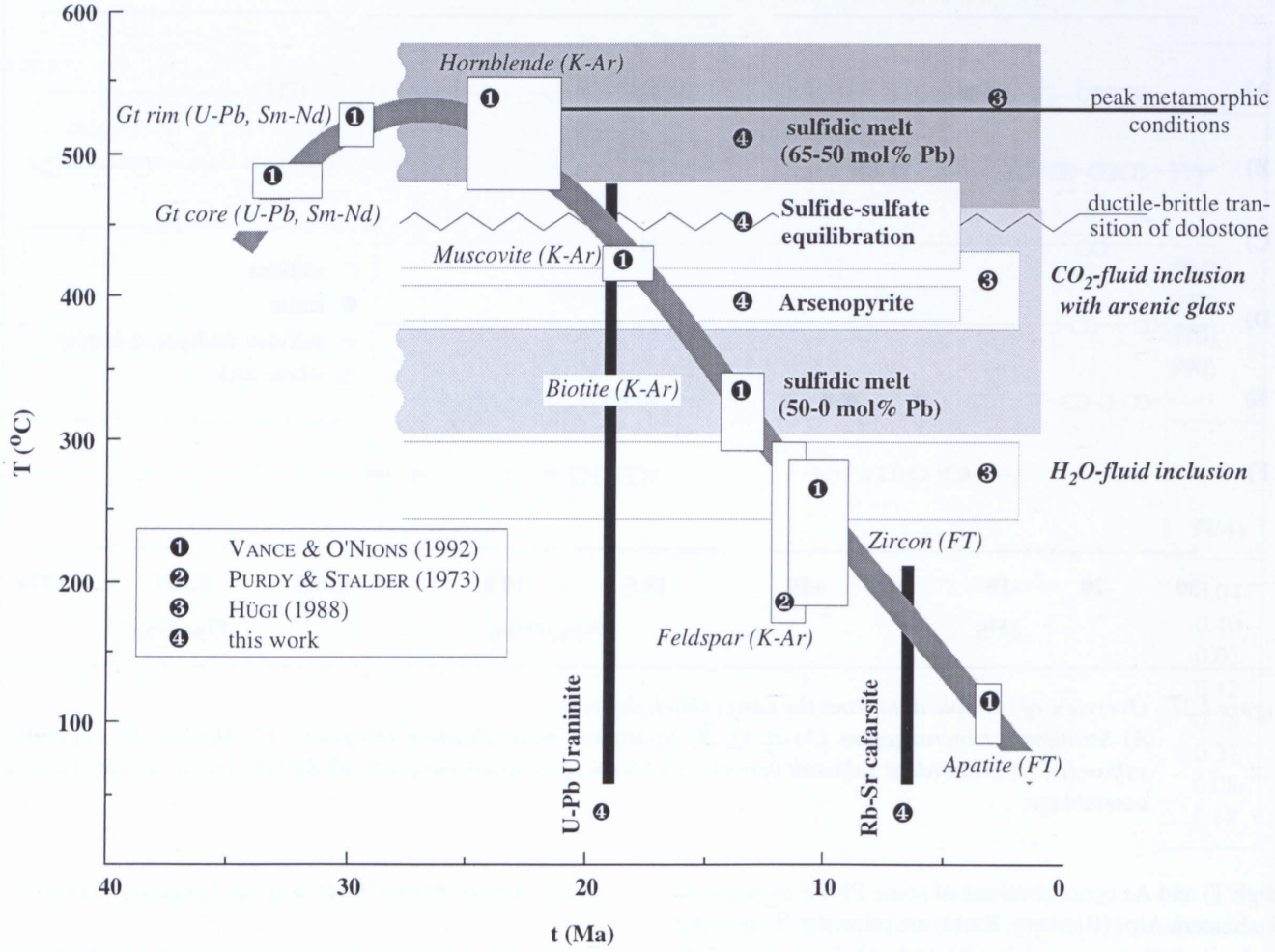

Figure I.28: Temperature-time plot for the Binn Valley region. The figure shows the T-t path of the Steinental after VANCE & O'NIONS (1992). See text for discussion.

interpretation is in agreement with the noted transition of ductile to brittle deformation of metadolostones and the assumed change to more hydrostatic pressure conditions at this time (section I.5.8). Figure I.29 also illustrates that the CO_2-rich fluid inclusions (partly As-glass-bearing; HÜGI, 1988) formed in the presence of the As-rich sulfidic melt.

I.10.4 Arguments in favor of isochemical metamorphism

The data presented in this work argue for an origin of the unique Lengenbach mineralogy as a result of an isochemical Alpine metamorphism. GRAESER (1965; 1968; 1975) proposed Alpine introduction of As, Tl and Cu into a pre-existing Fe-Pb-Zn mineralization at Lengenbach, based on the occurrence of the As minerals asbecasite (containing Tl and Sn) and cafarsite in Alpine fissures of the Monte Leone nappe. I assume a derivation of the Lengenbach element inventory from the basement now represented in the Monte Leone nappe as well, but during the Mesozoic. As-rich metarhyolites of the Monte Leone nappe are assumed to be the source rock of the mineralizing fluid.

Based on the new geochemical and isotopical data, following arguments in favor of a pre-Alpine origin of the Lengenbach element inventory followed by isochemical Alpine metamorphism can be summarized:

1st The association of Pb, Tl, Ag, As, Sb, Hg and Ba and their relative proportions are in no way unusual as primary constituents of sediment hosted sulfide deposits. A common source from strongly evolved continental crust is likely for these elements. Therefore, the element association present in the Lengenbach deposit can be explained by a single mineralizing event.

2nd The most intense stratiform pyrite-mineralization coincides with the strongest Tl-As mineralization at the Lengenbach deposit, indicating a common origin.

3rd The bulk of As-rich minerals has $\delta^{34}S$ and Pb-isotopic values almost equal to massive pyrite indicating no external source for these elements during Alpine times. Sulfosalts in the As-rich zone have $\delta^{34}S$-values closer to massive pyrite than in the other zones, showing that zones rich in As experienced the least external influ-

ence. Sulfur from two sulfides in an Cu-As occurrence in the Monte Leone gneiss are isotopically heavier ($\delta^{34}S$ = +4.7 and +7.9‰; HOEFS & GRAESER, 1968) than the heaviest Lengenbach sulfide sulfur ($\delta^{34}S$ = +3.4‰), indicating that interaction with sulfur from this source would have strongly influenced the isotopic composition of the Lengenbach deposit.

4th Mineralized metadolostones show no evidence of increased $^{87}Sr/^{86}Sr$ values that would have resulted from massive flushing by gneiss-derived fluids during Alpine times.

5th Arsenopyrite geothermometry, inclusions of sulfide melt and tectonically deformed tourmalines indicate that the associated elements As, Tl and B were already present before temperatures of metamorphism fell below 400°C. Hence they were not introduced during retrograde stages (<300°C) as suggested by GRAESER (1965; 1968).

6th Aqueous phases coexisting with a Pb-As-Tl-sulfide melt contained very high As-concentrations (in the 1000 ppm range) as is evident from abundant As-sulfide daughter mineral inclusions (HÜGI, 1988). This is good evidence that the system was closed because such high As-concentrations are unlikely for a metamorphic fluid of regional extent.

7th The C and O isotopic composition of rock forming (sugary) dolomite and dolomite in Alpine fissures and druses from the mineralized zones do not point to the influence of an external, metamorphic fluid.

8th Significantly different Pb isotope values of druse- versus massive sulfosalts indicate a different evolution of these two Pb reservoirs during Alpine time. I explain this by limited Pb isotope exchange between a former coexisting sulfide melt and a hydrothermal fluid. A difference in Pb isotopic compositions between massive and idiomorphic As-rich sulfosalt minerals are inconsistent with a late Alpine introduction of the whole Pb-As-association. The observed variations can best be explained by predominantly closed system evolution.

9th The enrichment of uranogenic lead in druses indicates the metacarbonates as the likely source rock of the radiogenic lead enriched in hydrothermally precipitated minerals.

Present evidence indicates therefore that the Lengenbach deposit is the result of isochemical Alpine metamorphism of an earlyer mineralization without a significant change in element inventory.

The present study focuses on the Lengenbach deposit. GRAESER (1965; 1968; 1969) and HOEFS & GRAESER (1968) additionally investigated samples from minor mineralization at other localities in the Binn Valley. These occurences differ significantly: Such occurrences have significantly lower total sulfide inventories and are characterized by isotopically heavier sulfides, higher Sb/As ratios and more radiogenic Pb than the Lengenbach deposit. The differences in S- and Pb isotope ratios may be interpreted as a result of the higher degree of equilibration with metamorphic fluids in these less intensely mineralized occurrences.

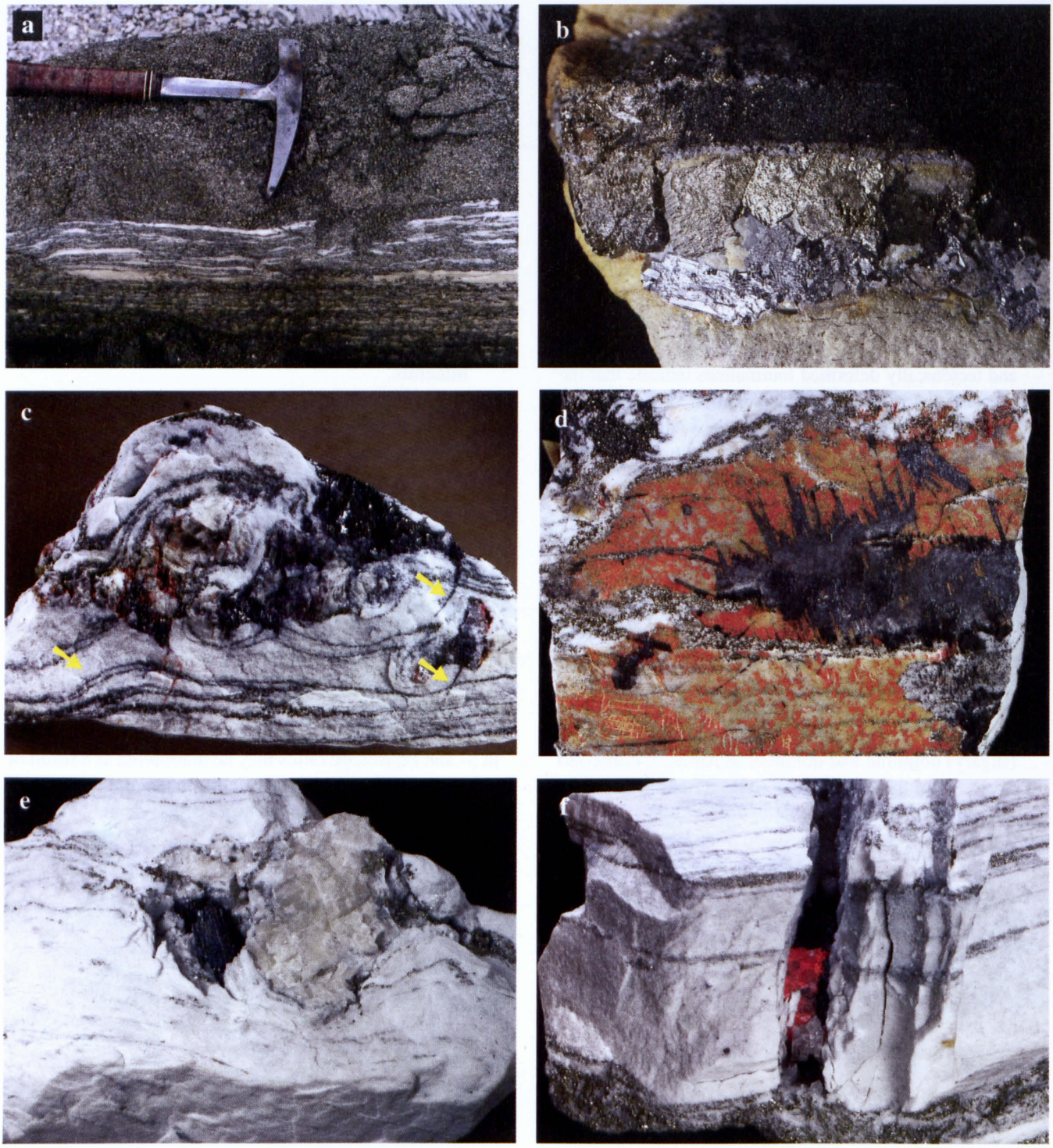

Plate I.1: *(above) Major structural types of sulfide mineralization at Lengenbach:*
a) Stratiform massive pyrite of the As(III)-rich zone.
b) Characteristic association of magnetite, pyrite and arsenopyrite in the reduced zone. Field of view 7 cm. NMBE B7153.
c) Massive sulfosalts and minor realgar in pressure shadows of dolomite porphyroclasts in the As(III)-rich zone. Note small discordant veinlets (arrows). Field of view 12 cm. L25251.
d) Discordant veinlet with sartorite and realgar. Field of view 11 cm. NMBE B9152.
e) Well crystallized sulfosalt (liveingite) in druse close to calcite porphyroclast. Field of view 9 cm. NMBE B1999.
f) Late (alpinotype) fissure with realgar and dolomite cutting stratiform pyrite. Field of view 11 cm. NMBE B8211.

Plate II.1: *(right side) Cu-As-F- mineralization of the Monte Leone nappe (Wanni region near P. Cervandone). The photo shows the slightly discordant biotite-epidote rocks with an adjacent occurrence of arsenates (cafarsite, tilasite, asbecasite).*

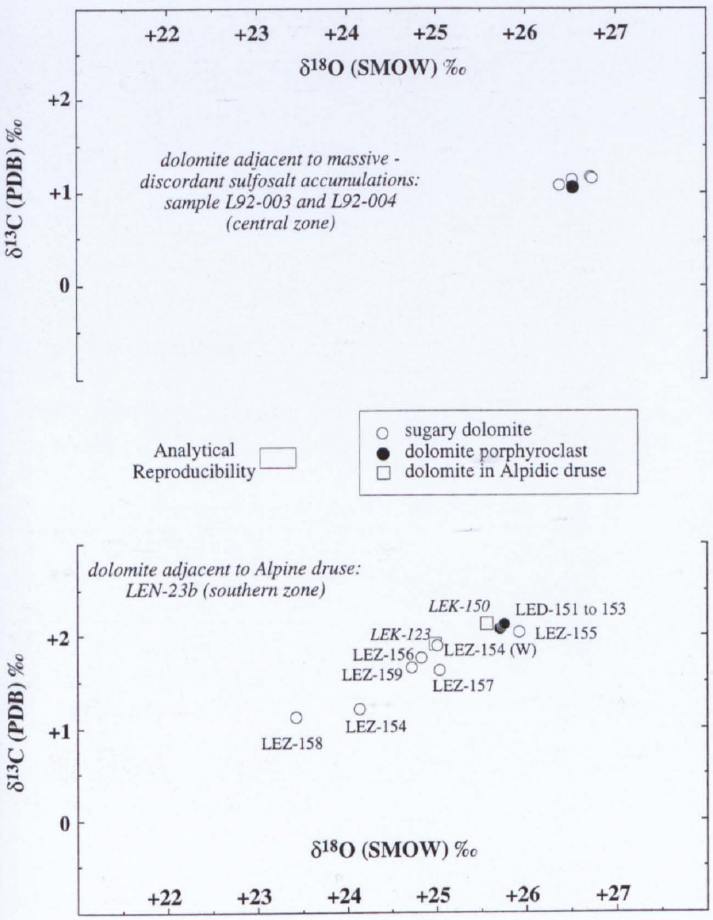

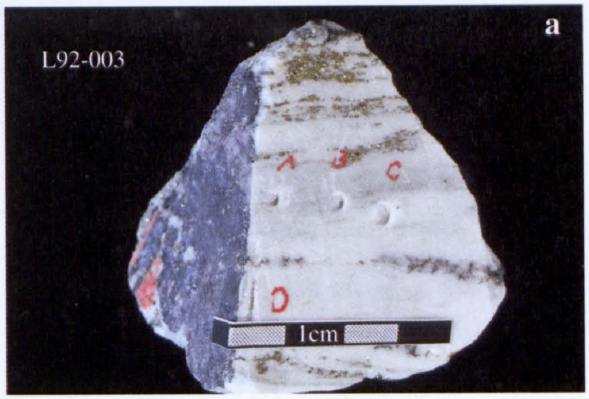

Discordant sulfosalt veinlet of baumhauerite and realgar in mineralized sugary dolomite.

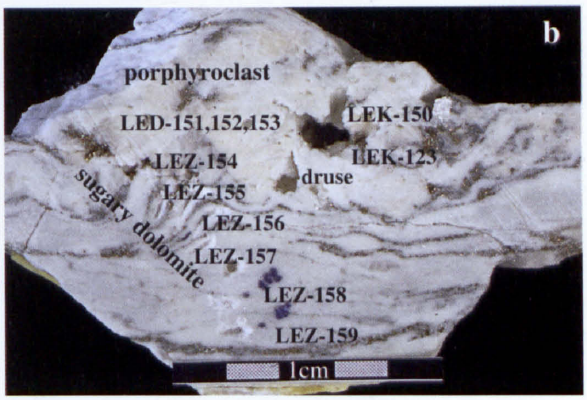

Alpine druse in sugary dolomite close to dolomite porphyroclast. Vuggy minerals: baumhauerite and dolomite.

Plate I.2: O- and C-isotopic composition of dolomite separates (sugary, idiomorphic and porphyroclastic) from the Lengenbach deposit close to sulfosalt accumulations and vuggy metadolomite (photos a and b).

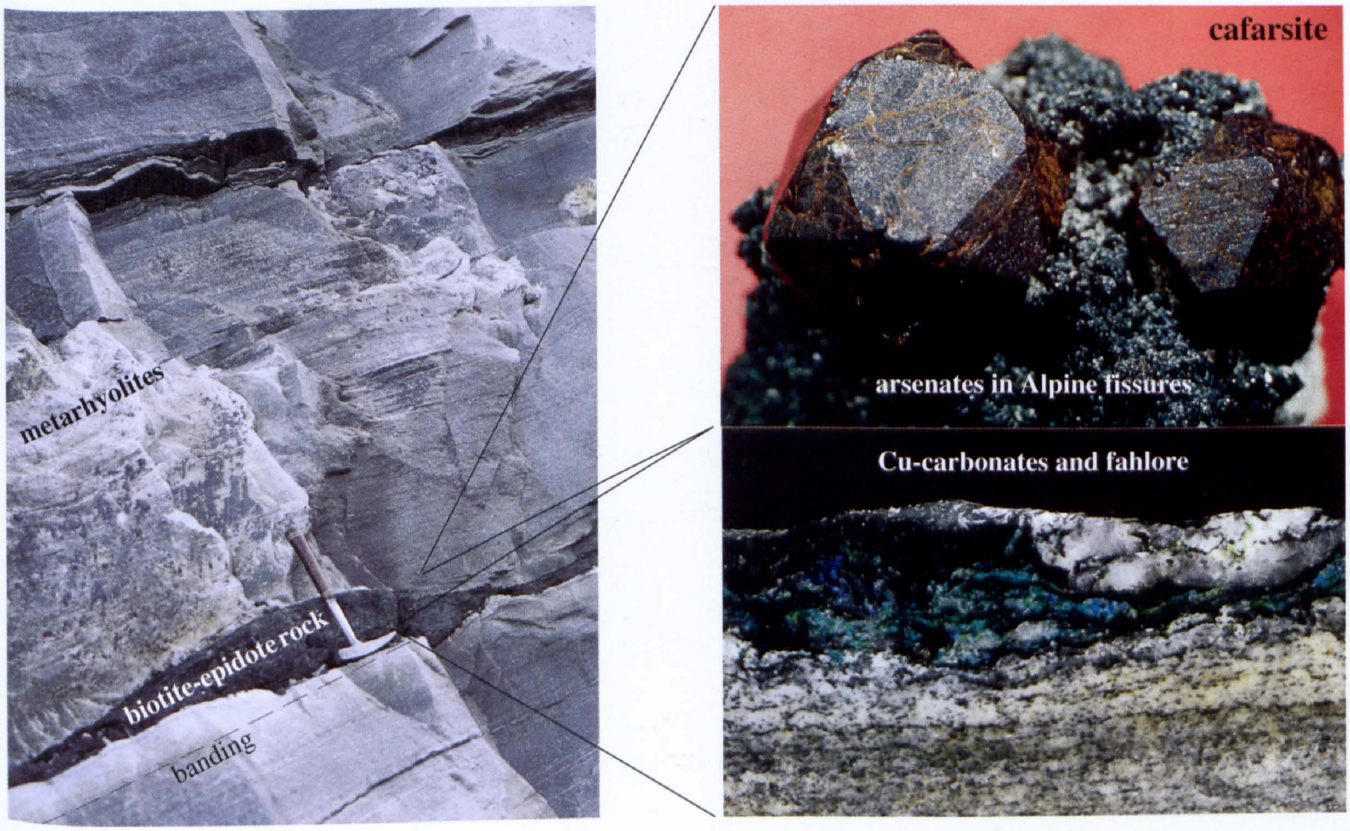

PART II:
GENESIS OF CU-AS-F- MINERAL OCCURRENCES IN THE BASEMENT GNEISSES OF THE MONTE LEONE NAPPE

II.1 Introduction

The Monte Leone nappe of southern Switzerland and northern Italy is well known for a large number of As-rich mineral occurrences. Fahlore and several arsenates occur in Alpine fissures and druses of the crystalline basement.

Previously, the occurrence of arsenic sulphosalt minerals in the Triassic metadolomites of the Binn Valley (e.g. the Lengenbach mineral deposit) was explained by addition of Cu and As from several Cu-As-F mineralizations located in the basement-gneisses a few km to the south (GRAESER, 1965, 1968; HÜGI, 1988). According to these authors, the metal enrichment in the basement was assumed to be of Hercynian age, whereas the formation of sulfoarsenides in the stratigraphically overlying Triassic dolomites was thought to be the result of metamorphic fluids, interacting during Alpine metamorphism with a pre-existing, stratiform Pb-Zn-Ba mineralization.

According to recent investigations, the formation of arsenic sulfosalts in the Triassic dolomites from the Binn Valley is considered to be the result of isochemical metamorphism. This part presents geochemical and isotopical data of basement rocks which indicate the source rocks of the mineralizing fluid. The data also help to clarify the petrogenesis of several Cu-As-F-occurrences in the basement rocks and finally explain their relation to the As-rich stratiform mineralization in the overlying Triassic dolostones.

II.2 Geologic setting

The complex structural framework of the Swiss Alps is the consequence of the complicated pattern of motion between the African and European plates since the early Mesozoic. The tectonic regime in the northern Penninic zone evolved from late Triassic extension to Tertiary subduction-related contraction (TRÜMPY, 1980; LEU, 1986a and 1986b; HSÜ, 1994). The late Triassic and Jurassic rifting resulted in thinning of the continental crust, formation of detachment structures along low-angle normal faults, asthenospheric uplift and extrusion of MORB-type basalts (see part III) on pelitic synrift-sediments (Bündnerschiefer, calcescisti or schistes lustrés). The Tertiary compression caused strong isoclinal folding during lower amphibolite-facies metamorphism. In the studied terrain, the P-T conditions during Alpine metamorphism reached 3 kbar and 520°C (FRANK, 1979; HÜGI, 1988).

The Penninic Monte Leone nappe includes two major lithologic groups: pre-Mesozoic gneisses forming the crystalline basement, and overlying Triassic to Cretaceous metasediments with minor interbedded amphibolites (fig. 1). The basement consists of various gneisses and an extensive ultramafic body (KEUSEN, 1972). Coarse grained, porphyroblastic augengneisses form the core of the Penninic nappe, whereas stratigraphically higher units comprise predominantly Permo-Carboniferous metasediments and metavolcanic rocks (BADER, 1934; HÜGI, 1988). Biotite-epidote rocks with numerous Cu-As-F-mineralized occurences are present in the basement rocks.

Several Cu-As-F occurrences are known from different localities of the Monte Leone nappe (fig. 1). The region around the Pizzo Cervandone is rich in rare arsenates (asbecasite [$Ca_3(Ti,Sn)(As_6Si_2Be_6)O_{20}$],
cafarsite [$Ca_{5.9}Mn_{1.7}Fe_3Ti_3(AsO_3)_{12} \cdot 4\text{-}5H_2O$],
chernovite [$(Y,La)AsO_4$],
cervandonite [$(Ce,La)(Fe,Ti,Al)_3SiAs(Si,As)O_{13}$],
fetiasite, gasparite-(Ce) [$(Ce,La)AsO_4$],
tilasite [$CaMg(F/AsO_4)$],
chalcophyllite [$(Cu,Al)_3\{(OH)_4/(AsO_4,SO_4)\} \cdot 6\,H_2O$],
chlorotil-agardite [$(Cu,Fe)_2Cu_{12}\{(OH)_{12}/(AsO_4)\} \cdot 6H_2O$],
strashimirite $Cu_4(OH/AsO_4)_2 \cdot 2.5\,H_2O$
and tirolite $Ca_2Cu_9\{(OH)_{10}/(AsO_4)_4\} \cdot 10H_2O$]),
occurring in fissures of a two-mica-gneiss (GRAESER & ROGGIANI, 1976).

Fahlore (tennantite), minor chalcopyrite and secondary copper minerals such as malachite and azurite as well as Ca- and REE-phosphates and fluorite coexist with these arsenates. Similar Cu-As-F-rich mineral associations in Alpine fissures occur 1 km east of the Lengenbach mineral deposit at Gorb and in the Mättital area (KRZEMNICKI, 1993) (fig. 1).

II.3 Samples and analytical procedure

2 to 5 kg of fresh rocks samples were crushed and milled for geochemical and isotopical analyses. If required, aliquots were dissolved for several hours in a microwave oven in a hot mixture of $HCl:HF:HNO_3 = 9:1:0.01$. The completness of dissolution was checked visually. The concentration of Si, Ti, Al, Fe, Mn, Mg, Ca, K, P, F, Ba, Rb, Zr, Y and S were determined by XRF (X-ray fluorescence) at the EMPA (Eidgenössische Materialprüfungsanstalt Dübendorf, Switzerland); U, Th, Sb, Au, Cs, Sc, Hf, Ta, Br, As and REE by

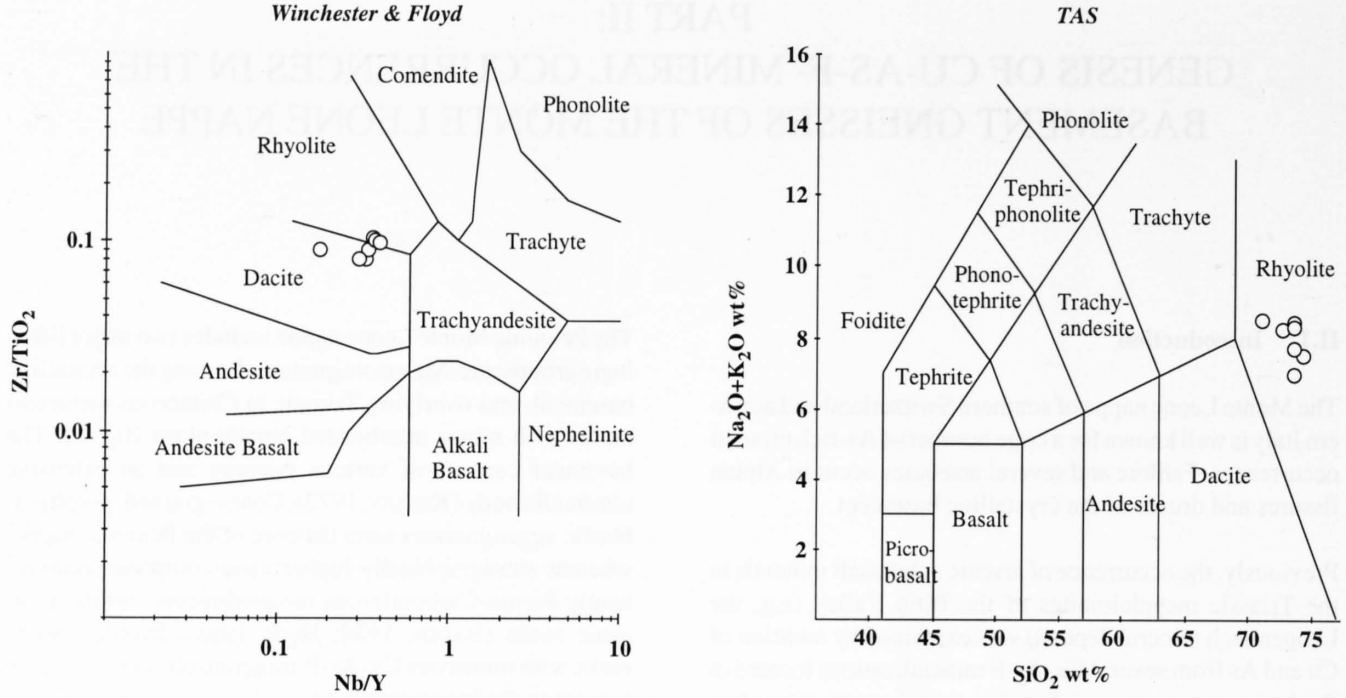

Figure II.1: Geochemical discrimination of two-mica-gneisses from the Monte Leone-nappe (WAG: 307, 311, 316, 324, 332, 220B, 220C). The diagrams show the classification according to WINCHESTER & FLOYD (1977) for immobile trace elements and after IRVINE & BARAGAR (1971) for alkali-silica (TAS).

INNA (Instrumental Neutron Activation Analyses); Sr, Pb, Cu, Zn, Ag, Mo, Nb, Cd, Li and Ga by ICP-OES (Inductively Coupled Plasma-Optical Emission Spectroscopy) and Tl by AAS (Atomic Absorption Spectroscopy). These analyses were performed at the Bondar Clegg Laboratories, Ottawa.

II.4 Geochemistry of basement rocks from the Monte Leone nappe

The geochemical analyses were performed on augengneisses, two-mica-gneisses and biotite-epidote rocks of the Monte Leone nappe (tab. 7.9). The investigation focused on two-mica gneisses and biotite-epidote rocks because the occurrence of arsenates in Alpine druses is restricted to these two rock types. The host rock of the mineralized zone in the basement is a leucrocratic two-mica gneiss. In thin section the rock appears homogeneous and equigranular. Potassium feldspar (mostly microcline) is common. Plagioclase ranges in composition from An_5 to An_{10}. Zircon-morphology and geochemical discriminatory analysis after SHAW (1972) indicate an igneous parentage (discrimination factor = +0.4 to +2.9). According to the geochemical discrimination of WINCHESTER & FLOYD (1977) and IRWINE & BARAGAR (1971), the rock has a rhyolitic or dacitic composition (fig. II.1).

Compared to rhyolitic rock standards (JR-1, RGM-1) or average rhyolites (WEDEPOHL, 1976) metarhyolites of the Monte Leone nappe are characterized by higher concentrations of MgO (0.58-1.14 wt%), Cu (5-520 ppm), Co (12-28 ppm), Ni (3-6 ppm), Cr (6-13 ppm), Ba (25-306 ppm), As (0.5-104 ppm), Pb (26-76 ppm) and Zn (26-87 ppm). The ages of these Penninic basement gneisses is not well constrained. U-Pb age determination of the Monte Leone gneiss indicates a Hercynian to Permian age (KÖPPEL et al., 1980), whereas Rb-Sr ages of the stratigraphically comparable Ganter and Eisten gneisses point to a Permian age (KRAMERS, 1970; STRECKEISEN et al., 1978).

Field observation revealed a strong correlation of the occurrence of arsenates, Cu-sulfides and Cu-carbonates with biotite-epidote rocks. Fissures with As-oxides are restricted to 1 to 2 meters in the footwall and hangingwall of these rocks. Biotite-epidote rocks are slightly discordant to the banding of the surrounding metarhyolites and show strong boudinage caused by the Alpine deformation (plate II.1). Structural, geochemical and isotopical investigations described in the following section indicate these rocks to be former shear-zones.

II.5 Geochemistry of biotite-epidote rocks – indications for pre-metamorphic alteration in shear zones

The gains and losses that took place during metasomatic alteration cannot be quantified without a knowledge of the relationship between compositional changes and volume changes that accompany the process. The chemical alteration can be quantified by calculations of gains and losses from chemical analyses and specific gravities of the unaltered and metasomatized rocks. In this work, mobile and non-mobile elements are discriminated by using the relative mobility diagrams of GRESENS (1967) for major elements and the diagram of MARQUER (1989) for trace elements (fig. II.2). The

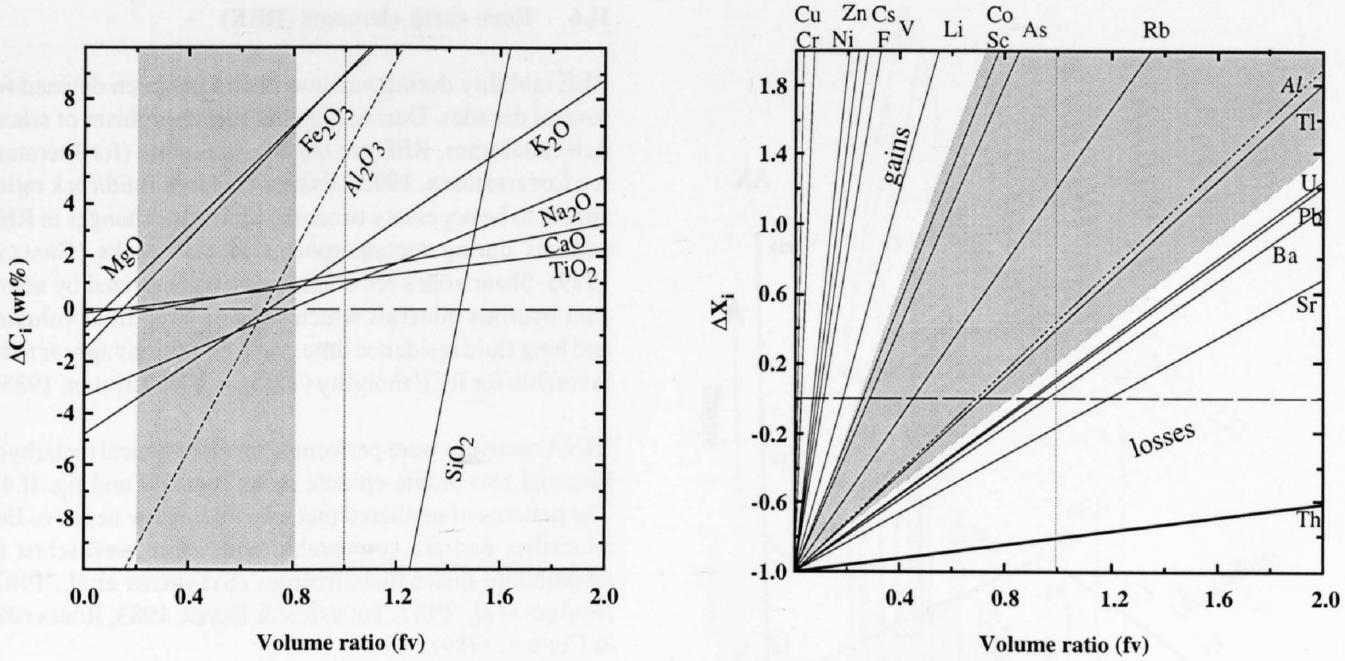

Figure II.2: Volume-composition relationship of major- and trace elements for altered rhyolites (after GRESENS, 1967 and MARQUER, 1989). The Δ-values were calculated for the transition of metarhyolites (WAG-307, WAG-311, WAG-316, WAG-324 ,WAG-332) to biotite-epidote rocks (WAN-14, WAG-220A). The grey zone indicate a geological reasonable volume ratio for shear zones (fv = 0.2 to 0.8).

importance of the composition-volume relationship was first recognized by GRESENS (1967), who used the specific gravity of the unaltered and altered rocks to combine mass balance and volume equation into one single equation, written as:

$$\Delta C_i = fv \cdot (d_{II}/d_I) \cdot C_{iII} - C_{iI}$$

where fv is given by the volume ratio between the transformed rock and the unaltered precursor. d_I and d_{II} are the densities of protolith (I) and altered rock (II), respectively. C_{iI} and C_{iII} are the weight percentages of the oxides or elements in the initial and modified rock.

In the diagram of MARQUER (1989), the mass variation of each element ΔX_i is normalized with respect to the content in the unaltered rock:

$$\Delta X_i = fv \cdot (d_{II}/d_I) \cdot (C_{iII}/C_{iI}) - 1$$

where X_i is the mass variation relative to the original rock volume. The comparison of elements with widely variable concentration ranges is facilitated by this type of diagram.

Chemical analyses of mineralized biotite-epidote rocks indicate an enrichment of Mg and Fe as well as of Cu, Cr, Ni, Zn, Cs, F, V, Li, Co, Sc, As, Rb (in decreasing order of enrichment, fig. II.2). Compared with adjacent unaltered metarhyolites, Si, Na and Th, Sr, Ba, Pb, U are depleted (fig. II.2). Al, known to be relatively immobile during hydrothermal alteration (KERRICH et al., 1980; MARQUER & PEUCAT, 1994) points to a volume ratio of 0.7.

Many studies have been published on chemical mass-transfer indicating changes in major and trace-element concentrations and strong modifications of isotope ratios in ductile shear zones (for references see MARQUER & PEUCAT, 1994). Up to now, however, little is known about chemical modifications in low-T shear zones.

MANATSCHAL (in press) investigated low angle detachment faults in the Lower Austroalpine Err nappe in eastern Switzerland. The faults are interpreted to accompany Mesozoic rifting. The onset of the detachment can be linked to brittle deformation (absence of plastic deformation in quartz indicates T<270°C) at low-grade metamorphic condition (alteration of potassium feldspar and plagioclase to albite, illite and chlorite). Chemical mass balances between the host rock in the footwall and the fault rocks along the detachment indicates an open system (MANATSCHAL & KNILL, 1995). If Al, Ti, Y and Zr are assumed to be immobile, a consistent gain in Mg and K as well as Cr, Ni, Zn, V, Rb, and a loss in Ca, Na, Si and Sr can be observed. These changes in chemistry reflect the breakdown of feldspar (loss of Na, Ca, Si, Sr) and the crystallization of the illite and chlorite (gain of Mg, K as well as Cr, Ni, Zn, V, Rb). Recently, JAIN et al. (1994) demonstrated that chlorite and illite concentrate significant amounts of trace elements such as V, Cr, Zn, Cd, Sn and As by adsorption.

The geochemistry and petrogenesis of biotite-epidote rocks from the Monte Leone nappe can also be explained by low-T hydrothermal alteration. Figure II.3 illustrates the dependence of chemical gains and losses on the ionic radius and valency. The enrichment of elements with a

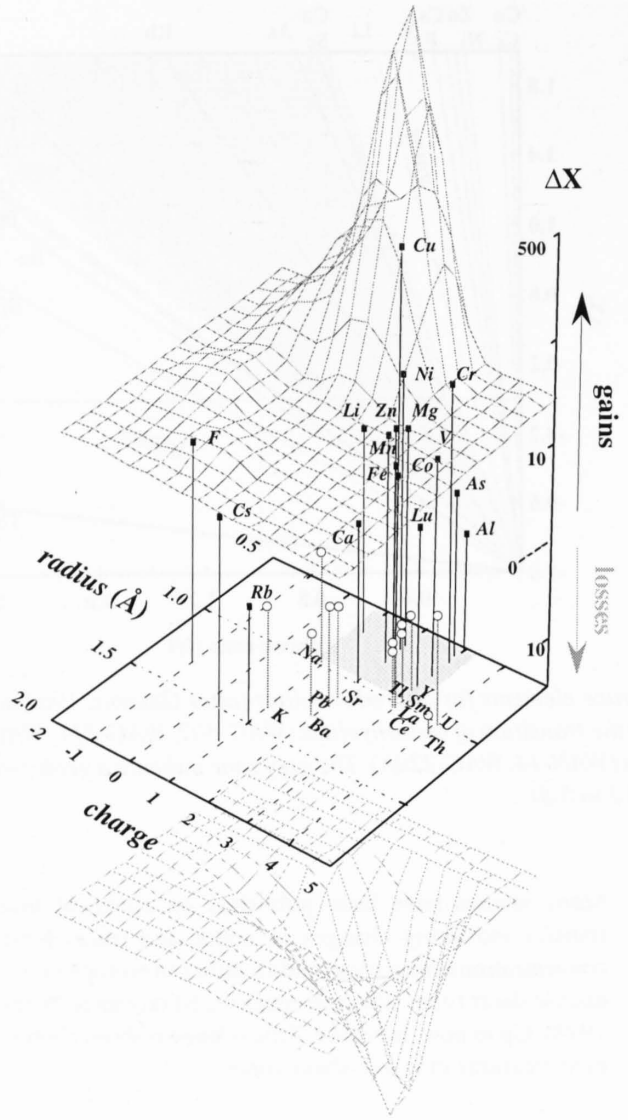

Figure II.3: Diagram of the chemical alteration for major and trace elements of biotite-epidote rocks in dependence of the ionic radius and valency. The factor ΔX_i (volume-composition relationship after MARQUER, 1989) was calculated by an assumed volume ratio of 0.7. Full symbols denote gains, open symbols losses. See figure II.2 and text for explanation of calculation.

ionic radius less than 0.8Å and the depletion of elements with higher ionic radius (>1.2Å) such as Sr, Pb, Ba, K suggest a hydrothermal alteration of feldspars to chlorite and clay minerals.

Similarities of geochemical characteristics of unmetamorphosed shear zones in the Austroalpine terrain and the metamorphosed biotite-epidote rocks of the Monte Leone nappe suggest a comparable petrogenesis (i.e. formation of clay minerals) and an isochemical recrystallization during Alpine, amphibolite facies metamorphism.

II.6 Rare earth elements (REE)

REE mobility during metamorphism has been debated for several decades. During regional metamorphism of silica-rich lithologies, REE are usually immobile (for literature see LOTTERMOSER, 1992). Extremely large fluid/rock ratios appear to be necessary to cause significant changes in REE patterns during metamorphism of acid rocks (GRAUCH, 1989). Shear zones are commonly characterized by abundant hydrous minerals which suggest large fluid volumes and long fluid residence time. Such conditions appear to be favorable for REE mobility (TAYLOR & MCLENNAN, 1985).

INNA-analyses were performed on three typical metarhyolites and two biotite-epidote rocks (tab. 7.9 and fig. II.4). The patterns of unaltered metarhyolites show negative Eu-anomalies and are comparable with other greenschist to amphibolite facies metarhyolites (SYLVESTER et al., 1987; NORMAN et al., 1987; THURSTON & FRYER, 1983; ROBERTSON & CONDIE, 1989).

Biotite-epidote rocks are depleted in LREE and slightly enriched in HREE with regard to the unmineralized rhyolitic host rocks. This REE pattern is typical for hydrothermally altered rocks (BAKER & HELLINGWERF, 1988; SCHADE et al., 1989; LOTTERMOSER, 1992). The bird-wing shaped REE profile of biotite-epidote rocks with the depletion of LREE indicates low-T hydrothermal alteration with the breakdown of feldspar and the formation of clay minerals.

Several arsenates such as cervandonite, chernovite or gasparite as well as monazite contain significant amounts of LREE. Moreover, KRZEMNICKI (1993) emphasized an enrichment of La, Ce and Nd in the most common arsenate mineral cafarsite from the Monte Leone nappe. The occurrence of these LREE-enriched minerals is restricted to Alpine fissures close to biotite-epidote rocks, which are thought to be the source rock for Cu and As, but also LREE in a late Alpine

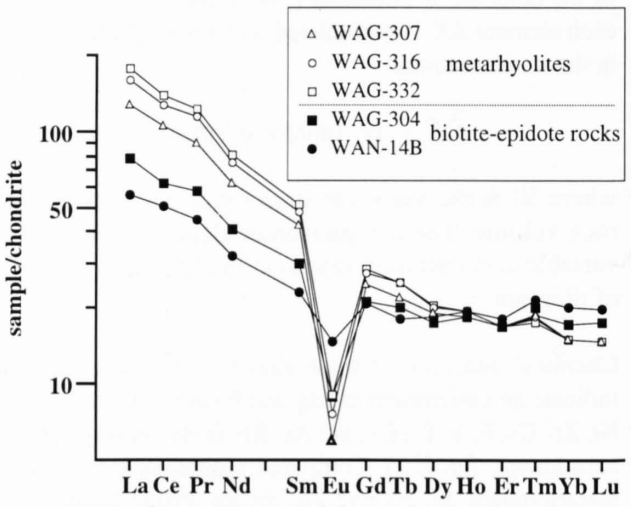

Figure II.4: Chondrite-normalized (NAKAMURA, 1974) REE pattern of metarhyolites and biotite-epidote rocks of the Monte Leone nappe.

fluid. The LREE are supposed to have been preferentially released in shear zones prior to the Alpine metamorphism by hydrothermal alteration.

II.7 Rb-Sr isotopes of whole rock samples from the Monte Leone nappe

Rb-Sr whole rock analyses were performed on augengneisses, metarhyolites and biotite-epidote rocks from the Monte Leone nappe (tab. 7.9 and fig. II.5). The fit of the isotopic compositions of three augengneisses from the core of the nappe defines a regression line of about 325 Ma and indicates a Hercynian age for these basement rocks. Five Permian metarhyolites from the region around the Pizzo Cervandone define an isochron of 185 ± 17 Ma. Comparable Rb-Sr whole rock ages in the central Alps have been interpreted as isotopic resetting caused by Mesozoic hydrothermal alteration (ABRECHT & SCHALTEGGER, 1988; SCHALTEGGER, 1990).

MARQUER & PEUCAT (1994) analyzed shear zones from granites in the central Swiss Alps for their Rb-Sr systematics. They observed chemical and isotopic modifications related to external derived fluid circulation and progressive mineral changes. Their Rb-Sr isotopic dating of shear zones recorded spurious ages caused by chemical and mineralogical changes in the shear zones.

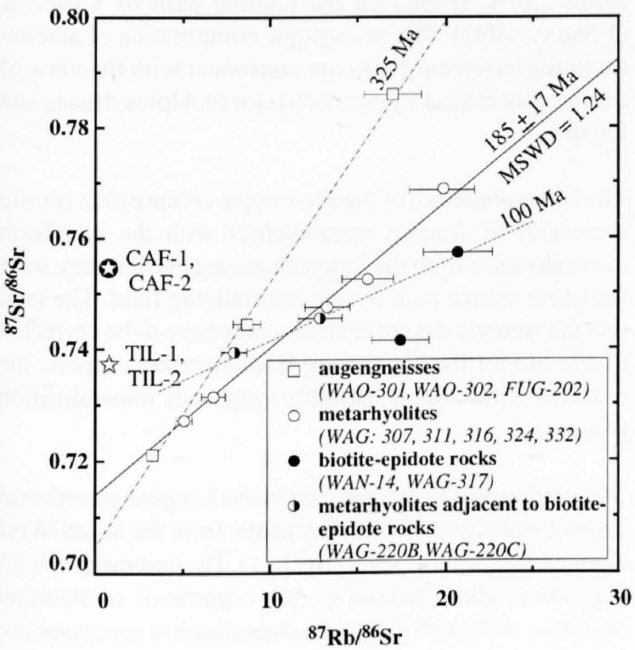

Figure II.5: Rb-Sr evolution diagram for whole-rock samples and Alpine arsenates (CAF-1, CAF-2, TIL-1, TIL-2; see tab. II.1) of the Monte Leone nappe. The fit to the 5 metarhyolites yields an age of 185 ± 17 Ma and initial $^{87}Sr/^{86}Sr$ = 0.7135 ± 20 with MSWD (mean standard weighted deviation) = 1.24. The isochron fit was calculated by the York-fit model with $\lambda = 1.42 \times 10^{-11}$ a^{-1}. Rb and Sr concentrations were determined by XRF and ICP-OES respectively.

Biotite-epidote rocks as well as a metarhyolite (WAG-220B) close (d = 5 cm) to these rock type deviate from the isochron defined by metarhyolites, whereas a sample (WAG-220C) farther from the shear zone (d = 10 cm) fits the latter. Chemical and mineralogical changes in tectonized zones and their immediate neighborhood explains the fictitious age of about 100 Ma defined by three samples from a profile of unaltered metarhyolite (WAG-220C) to biotite-epidote rock (WAN-14).

II.8 Sr isotopic composition of Alpine arsenates

The Sr isotopic compositions of Alpine arsenates in two different fissures from the Monte Leone nappe were determined on 2 cafarsite and 2 tilasite crystals occurring within less than 0.5 m to the biotite-epidote rocks WAN-14 and WAG-317 respectively. Arsenates of the same fissure have a comparable $^{87}Sr/^{86}Sr$ ratio, whereas the isotope compositions of minerals in different fissures are significantly different (tab. II.1). A «two-point-isochron-model-age» can be calculated for these arsenates assuming that the initial Sr-isotope ratio of the hydrothermally precipitated minerals was identical to the one of the assumed source rock.

In their investigation of hydrothermal alteration around Alpine fissures in granites, MERCOLLI et al. (1984) demonstrated only local leaching of the host rock. The chemical components of various Alpine fissure minerals may therefore often derive mainly from the adjacent host rock. The occurrence of arsenate-bearing fissures is restricted to around biotite-epidote rocks, which are by analogy thought to be the source rock for Alpine mobilized Cu, As, REE and also Sr. In order to determine a model-age of arsenates in Alpine

Table II.1: Rb and Sr isotope compositions of arsenates (single grains) from Alpine fissures of the Monte Leone nappe. Rb and Sr concentrations were determined by AA. The ages were calculated using the initial $^{87}Sr/^{86}Sr$-ratio of the adjacent biotite-epidote rock and therefore presuppose equilibration of the Alpine fluids with these rocks. (WAN-14 for cafarsite and WAG-317 for tilasite).

Cafarsite [$Ca_{5.9}Mn_{1.7}Fe_3Ti_3(AsO_3)_{12} \cdot 4\text{-}5H_2O$]:

sample	$^{87}Sr/^{86}Sr$	Rb (ppm)	Sr (ppm)	t (Ma) ± 2σ
CAF-1	0.757149 ± 07	5	104	6.7 ± 0.4
CAF-2	0.757129 ± 11	6	111	6.8 ± 0.4

Tilasite [$CaMg(F\backslash AsO_4)$]:

sample	$^{87}Sr/^{86}Sr$	Rb (ppm)	Sr (ppm)	t (Ma) ± 2σ
TIL-1	0.739718 ± 17	5	55	6.9 ± 0.4
TIL-2	0.739738 ± 12	5	52	6.8 ± 0.4

fissures, biotite-epidote rocks were assumed as the exclusive source rock. Additional Sr sources such as the unaltered adjacent metarhyolites would cause spurious ages.

The amphibolite facies metamorphism caused recrystallization and homogenization of Sr isotopes among rock forming minerals within basement rocks of the terrain (JÄGER et al., 1967). Thus, the $^{87}Sr/^{86}Sr$ ratio of the late Alpine fluid would not be sensitive to the mineral phase that is predominantly leached.

These assumptions are confirmed by comparable age determinations of two independent mineral-host rock systems. The calculated Rb-Sr-model ages of 6.3 to 7.3 Ma point to a late Alpine mobilization of As and Cu in vugs and fissures in the basement rocks. U-Pb ages of uraninites from the Lengenbach mineral deposit define an age of 18.5 ± 0.5 Ma (Part I). The Rb-Sr-model-ages of arsenates from the basement indicate a much later mobility of As in the crystalline basement rocks. Nevertheless, the calculated Rb-Sr-ages of Alpine minerals from the Monte Leone nappe must be interpreted with caution.

II.9 Pb isotopic composition of basement rocks

Apart from the redox-sensitive elements (U, V, Mo) most of the enriched elements (Pb, Zn, Tl, Ag, Sb, Ba, Hg) of the carbonate-hosted Lengenbach deposit are thought to be derived from an external source. Many stratiform to stratabound deposits are known to be formed by the leaching of elements from basement rocks, followed by precipitation in an overlying sedimentary environment (EVANS, 1980; LYDON, 1983). Pb isotopes are a powerful tool to delineate the general source areas of the Pb concentrated in stratiform ore deposits (KÖPPEL, 1988; KÖPPEL & SCHROLL, 1988). Furthermore, a comparison of the ore-Pb with the trace-Pb of an assumed source rock offers the opportunity to designate or exclude possible source rocks of a deposit.

Pb isotopes were therefore analyzed in whole rock samples of gneisses from the Monte Leone nappe. The isotopic compositions of all analyzed samples (augengneisses, metarhyolites, biotite-epidote rocks) are more radiogenic than the stratiform mineralization from the Lengenbach deposit (fig. II.6). However, after correcting for in situ produced ^{207}Pb and ^{206}Pb during the past 200 Ma, the values of the basement rocks are similar to those of stratiform minerals from the Lengenbach deposit. Only two augengneiss-samples show a more radiogenic Pb isotope signature after correction.

II.10 Discussion and conclusion of part II

Rb-Sr-isotopic investigations of Alpine biotites in fissures from the Simplon-area yield an age of 10 ± 5 Ma (JÄGER et al., 1967). The model ages of arsenates from the Monte Leone nappe confirm these results which point to late Alpine formation of some fissure minerals at temperatures

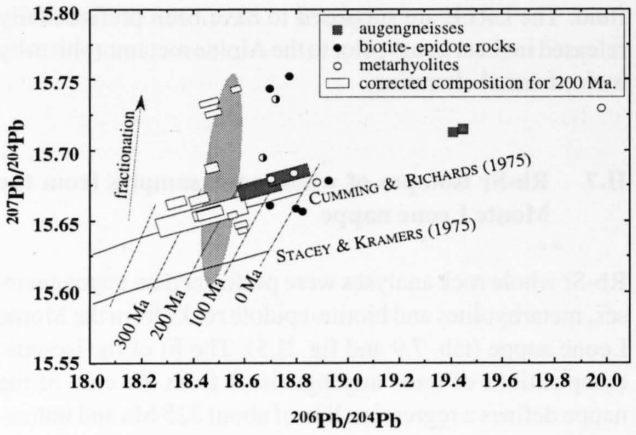

Figure II.6: Pb-isotope evolution diagram for whole-rock samples of Monte Leone gneisses. The stippled field defines the composition of the stratiform mineralization at the Lengenbach deposit. High $^{207}Pb/^{204}Pb$ values of some mineralized samples can be explained by fractionation during the analytical procedure (see section 6.1.4). The errors of the corrected compositions (rectangles) were calculated assuming an uncertainty at the given concentration level of 4% for U and Th (INAA) and 8% for Pb (ICP-OES).

below 250°C (based on the cooling path of VANCE & O'NIONS, 1992). The Sr-isotopic composition of arsenates in the basement rocks are consistent with the view of a relatively closed-system behavior in Alpine druses and fissures.

The correspondence of the Pb isotopic composition (in situ corrected) of As-rich metarhyolites with the stratiform mineralization from the Lengenbach argues that they were the likely source rock for the mineralizing fluid. The fact, that the isotopic data of metarhyolites have to be corrected to 200 Ma for the two sets of data to overlap supports the model of a pre-Alpine, possibly syngenetic mineralization process.

The similarity of Pb isotope data for the Lengenbach mineral deposit with those of Bleiglanzbänke from the South-West German Keuper is evident (fig. I.11). The basement of both deposits is characterized by the occurrence of Permian rhyolites. Although different mineralization processes are postulated for the two deposits, the source for Pb and also As, Zn and Ba in the Triassic sediments is thought to be a uniform metal source, which could be the Permian volcanic rocks.

The resetting of the Rb-Sr isotopic system in metarhyolites points to a hydrothermal activity during early Mesozoic times. This is in agreement with the suggestion by LYDON (1983), that metals can only be effectively leached from rock forming minerals during destructive mineral transformations.

LEEDER (1982) implied that the hydrothermal convection, responsible for stratiform Pb-Zn-mineralization in Ireland, was generated as a response to an increase in geothermal gradient as the crust thinned due to extension. RUSSELL (1968, 1983) also explained the formation of Irish exhalative sedimentary Pb-Zn deposits (e.g. Silvermines, Navan) as a result of processes in an extensional stress regime and of leaching of Lower Paleozoic metasediments. Biotite-epidote rocks from the basement of the Monte Leone are interpreted as metamorphosed shear zones. Their occurrence supports the existence of an early Mesozoic rifting stage which was accompanied by the leaching of rhyolitic basement rocks.

PART III:
GEOCHEMISTRY OF MESOZOIC AMPHIBOLITES IN THE BINN VALLEY

III.1 Introduction

In the Central Alps, several ophiolitic sequences, which are considered to represent remnants of the North Penninic or Valais oceans, occur as isolated bodies in pelitic sediments. According to their stratigraphic position, two sequences can be distinguished in the Binn Valley:

1st Basic and minor ultrabasic rocks in monotonous, calcareous schists of Mesozoic age (Bündnerschiefer, calcescisti or schistes lustrés).

2nd An ultrabasic complex (Geisspfad serpentinite body; fig. 1) with minor basic layers, occurring in pre- Mesozoic gneisses of the Monte Leone nappe. KEUSEN (1972) explained the existence of these layered spinel-lherzolites, pyroxenites and dunites as a result of fractional crystallization of an ultramafic magma in the upper mantle. The primary minerals of the Geisspfad rocks have been almost completely changed by serpentinization, rodingitization and Alpine regional metamorphism. Furthermore the Alpine orogeny caused the emplacement of this complex.

This part describes the geochemistry of Mesozoic amphibolites that occur close to the stratiform polymetallic sulfide mineralization in the Binn Valley. GIUSCA (1930) and BADER (1934) assumed that the formation of carbonate hosted Pb-Zn-Tl-As-Ba mineralization in the Binn Valley (e.g. Lengenbach deposit) were related to the extrusion of Mesozoic basic magmas. This suggestion was supported by the observation that Mesozoic amphibolites occur close to or in contact to the underlying, mineralized Triassic metadolostones. BADER (1934) described a doubtful thermal contact between metasediments and metavolcanics (formation of biotite-chlorite-rich amphibolites at the contact to the metapelites), which would indicate late Triassic or later magmatic activity. Alpine amphibolite-facies regional metamorphism and accompanying isoclinal folding does not allow a detailed stratigraphic reconstruction of Mesozoic metasediments and metavolcanics. Field observations have shown that Mesozoic basic rocks of the Monte Leone nappe mainly occur close or in contact to the stratigraphically underlying Triassic metadolostones (BADER, 1934; GRAESER, 1968; LEU, 1986b; DIETRICH & OBERHÄNSLI, 1975).

The aim of this part is to characterize geochemically and isotopically the Mesozoic basic rocks occurring in the hangingwall to the stratiform Pb-Zn-Tl-As-Ba mineralization in the Binn Valley and to illuminate their relations to the mineralizing process.

III.2 Geological framework

In the late Triassic to early Jurassic, rifting developed between the European continent and the Apulian plate (CHANNELL & HORVATH, 1976; FRISCH, 1979; DERCOURT et al., 1986; HSÜ, 1994). This rifting evolved to a narrow oceanic basin, the South Penninic or Ligurian-Piemontais ocean, in the middle Jurassic to early Cretaceous. The existence of oceanic crust has been widely accepted for the South Penninic ocean (LAUBSCHER, 1969; DEWEY & BIRD, 1970; OBERHÄNSLI & DIETRICH, 1975; WEISSERT & BERNOULLI, 1985; PFEIFFER et al., 1989). Recently, DUERR et al. (1993) showed that several ophiolitic rocks of the Central Alps represent remnants of oceanic crust, thus indicating the former existence of oceanic crust also in the North Penninic or Valais domain. The stratigraphic position of metabasalts from Visp is ambiguous, because the Mesozoic cover in this area belongs to both the Monte Leone and Bernhard nappe. On the basis of their tectonic position, the Mesozoic amphibolites in the Binn Valley belong clearly to the North Penninic trough (LEU, 1986b).

III.3 Samples, petrography and mineralogy

Field relations, mineralogy and major element geochemistry of Mesozoic ophiolites from the Binn Valley were described in detail by PREISWERK (1907), BADER (1934), LÜTHY (1965), HANSEN (1972), JEANBOURQUIN (1981) and LEU (1986a; 1986b).

In this study two amphibolite samples were collected approx. 50 m into the hangingwall of the Lengenbach deposit. The thickness of amphibolites in the Binn Valley varies from a few centimeters to several meters. BIA-207 (Bänderamphibolit or greenschist) is a fine grained and banded albite amphibolite with epidote, carbonate and rutile whereas BIA-202 (gabbro amphibolite or metagabbro) is a coarser grained biotite-albite amphibolite with large (up to 6mm) pyrite crystals and minor epidote.

The results of the combined XRF, ICP-OES and AA-analyses of the two samples are summarized in table A2.9.

The geochemical data of amphibolites from the Binn Valley are compared with data of other metabasalts from the Central Alps (DUERR et al., 1993).

Mineral fractions for isotope analyses were obtained by hand-picking. Pure samples of feldspar were cleaned ultrasonically in water, leached in HCl and dissolved in a hot mixture of $HCl:HF:HNO_3 = 9:1:0.01$.

III.4 Element mobility

DUERR et al. (1993) showed that the major element content of the metabasalts from the Central Alps are significantly influenced by geochemical alteration during sea floor metasomatism as well as by regional metamorphism. Intense hydration and carbonatisation of some of these rocks is evident from the high loss on ignition (l.i.>1%) and elevated CaO contents.

The geochemical characteristics of these metabasalts were explained by K-metasomatism and carbonatisation. The carbonatized metabasalts from the Central Alps are poor in SiO_2 whereas the Al_2O_3 content is not influenced (fig. III.1a and fig. III.1b). High Al_2O_3 concentration correlates with low CaO and high K_2O contents. (fig. III.1a and fig. III.1d). This is interpreted in terms of break down of the anorthite component accompanied by a loss of Ca and K-metasomatism. The occurrence of metamorphic mica also indicates alteration caused by a high geochemical gradient between the metabasalts (primarily poor in K_2O) and surrounding metapelitic sediments during regional metamorphism. The alteration pattern is different from spilitization (fig. III.1c).

To avoid misinterpretation due to alteration effects, my interpretation of the protolith and the geotectonic environment is therefore mainly based on abundances and ratios of trace elements generally considered as being immobile during weathering, low to medium grade metamorphism and metasomatism. Immobility up to the amphibolite facies has been shown for Ti, Zr, Nb, Y, Cr and with limitations for P (e.g. CANN, 1970; HUMPHRIS & THOMPSON, 1978).

Since these elements, except Cr, behave incompatibly during basalt fractionation, a method of testing their immobility is to plot their concentrations against each other (CANN, 1970). A good positive correlation exists between Ti, Y, P, and Zr for samples from the Binn Valley as well as for 25 samples from the Central Alps and therefore indicates the immobility of these elements (fig. III.1).

Geochemical discrimination of metabasalts requires a screening of the analyses to remove those with a «cumulate» composition (PEARCE, 1983). «Cumulate» in this context refers to any plutonic or volcanic rocks that deviate significantly from a true melt composition. One simple screen is a covariation diagram of Al_2O_3 against TiO_2, as illustrated in fig. III.2 a. Samples that plot outside the basalt melt field should not be used in basalt discrimination diagrams; if they are plotted, the chemical effects of crystal cumulation or strong alteration must be taken into account. Most of the metabasalt from the Central Alps (including those from the Binn Valley) plot within the field of basaltic liquids. The elevated Al-content of some samples can be explained by strong K-metasomatism (see above).

Screening of evolved rocks can be carried out effectively by using the Ti/Zr ratio (WINCHESTER & FLOYD, 1977; STILLMAN & WILLIAMS, 1978; PEARCE et al., 1981). The reason why this ratio discriminates between basic and evolved lavas is well-understood. Olivine, pyroxene and feldspar, the predominant crystallizing phases in basic magmas, do not have a significant effect on the Ti/Zr ratio of the melt. However, once a Ti-bearing oxide becomes a crystallizing phase, Ti becomes depleted in the magma while Zr continues to be enriched. Since crystallization of this oxide phase correlates with a rapid increase in the SiO_2 content of the magma, the change from basic to acid composition is accompanied by a decrease in the Ti/Zr ratio. In tholeiite basaltic melts, however, both Ti and Zr become increasingly enriched in early stages of magma evolution, since a low oxygen fugacity prevents early precipitation of FeTi-oxides. This trend is displayed by the samples from the Penninic metabasalts of the Central Alps. Their subalkalic or tholeiitic character is supported by additionally taking P into consideration (fig. III.2c).

III.5 Geotectonic environment

Plots of Ti vs. V are diagnostic for volcanic rocks and can be used to determine possible tectonic settings of ophiolites (SHERVAIS, 1982). Vanadium (like Cr) differs from Ti and other trace transition metals such as Ni, Co, Sc by having three common valence states under terrestrial conditions that exhibit strongly contrasting geochemical behavior. Reduced vanadium (V^{3+}) has ionic characteristics similar to the compatible trace transition metals and commonly substitutes for other trivalent cations in spinel and pyroxene. The more oxidized species (V^{4+}, V^{5+}) are cations with high charges and low radius/charge ratios, similar to Ti^{4+}. The basis of the geochemical discrimination is the variation in the crystal/liquid partition coefficients for V, which range with increasing oxygen fugacity from >1 to <<1. Since the partition coefficients for Ti are almost always <<1, the depletion of V relative to Ti is a function of the fO_2 of the magma and its source, the degree of partial melting and subsequent fractional crystallization.

This study shows that metabasalts from the Penninic Central Alps (including those from the Binn Valley) have Ti/V ratios similar to MORB (fig. III.2d).

DUERR et al. (1993) showed that the concentrations of elements with intermediate ionic potential (P, Zr, Ti, Y, Cr) in Mesozoic metabasalts from the Central Alps are slightly lower compared to average N-type MORB. This geochemical characteristic was interpreted as an indication for formation at a slowly spreading ridge. Paleogeographic recon-

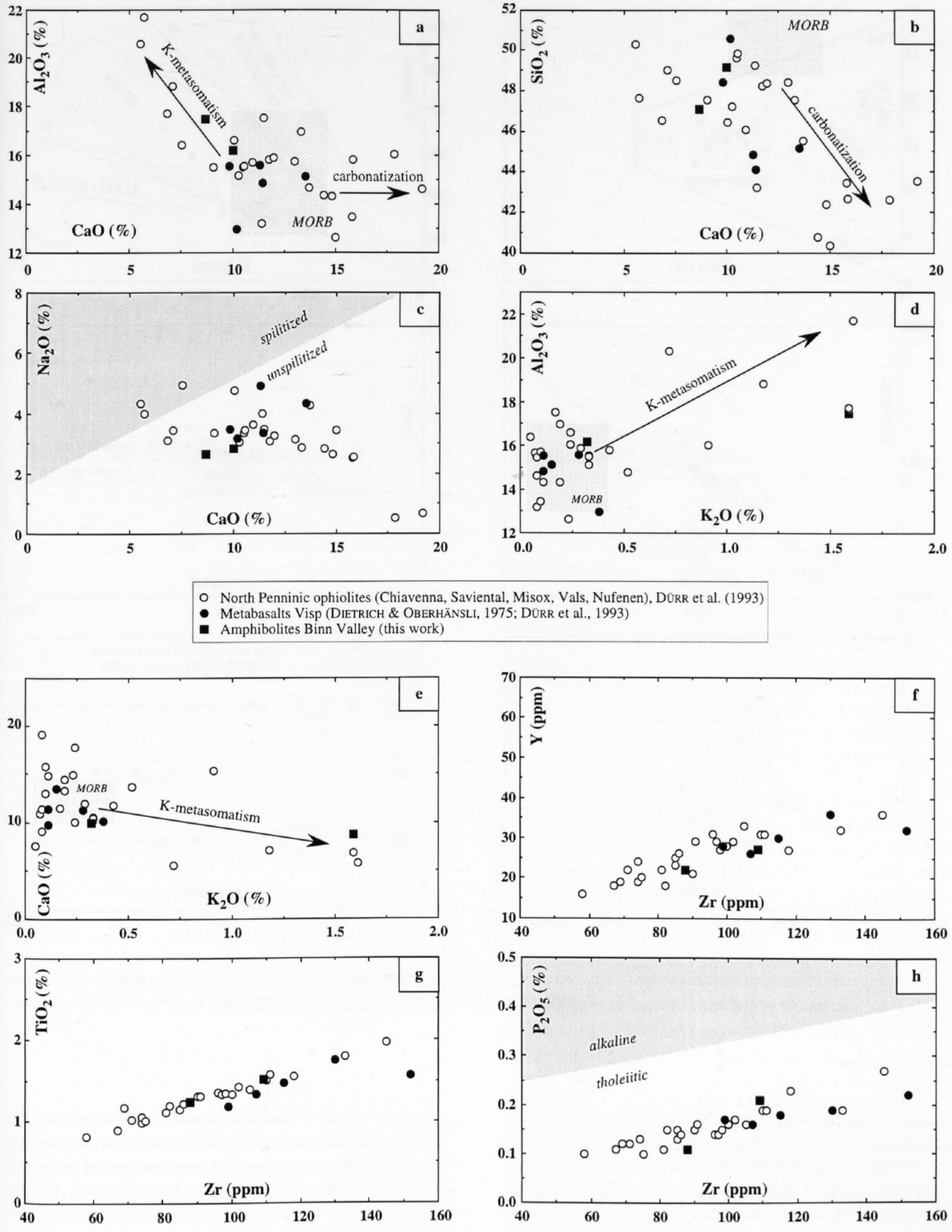

Figure III.1: Geochemical discrimination diagrams for North Penninic ophiolites from the Alps. Correlation diagrams f, g and h test the immobility of incompatible trace elements. Good correlation of Y, Zr, Ti and P points to the immobility of these elements. c: diagram after STILLMANN & WILLIAMS (1978) for the discrimination of spilites.

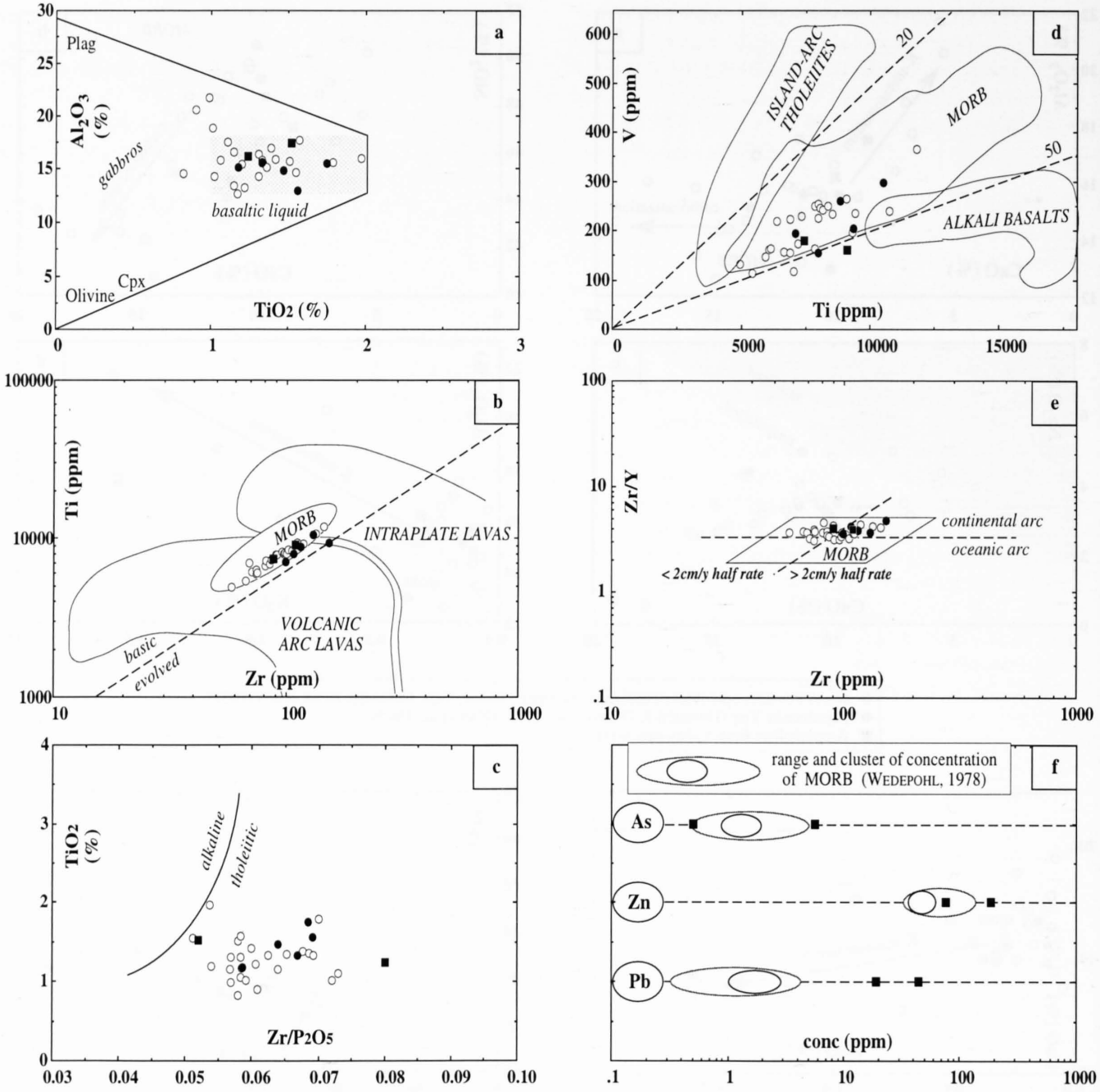

Figure III.2: Geochemical discrimination diagrams (a-e) for North Penninic ophiolites from the Alps. See text for discussion. f: As, Zn and Pb concentration of amphibolites from the Binn Valley in comparison to typical MORB-values.

structions confirm this concept (DERCOURT et al., 1986). In accordance, the Zr/Y-Zr diagram (fig. III.2e) which enables to distinguish between MORB from slow (bilateral spreading rate <2cm/y) and faster spreading ridges, suggests slow spreading rates for most North Penninic metabasalts. The distinction between ridges with different spreading rates is thought to be due to a generally larger and more stable magma chamber under fast spreading ridges, allowing mixing of the primitive, newly generated magma with magma in the chamber enriched by fractionation (NISBETT & FOWLER, 1978). The resulting displacement towards higher Zr values is therefore roughly correlative with the spreading rate (PEARCE 1980; 1983). However, the estimation of spreading rates from the geochemistry of deformed and metamorphosed basalts alone is problematic. Figure III.2e illustrates that the geochemical characteristic of metabasalts from the Central Alps indicates different spreading rates depending on the paleogeographic position. Samples from the eastern Central Alps (Chiavenna, Misox, Safiental, Nufenen, Vals) indicate slow spreading, whereas metabasalts to the West (Visp, Binn Valley) point to a faster spreading.

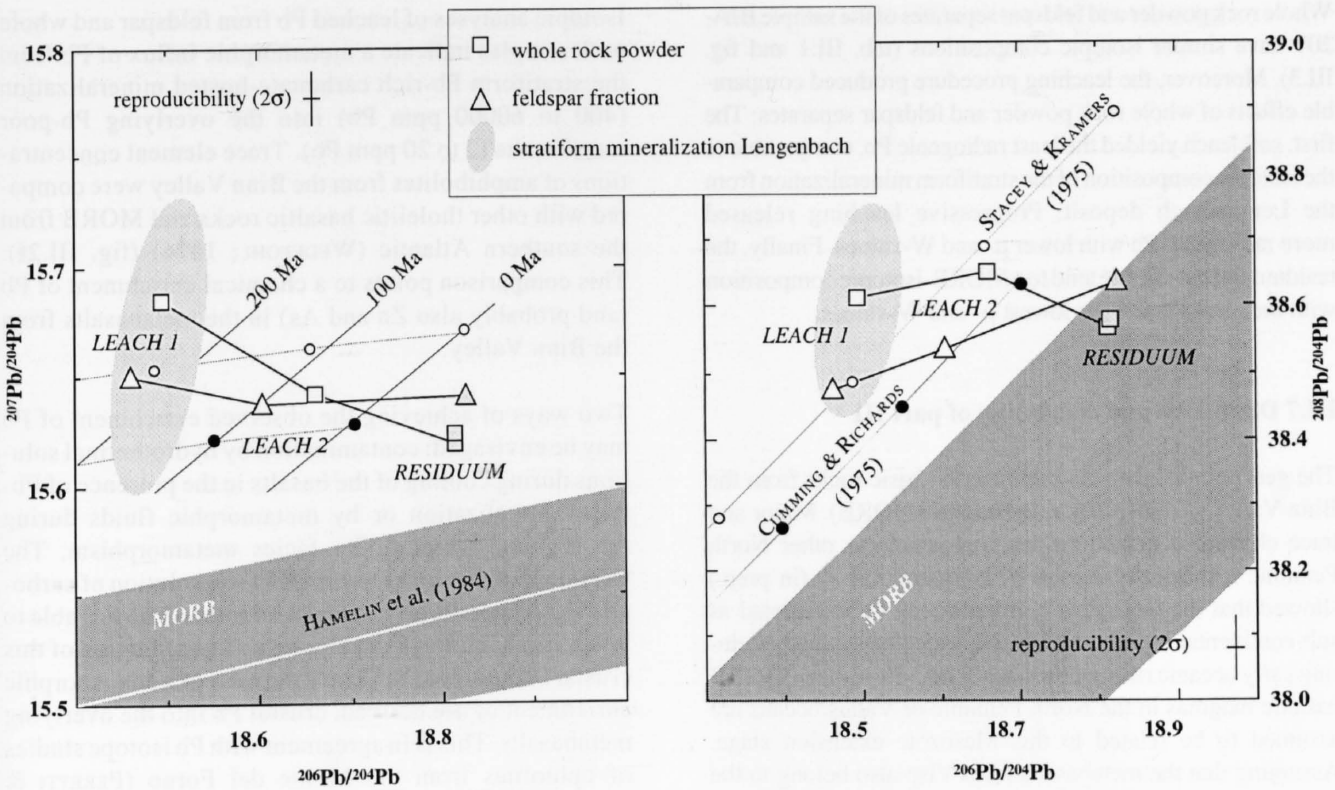

Figure III.3: *$^{208}Pb/^{204}Pb$-$^{207}Pb/^{204}Pb$-$^{206}Pb/^{204}Pb$ diagrams of amphibolite BIA-207 from the Binn Valley. The evolution curves for the average crust are shown according to the models of STACEY & KRAMERS (1975) and CUMMING & RICHARDS (1975). The reference line after HAMELIN et al. (1984) represent the average of MORB from the Atlantic and Pacific oceans.*

III.6 Pb isotopes

Acid leach and residuum of the amphibolite sample BIA-207 were analyzed for their Pb isotopic composition. A multiple-step leaching procedure was performed on feldspar separates (400 mg) as well as whole rock powder (800 mg with 19 ppm Pb). First, the samples were treated with 1N HCl during 30 minutes at 60°C (one respectively two times). The residuum was then leached again in 1N HCl during 60 minutes at 100°C before totally dissolved in a HCl-HF-HNO_3-mixture. Pb was extracted from all solutions using a HBr-cation exchange technique.

Table III.1: *Pb isotopic compositions (leaches and residuum) of amphibolite sample BIA-207 from the Binn Valley. The μ and W values as well as the model ages were calculated according the evolution model of STACEY & KRAMERS (1975).*

sample	BIA-207.F.L1	BIA-207.F.L2	BIA-207.F	BIA-207.G.L0	BIA-207.G.L1	BIA-207.G.L2	BIA-207.G
	Fsp separate	*Fsp separate*	*Fsp separate*	*whole rock*	*whole rock*	*whole rock*	*whole rock*
	Leach 1 (60°C)	Leach 2 (100°C)	Residuum	Leach 1 (60°C)	Leach 2 (60°C)	Leach 3 (100°C)	Residuum
$^{206}Pb/^{204}Pb$	18.463 ± 0.015	18.605 ± 0.010	18.828 ± 0.002	18.493 ± 0.004	18.660 ± 0.002	18.814 ± 0.002	18.815 ± 0.002
$^{207}Pb/^{204}Pb$	15.650 ± 0.013	15.638 ± 0.008	15.641 ± 0.002	15.685 ± 0.003	15.643 ± 0.001	15.620 ± 0.002	15.624 ± 0.002
$^{208}Pb/^{204}Pb$	38.474 ± 0.032	38.535 ± 0.020	38.635 ± 0.005	38.613 ± 0.009	38.652 ± 0.003	38.568 ± 0.005	38.580 ± 0.006
t (Ma)	224	93	-69	334	63	-105	-97
μ	9.88	9.8	9.77	10.17	9.81	9.68	9.7
W	38.18	37.22	36.25	40.08	37.53	35.61	35.73
k (= W/μ)	3.9	3.8	3.7	3.9	3.8	3.7	3.7

Whole rock powder and feldspar separates of the sample BIA-207 have similar isotopic compositions (tab. III.1 and fig. III.3). Moreover, the leaching procedure produced comparable effects of whole rock powder and feldspar separates: The first, soft leach yielded the least radiogenic Pb, comparable to the isotopic composition of the stratiform mineralization from the Lengenbach deposit. Progressive leaching released more radiogenic Pb with lower μ- and W-values. Finally, the residuum of the sample tend to a MORB-isotopic composition with the most Pb and the lowest μ- and W-values.

III.7 Discussion and conclusion of part III

The geochemical data discriminate the basic rocks from the Binn Valley as mid-ocean ridge basalts (MORB). Major and trace element distributions are comparable to other North Penninic metabasalts. Recently, PASTORELLI et al. (in prep.) showed that the Geisspfad peridotites can be interpreted as sub-continental lithospheric mantle which was exhumed during early oceanic rifting processes. The extrusions of MORB basaltic magmas in the North Penninic or Valais oceans are assumed to be related to this Mesozoic extension stage. Assuming that the metabasalts from Visp also belong to the Mesozoic cover of the Monte Leone nappe, we can suspect a higher spreading rate in this paleogeographic terrain. The interpretation is based on the higher Zr contents of metabasalts from this region (fig. III.2e). This work supports the idea that rifting in the western part of the northern Penninic realm started in late Triassic time (which is also documented by the extrusion of metabasalts in the hangingwall of the Triassic dolostones in this region). It is therefore also likely that hydrothermal activity occured in late Triassic times.

Isotopic analyses of leached Pb from feldspar and whole rock samples indicate a metamorphic influx of Pb from the stratiform Pb-rich carbonate-hosted mineralization (400 to 60000 ppm Pb) into the overlying Pb-poor metabasalts (2 to 20 ppm Pb). Trace element concentrations of amphibolites from the Binn Valley were compared with other tholeiitic basaltic rocks and MORB from the southern Atlantic (WEDEPOHL; 1976) (fig. III.2f). This comparison points to a chemical enrichment of Pb (and probably also Zn and As) in the metabasalts from the Binn Valley.

Two ways of achieving the observed enrichment of Pb may be envisaged: contamination by hydrothermal solutions during cooling of the basalts in the presence of Pb-rich mineralization or by metamorphic fluids during the regional, amphibolite facies metamorphism. The treatment of the samples with HCl (dissolution of carbonates and interstitially, surface-adsorbed Pb) was able to lower this common Pb component. The reduction of this crustal Pb component favors the idea of a metamorphic enrichment of ore derived, crustal Pb into the overlying metabasalts. This is in agreement with Pb isotope studies of ophiolites from the Monte del Forno (PERETTI & KÖPPEL, 1986) indicating an enrichment of crustal Pb in metabasalts during regional metamorphism of rocks close (<10 m) to the contact with metasediments. The pre-Alpine, initial Pb isotopic composition of metabasalts from the Binn Valley is thought to be comparable to average MORB-composition. The data point to a restricted late stage metamorphic enrichment of common Pb derived from the stratiform carbonate-hosted mineralization into the nearby, overlying metabasalts.

IV GENERAL CONCLUSIONS

IV.1 Classification of the Lengenbach deposit

IV.1.1 Sediment hosted Pb-Zn deposits

Two major types of sediment hosted Pb-Zn can be distinguished:

1st *Sediment-hosted massive sulfide deposits* of Pb and Zn (LARGE, 1980; 1988; SANGSTER, 1983). These massive to semi-massive deposits occur in extensional basins and are hosted in sedimentary rocks such as shales or carbonates. They are typically fine-grained and stratiform down to the hand-specimen scale. They are also commonly referred to as «sediment hosted stratiform deposits» or «sedimentary-exhalative Pb-Zn» or «sedex» deposits because they are considered to have formed mainly through exhalation of basinal brines at the sea floor and/or «inhalation» into poorly consolidated sediments below the surface.

2nd *Mississippi Valley-type (MVT) ore deposits* (e.g. ANDERSON & MACQUEEN, 1988). These stratabound Zn-Pb-(F-Ba) deposits are mainly, but not exclusively, hosted by carbonate rocks deposited at the margins of tectonically stable platforms. Even if at the deposit scale they have in places tabular morphologies parallel to bedding, closer examination often reveals cross-cutting relationships at outcrop and hand-specimen scale. In comparison with the above ore type, they are generally coarser-grained. Vein-type morphologies with similar mineral assemblages are considered to be related products of the mineralization processes. Mississippi Valley-type deposits are usually interpreted as having been formed by precipitation from saline hot basinal brines during burial diagenesis and later evolutionary stages of the host rocks.

A detailed comparison between these two types of ore deposits has been published by SANGSTER (1990) as well as FONBOTÉ & BONI (1994) who give abundant references. Additional recent reviews can be found in EIDEL (1991) and RUSSELL & SKAULI (1991).

The classification of sediment hosted Pb-Zn deposits of the Alpine realm has for a long time been a matter of discussion. The term «Alpine-type» or «Bleiberg-type» is used for Pb-Zn deposits in the Eastern Alps, e.g., Bleiberg-Kreuth in Austria, Mezica in Slovenia or Raibl and Salafossa in Italy, which are hosted in Middle-Upper Triassic carbonate successions. A problem of classification is that the term «Alpine-type» has often been accompanied by a genetic connotation. Several authors (e.g. SCHNEIDER, 1964; BRIGO et al., 1977; KLAU & MOSTLER, 1983) interpreted the Alpine carbonate-hosted Pb-Zn deposits to be at least in part syngenetic, in contrast to the American MVT deposits which are clearly epigenetic. BECHSTÄDT (1973), BECHSTÄDT & DÖHLER-HIRNER (1983), ZEEH & BECHSTÄDT (1994) suggested that the main characteristic of the Alpine deposits are similar to those of typical MVT and that also the Alpine deposits appear to have formed long after sedimentation of the carbonate host rock. SAWKINS (1990) concluded that «Alpine-type» deposits appear to be fairly typical MVT in affiliation, but that their tectonic setting can be related to widespread rifting events in the area.

IV.1.2 Petrogenesis of the Lengenbach deposit

Due to the metamorphic overprinting, the origin of the Lengenbach deposit must be deduced from geochemistry, isotopic data and geometric arguments. The light S isotopic composition (initially around -25‰) of the stratiform sulfides indicates that open system bacterial sulfate reduction was a major source of S and demonstrates precipitation at or near the sea floor. Only the comparatively small amounts of isotopically heavy sulfide S in the reduced zone of the deposit may be derived directly from the hydrothermal fluids. Large amounts of Fe, Pb, Zn, As, Tl, Cu and other elements present in a surrounding carbonate host rock are best explained by hydrothermal supply. The Eu-enrichment in mineralized samples is consistent with a hydrothermal supply as well.

Light S isotope ratios of the stratiform mineralization combined with a high pyrite content as well as the extensional tectonic setting (SANGSTER & LEACH, 1995) are unusual for MVT deposits. Indications of strong interaction between the precipitated mineralization and oxygenated sea water are the observed light sulfur isotopes indicating open system sulfate reduction, the enrichments of redox-sensitive elements such as U, Mo, V and Cr that were possibly precipitaded from sea water and the close association with barite which contains sea water derived Sr and sulfate. A relatively stable system of prolonged seawater-hydrothermal water interaction is possible only if the hydrothermal fluid had a high salinity and was trapped in brine pools at the sea floor or within shallow cavities of karst- or tectonic origin (fig. IV.1). The dominance of isotopically light primary sulfide however indicates that the input of hydrothermal sulfide

was insignificant. The silicate-rich bands represent either a sediment deposited from particles in the hydrothermal fluid or carbonate dissolution residues within feeder zones.

The source rock of the metals in the hydrothermal fluids were likely the rhyolitic basement rocks now represented in the Monte Leone nappe.

During Alpine metamorphism under upper greenschist or lower amphibolite grade conditions (500°C), ore minerals recrystallized and released Tl, As, Sb and other minor elements to form a Pb-As-Tl-rich sulfide melt. Due to redox conditions buffered by barite and pyrite, As remained in the trivalent state and precluded arsenopyrite formation. During slow cooling, a sulfide melt underwent fractional crystallization in equilibrium with an aqueous fluid phase leading to the formation of massive (from the melt) and idiomorphic (from the fluid) sulfides.

The isotopical investigations of different types of minerals from the mineralization shows that minerals in druses can be best explained by isochemical crystallization during retrograde Alpine metamorphism.

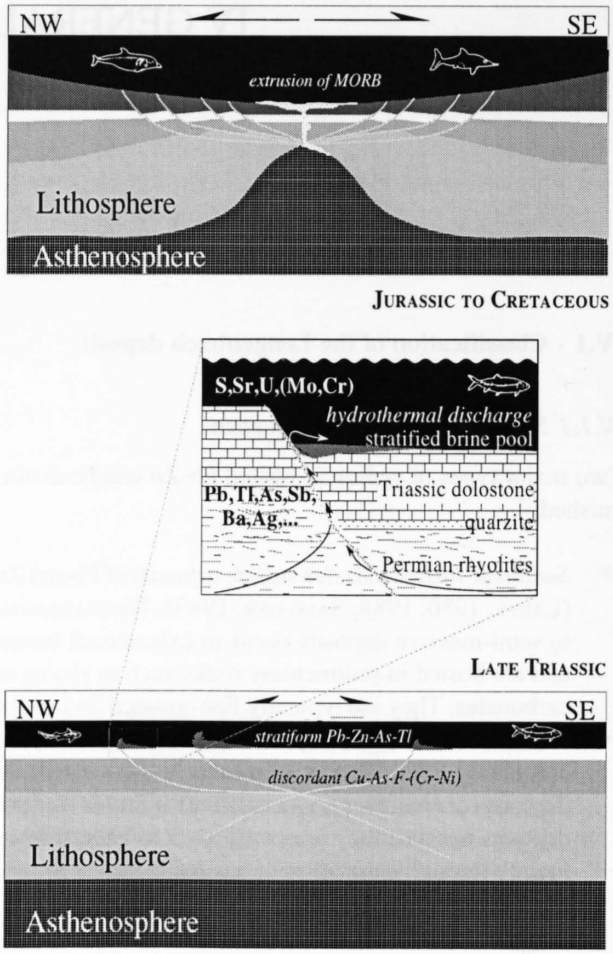

Figure IV.1: Conceptual model for the origin of the primary Lenganbach deposit.

REFERENCES

ABRECHT, J. & SCHALTEGGER, U. (1988): Aplitic intrusions in the Central Aar massif basement: Geology, petrography and Rb/Sr data. Eclogae geol. Helv. 81, 227–239.

AMSTUTZ, G.C. & FONTBOTÉ, L. (1985): Correlative observations on the lead–zinc–(barite–fluorite) occurrences in the germanic triassic lithofacies of Central Europe. Geol. Jb. D70, 179–211.

ANDERSON, G. M. & MACQUEEN, R. W. (1988): Mississippi Valley–type lead–zinc deposits. In: Roberts, R. G. & Sheahan, P. A. (eds): Ore deposit models. Geoscience Canada, Reprint Series 3, 79–90.

ARRIBAS, JR., A. & TOSDAL, R.M. (1994): Isotopic Composition of Pb in Ore Deposits of the Betic Cordillera, Spain: Origin and Relationship to Other European Deposits. Econ. Geol. 89, 1074–1093.

BADER, H. (1934): Beitrag zur Kenntnis der Gesteine und Minerallagerstätten des Binnentals. Schweiz. Mineral. Petrogr. Mitt. 14, 319–441.

BAERTSCHI, P. (1957): Messung und Deutung relativer Häufigkeitsvariationen von ^{18}O und ^{13}C in Karbonatgesteinen und Mineralien. Schweiz. Mineral. Petrogr. Mitt. 37, 73–152..

BAKER, J.H. & HELLINGWERF, R.H. (1988): Rare Earth Element Geochemistry from Western Bergslagen, Central Sweden. Min. Pet. 39, 231–244.

BECHSTÄDT, T. & DÖHLER–HIRNER, B. (1983): Lead–zinc deposits of Bleiberg–Kreuth. In: Scholle, P. Bebout, D.G., Moore, C.H. (eds): Carbonate depositional environments. Am Assoc. Petrol. Geol. Mem. 33, 55–63.

BECHSTÄDT, T. (1973): Zyklotheme im hangenden Wettersteinkalk von Bleiberg–Kreuth (Kärnten/Oesterreich). Veröffentl. Univ. Innsbruck (Festschrift Heissel) 86, 25–55.

BIELICKI, K.H. & TISCHENDORF, G. (1991): Lead isotope and Pb–Pb model age determinations of ores from Central Europe and their metallogenetic interpretation, Contributions to Mineralogy and Petrology 106, 440–461.

BOAST, A.M., COLEMAN, M.L., HALLS, C. (1981): Textural and Stable Isotopic Evidence for the Genesis of the Tynagh Base Metal Deposit, Ireland. Econ. Geol. 76, 27–55.

BOTTINGA, Y. (1968): Calculation of fractionation factors for carbon and oxygen exchange in the systen calcite–carbon dioxide–water. J. Phys. Chem. 72, 4338–1275.

BRETT, R. & KULLERUD, G. (1967): The Fe–Pb–S system, Econ. Geol. 62, 354–369.

BREVART, O., DUPRÉ, B., ALLÈGRE, C.J. (1982): Metallogenic Provinces and the Remobilization Process Studied by Lead Isotopes: Lead–Zinc Ore Deposits from the Southern Massif Central, France. Econ. Geol. 77, 564–575.

BRIGO, L. & CERRATO, P. (1994): Trace Element Distribution of Middle–Upper Triassic Carbonate–Hosted Lead–Zinc Mineralizations: The Example of the Raibl Deposit (Eastern Alps, Italy). In: Fontboté, L. & Boni, M. (eds): Sediment–Hosted Zn–Pb Ores. Spec. Publ. No. 10 Soc. Geol. Applied to Mineral Deposits, Springer.

BRIGO, L., KOSTELKA, L., OMENETTO, P., SCHNEIDER, H.J., SCHROLL, E., SCHULZ, O. STRUCL, I. (1977): Comparative reflections on four Alpine Pb–Zn Deposits. In: Klemm, D.D., Schneider, H.–J. (eds): Time– and Strata–Bound Ore Deposits. Springer, Berlin, Heidelberg, New York, 273–293.

CAMPBELL, A.C., PALMER, M.R., KLINKHAMMER, G.P., BOWERS, T.S., EDMOND, J.M., LAWRENCE, J.R., CASEY, J.F., THOMPSON, G., HUMPHRIS, S., RONA, P. , KARSON, J.A. (1988): Chemistry of hot springs on the Mid–Atlantic Ridge. Nature 335, 514–519.

CANN, J. R. (1970): Rb, Sr, Y, Zr, and Nb in some ocean floor basaltic rocks. EPSL 10, 7–11.

CHABU, M. & BOULÈGUE, J. (1992): Barian Feldspar and Muscovite from the Kipushi Zn–Pb–Cu Deposit, Shaba, Zaire. Can. Min. 30, 1143–1152.

CHANG, L.L.Y. & BEVER, J.E. (1973): Lead sulphosalt minerals: crystal structures, stability relations, and paragenesis. Mineral. Sci. Engng. 5, 3, 181–191.

CHANNEL, J.E.T & HORVATH, F. (1976): The African/Adriatic promontory as a paleographical premise for the Alpine orogeny and plate movements in the Carpatho–Balkan region. Tectonophysics 35, 71–101.

CHAREF, A. AND SHEPPARD S.M. (1984): Carbon and oxygen isotope analyses of calcite or dolomite associated with organic matter. Isotope Geoscience 2, 325–333.

COCHERIE, A., CALVEZ, J.Y., OUDIN–DUNLOP, E. (1994): Hydrothermal activity as recorded by Red Sea sediments: Sr–Nd isotopes and REE signatures. Marine Geology 118, 291–302.

CRAIG J.R. (1974): Sulfosalts. In: P.H. Ribbe (ed): Sulfide Mineralogy, Mineralogical Society of America, Short Course Note V1, 91–110.

CUMMING, G.L., KÖPPEL, V., FERRARIO, A. (1987): A lead isotope study of the northeastern Ivrea Zone and the adjoining Ceneri zone (N–Italy): evidence for a contaminated subcontinental mantle. Contr. Mineral. Petrol. 97, 19–30.

CUMMING, G.L. & RICHARDS, J.R. (1975): Ore lead isotope ratios in a continuously changing earth. Earth Planet. Sci. Lett. 28, 155–171.

CURTI, E. (1987): Isotope geochemistry and fluid inclusion studies on the late metamorphic gold–quartz veins of the

Monte Rosa area, Northwestern Alps, Italy: the origin of metals and fluids. Unpubl. PhD thesis, ETH Zuerich, 121.

CURTI, E. (1987): Lead and oxygen isotope evidence for the origin of the Monte Rosa gold lode deposits (Western Alps, Italy): A comparison with Archean lode deposits. Econ. Geol. 82, 2115–2140.

DEGENS, E.T. (1964): Oxygen and carbon isotope ratios in coexisting calcites and dolomites from recent and ancient sediments. Geochim. Cosmochim. Acta 28, 23–42.

DERCOURT, J. ZONENSHAIN, L.P., RICOU, L.–E., KAZMIN, V.G., LE PICHON, X., KNIPPER, A.L., GRANDJACQUET, C., SBORTSWHIKOV, I.,M.,GEYSSANT, J., LEPVRIER, C., PECHERSKY, D.H., BOULIN, J., SIBUET, J.–C., SAVOSTIN, L.A., SOROKHTIN, O., WESTPHAL, M., BAZHEINOV, M.L., LAUER, J.P.AND BIJU–DUVAL, B. (1986): Geological evolution of the Thetys belt from the Atlantic to the Pamirs since the Lias. Tectonophysics 123, 241–315.

DEWEY J.F. & BIRD J.M., (1970): Mountain belts and the new global tectonics. J. Geophys. Res. 75, 2625–2647.

DIAMOND, L.W. (1990): Fluid inclusion evidence for p–V–T–X evolution of hydrothermal solutions in late Alpine fold–quartz veins of Brusson, Val dÀyaz, North West Italian Alps. Amer. J. Science 290, 912–958.

DIETRICH, V. & OBERHÄNSLI, R. (1975): Die Pillow–Laven des Vispertales. Schweiz. Mineral. Petrogr. Mitt. 55, 79–87.

DILLEN, H., GIJBELS, R., STALDER H.A., EDENHARTER, A. (1984): Untersuchung einiger Spurenelemente in alpinen Kluftpyriten mit der Ionenmikrosonde. Schweiz. Mineral. Petrogr. Mitt. 64, 27–48.

DUERR, S. B., RING, U., FRISCH, W. (1993): Geochemistry and geodynamic significance of North Penninic ophiolites from the Central Alps. Schweiz. Mineral. Petrogr. Mitt. 73, 407–419.

EIDEL J. J. (1991): Basin analysis for the mineral industry. In: Force E, R., Eidel, J. J., Maynard, J. B. (eds): Sedimentary and diagenetic mineral deposits: a basin analysis approach to exploration. Rev. Econ. Geol., Society of Economic Geologist (El Paso) 5, 1–15.

EVANS, A.M. (1980): An Introduction to Ore Geology. Blackwell, 231 pp.

FONTBOTÉ, L. & BONI, M. (1994): Sediment–Hosted Zinc–Lead Ores – An Introduction. In: Fontboté, L. & Boni, M. (eds): Sediment–Hosted Zn–Pb Ores. Spec. Publ. No. 10 Soc. Geol. Applied to Mineral Deposits, Springer, 3–13.

FRANK, E. (1979): Metamorphose mesozoischer Gesteine im Querprofil Brig–Verampio: Mineralogische–petrographische und isotopengeologische Untersuchungen. Unpubl. PhD Thesis, Univ. Bern.

FREY, M., HUNZIKER, J.C., FRANK, W., BOCQUET, J., DAL PIAZ, G.V., JÄGER, E., NIGGLI, E. (1974): Alpine Metamorphism of the Alps. A Review. Schweiz. Mineralog. Petrogr. Mitt. 54, 247–290.

FRIEDMAN, I. & O'NEIL, J.R. (1977): Compilation of stable isotope fractionation factors of geochemical interest. In: M. Fleischer (ed.): Data of Geochmistry, 6th ed. U.S. Gov. Printing Office, Washington, D.C.

FRISCH, W. (1979): Tectonic progradation and plate tectonic evolution of the Alps. Tectonophysics 60, 121–139.

FU, M., CHANGKAKOTI, A., KROUSE, H.R., GRAY, J.,, KWAK, T. A. P. (1991): An Oxygen, Hydrogen, Sulfur, and Carbon Isotope Study of Carbonate–Replacement (Scarn) Tin Deposit of the Dachang Tin Field, China. Economic Geology 86, 1683–1703..

GALKIEWICZ, T. (1967): Genesis of Silesian–Cracovian zinc–lead deposits. Econ. Geol. Monograph 3, 156–168.

GASSER, U. (1974): Zur Struktur und Geochemie der stratiformen Sulfidlagerstätte Meggen (Mitteldevon, Rheinisches Schiefergebirge). Geol. Rundsch. 63, 52–73.

GASSER, U. & THEIN, J. (1977): Das syngenetische Sulfidlager Meggen im Sauerland (Struktur, Geochemie, Sekundardispersion). Forschungsbericht des Landes Nordrhein–Westfalen No. 2620 / Fachgruppe Chemie. Westdeutscher Verlag, 171 pp.

GIUSCA, D. (1930): Die Erze der Lagerstätte vom Lengenbach im Binnental (Wallis). Schweiz. Mineral. Petrogr. Mitt. 10, 152–177.

GRAESER, S. (1965): Die Mineralfundstellen im Dolomit des Binntales. Schweiz. Mineral. Petrogr. Mitt. 45, 597–795.

GRAESER, S. (1966): Asbecasit und Cafarsit, zwei neue Mineralien aus dem Binnatal (Kt. Wallis). Schweiz. Mineral. Petrogr. Mitt. 46: 367–375.

GRAESER, S. (1968): Lead isotopes and minor elements in galenas and sulphosalts from Binnatal. Earth Planet. Sci. Lett. 4, 384–392.

GRAESER, S. (1969): Minor elements in sphalerite and galena from Binnatal. Contr. Mineral. Petrol. 24, 156–163.

GRAESER, S. (1975): Die Mineralfundstelle Lengenbach, Binntal. Schweiz. Mineral. Petrogr. Mitt. 55, 143–149.

GRAESER, S. (1981): Das Binntal, Lapis 12, 9–27.

GRAESER, S. (1990): Binn – Tal der Mineralien. Minaria Helvetica 10b, 14–41.

GRAESER, S. & GUGGENHEIM, R. (1990): Brannerite from Lengenbach, Binntal (Switzerland). Schweiz. Mineral. Petrogr. Mitt. 70, 325–331.

GRAESER, S. & ROGGIANI, A.G. (1976): Occurence and genesis of rare arsenate and phosphate minerals around Pizzo Cervandone, Italy/Switzerland. Soc. Italiana di Mineralogia e Petrologia 32, 279–288.

GRAESER, S., SCHWANDER, H., STALDER, H.A. (1973): A solid solution series between xenotime (YPO_4): and chernovite ($YAsO_4$). Mineral. Mag. 39, 145–151.

GRAUCH, R.I. (1989): Rare earth elements in metamorphic rocks. In: Geochemistry and mineralogy of rare earth elements, Rewiews in Mineralogy, Min. Soc. of Am.

GRESENS, R.L. (1967): Composition–volume relationships of metasomatism. Chem. Geol. 2, 47–65.

GUSTAFSON, L.B. & WILLIAMS, N. (1981): Sediment–Hosted Stratiform Deposits of Copper, Lead, and Zinc. Econ. Geol. 57th Anniversary Vol., 139–178.

HAMELIN, B., DUPRÉ, B., ALLÈGRE, C.J. (1984): Lead–strontium isotopic variations along the East Pacific Rise and the Mid–Atlantic Ridge: a comparative study. EPSL 67, 340–350.

HANNAK, W.W. (1981): Genesis of the Rammelsberg ore deposit near Goslar / Upper Harz, Federal Republic of Germany. Handbook of stratiform and stratabound ore deposits 9, 551-642.

HANNINGTON, M.D., HERZIG, P.M., SCOTT, S.D. (1990): Auriferous hydrothermal precipitates on the modern seas floor. In Foster, R.P. (ed): Gold metallogeny and exploration, 249–282.

HANSEN, J.W. (1972): Zur Geologie, Petrographie und Geochemie der Bünderschiefer–Serien zwischen Nufenenpass (Schweiz) und Cascata Toce (Italia). Schweiz. Mineral. Petrogr. Mitt. 52, 109–153.

HARRIS, D.C. (1989): The Mineralogy and Geochemistry of the Hemlo Gold Deposit, Ontario. Geol. Surv. Canada, Econ. Geol. Report 28, 88 pp.

HEINRICH, C.A. & EADINGTON, P.J. (1986): Thermodynamic predictions of the hydrothermal chemistry of arsenic, and their significance for the paragenetic sequence of some cassiterite–arsenopyrite–base metal sulfide deposits. Econ. Geol. 81, 511–529.

HERZIG, P.M., HANNINGTON, M.D., SCOTT, S.D, MALIOTIS, G., RONA, P.A., THOMPSON, G. (1991): Gold–rich sea–floor gossans in the Troodos ophiolite and on the Mid–Atlantic Ridge. Econ. Geol. 86, 1747–1755.

HOEFS, J. & GRAESER, S. (1968): Schwefelisotopenuntersuchungen an Sulfiden und Sulfosalzen des Binnatales. Contr. Mineral. Petrol. 17, 165–172.

HOEFS J. & STALDER H.A. (1977): Die C–Isotopenzusammensetzung von CO_2–haltigen Flüssigkeitseinschlüssen in Kluftquarzen der Zentralalpen. Schweiz. Mineral. Petrogr. Mitt. 57, 329–347.

HOERNLE, K.A. & TILTON, G.R. (1991): Sr–Nd–Pb isotope data for Fuerteventura (Canary Islands): basal complex and subareal volcanics: applications to magma genesis and evolution. Schweiz. Mineral. Petrogr. Mitt. 71, 3–18.

HOFMANN, B. (1994): Formation of a sulfide melt during Alpine metamorphism of the Lengenbach polymetallic sulfide mineralization, Binntal, Switzerland. Mineralium Depos. 29, 439–442.

HOFMANN, B., GRAESER, S., IMHOF, T., SICHER, V., STALDER, H.A. (1993): Mineralogie der Grube Lengenbach, Binntal, Wallis. Jahrb. Naturhist. Mus. Bern 11, 3–90.

HOFMANN, B. & v. GEHLEN, K. (1993): Formation of stratiform sulfide mineralizations in the Lower Muschelkalk (Middle Triassic) of Southwestern Germany and Northern Switzerland: constraints from sulfur isotope data. Schweiz. Mineral. Petrogr. Mitt. 73, 365–374.

HSÜ, K.J. (1994): The Geology of Switzerland–An introduction to tectonic facies. Princeton University Press, Princeton, New Jersey, pp.250.

HÜGI, M. (1988): Petrographie und Mineralogie der Lercheltinizone (Monte–Leone–Decke, Binntal, VS). Unpubl. Masters Thesis, University of Bern, 131 .

HUMPHRIS, S.E. & THOMPSON, G. (1978): Hydrothermal alteration of oceanic basalts by seawater. Geochim. Cosmochim. Acta 42, 107–125.

IRVINE, T.N. & BARAGAR, W.R. (1971): A guide to the chemical classification of the common volcanic rocks. Can. J. of Earth Sci. 8, 523–548.

JÄGER, E., NIGGLI, E., WENK, E. (1967): Rb–Sr Altersbestimmungen an Glimmern der Zentralalpen. Beiträge zur Geologischen Karte der Schweiz, Schweizerische Geologische Kommission.

JAIN, J.C., MERMUT, A.R., KERRICH, R., HI D.C. (1994): Trace element concentrations of the clay minerals coyiety source clay minerals, chlorites, and vermiculites determined by the ICP–MS technique. Abstract 31st Annual Meeting of Clay Minerals Society, Saskatoon, Canada, 111.

JEANBOURQUIN, P. (1981): Géologie et pétrographie dans la region du Simplon. Unpubl. diploma thesis University of Lausanne.

KAPLAN, I.R., SWEENEY, R.E., NISSENBAUM, A. (1969): Sulfur Isotope Studies on Red Sea Geothermal Brines and Sediments. In: Degens, E.D. & Ross, D.A. (eds): Hot brines and Recent Heavy Metal Deposits in the Red Sea. Springer, Berlin, 474–498.

KERRICH, R., ALLISON, I., BARNETT, R.L. MOSS, S., STARKEY, J. (1980): Microstructural and chemical transformations accompanying deformation of granite in a shear zone at Miéville, Switzerland; with implications for stress corrosion cracking and superplastic flow. Contrib. Mineral. Petrol. 73, 221–242.

KEUSEN, H.R. (1972): Mineralogie und Petrographie des metamorphen Ultramafitit–Komplexes vom Geisspfad (Penninische Alpen). Schweiz. Mineral. Petrogr. Mitt. 52, 385–478.

KLAU, W. & MOSTLER, H. (1983): Alpine Middle and Upper Triassic Pb–Zn deposits. In: Kisvarsanyi, G.G., S.K., Pratt, W.P., Koenig, J.W. (eds): International Conference on Mississippi Valley type lead–zinc deposits. Proc Vol., Rolla, University of Missouri Rolla, 113–128.

KOEPNICK, R.B., DENISON, R.E., BURKE, W.H, HETHERINGTON, E.A., DAHL, D.A. (1990): Construction of the Triassic and Jurassic portion of the Phanerozoic curve of seawater $^{87}Sr/^{86}Sr$. Chem. Geol. (Isot. Geosc. Sec.) 80, 327–349.

KÖPPEL, V. (1983): Summary of lead isotope data from ore deposits of the eastern and southern Alps: Some metallogenetic and geotectonic implications. In: Schneider, H.–J. (ed): Mineral Deposits of the Alps and of the Alpine Epoch in Europe. Springer, Berlin Heidelberg, 162–168.

KÖPPEL, V. (1988): Ore and rock lead isotope systematics in different tectonic units of the Alps, a summary. In: Zuffar'days Symposium held in Cagliari, 57–60.

KÖPPEL, V., GÜNTHERT, A., GRÜNENFELDER, M. (1980): Patterns of U–Pb zircon and monazite ages in polymetamorphic units of the Swiss Central Alps. Schweiz. Mineral. Petrogr. Mitt. 61, 97–119.

KÖPPEL, V. & SCHROLL, E. (1988): Pb–isotope evidence for the origin of lead in strata–bound Pb–Zn deposits in triassic carbonates of the Eastern and Southern Alps. Mineralium Depos. 23, 96–103.

KRAMERS, J.D. (1970): Die Stirnpartie der Monte–Leone–Decke zwischen Heiligkreuz (Längtal bei Binn) und dem Gantertal (Simplonstrasse). Unpubl. Masters Thesis, University of Bern, 120.

KREBS, W. (1981): The geology of the Meggen ore deposit. In: Wolf, K.H. (ed.): Handbook of stratiform and strata-bound ore deposits, Vol. 9. Elsevier, Amsterdam, 509–549.

KRZEMNICKI, M. (1992): Spezielle Mineralisationen im Grenzbereich M.–Leone–Decke/ Berisalserie. Schweiz. Mineral. Petrogr. Mitt. 72, 155.

KRZEMNICKI, M. (1993): Rare Earth Element–zoning in cafarsite from the Binnatal–region (Switzerland). Terra nova 5, 492–493.

KU, T.–L. (1969): Uranium Series Isotopes in Sediments from the Red Sea Hot–Brine Area. In: Degens, E.T. & Ross, D.A. (eds): Hot brines and Recent Havy Metal Deposits in the Red Sea. Springer, Berlin: 512–524.

KUCHA, H. & VIAENE, W. (1993): Compounds with mixed and intermediate sulfur valences as precursors of banded sulfides in carbonate–hosted Zn–Pb deposits in Belgium and Poland. Mineralium Depos. 28, 13–21.

KUTOGLU, A. (1961): Roentgenographische und thermische Untersuchungen im quasibinaeren System PbS–As_2S_3. Jb. Min. Mh 2, 68–72.

LARGE, D. E. (1980): Geological parameters associated with sediment–hosted, submarine exhalative Pb–Zn deposits: an empirical model for mineral exploration. Geol. Jahrb. (Hannover) D40, 59–129.

LARGE, D. E. (1988): The evaluation of sedimentary basins for massive sulfide mineralization. In Friedrich, G. H. & Herzig, P.M. (eds): Base metal sulfide deposits. Springer, Berlin, Heidelberg, New York, 3–12.

LATTANZI, P., CURTI E., BASTOGI, M. (1989): Fluid inclusion studies of the gold deposits of the upper Anzasca valley, Northwestern Alps, Italy. Econ. Geol. 84, 1382–1397.

LAUBSCHER H.P. (1969): Mountain building. Tectonophysics 7, 173–182.

LAWRENCE, L.J. (1967): Sulphide neomagmas and highly metamorphosed sulphide deposits. Min. Dep. 2, 5–10.

LE GUEN, M., ORGEVAL, J.–J., LANCELOT, J. (1991): Lead isotope behaviour in a polyphased Pb–Zn ore deposit: Les Malines (Cévennes, France). Mineralium Depos. 26, 180–188.

LEBLANC, M. & ARNOLD, M. (1994): Sulfur isotope evidence for the genesis of distinct mineralizations in the Bleïda stratiform copper deposit (Morocco). Econ. Geol. 89, 931–935.

LEEDER, M.R. (1982): Upper Palaeozoic basins of the British Isles–Caledonide inheritance versus Hercynian plate margin processes. J. Geol. Soc. London 139, 481–490.

LEU, W. (1986): Lithostratigraphie und Tektonik der nordpenninischen Sedimente in der Region Bedretto–Baceno–Visp. Eclogae geol. Helv. 79, 769–824.

LEU, W. (1986): Geologie und Tektonik der Bündnerschiefer–Serien in der Umgebung des Lago del Sabbione (Südlich des Griespasses, Italien). Unpubl. PhD thesis, University of Bern.

LIPPOLT, H.J., SCHORN, U., PIDGEON, R.T. (1983): Genetic implications of new lead isotope measurements on Schwarzwald vein and Upper Triassic sediment galenas. Geol. Rundsch. 72, 77–104.

LOTTERMOSER, B.G. (1992): Rare earth elements and hydrothermal ore formation processes. Ore Geology Reviews 7, 25–41.

LÜTHY, H.J. (1965): Geologie der gotthardmassivischen Sedimentbedeckung und der penninischen Bünderschiefer im Blinnental, Rappental und Binnental (Oberwallis). Unpubl. PhD thesis, University of Bern.

LYDON, J.W. (1983): Chemical parameters controlling the origin and deposition of sediment–hosted stratiform lead–zinc deposits. In: Short Course in Sediment–hosted stratiform lead–zinc deposits, Min. Ass. Can., 175–250.

MANATSCHAL, G. (1995): Jurassic rifting and formation of a passive continental margin (Platta and Err nappes, Eastern Switzerland): geometry, kinematics and geochemistry of fault rocks and a comparison with the Galicia margin. Unpubl. PhD thesis, ETH-Zürich, 220 pp.

MANATSCHAL, G. & KNILL, M. D. (1995): Geochemical characteristics of Mesozoic detachment faults accompamying rifting in the Swiss Alps. Abstract Goldschmidt Conference, Pennsilvania, 1995.

MANTIENNE, J. (1974): La minéralisation thallifère de Jas Roux (Hautes–Alpes). Thèse, Université de Paris, 146 pp.

MARQUER, D. & PEUCAT, J.J. (1994): Rb–Sr systematics of recrystallized shear zones at the greenschist–amphibolite transition: examples from granites in the Swiss Central Alps. Schweiz. Mineral. Petrogr. Mitt. 74, 343–358.

MARQUER, D. (1989): Transfer de matière et déformation des granitoïdes – Aspects méthodoligiques. Schweiz. Mineral. Petrogr. Mitt., 69, 15–35.

MATTE, P. (1991): Accretionary history and crustal evolution of the Variscan belt in Western Europe. Tectonophysics 196, 309–337.

MCGOLDRICK, P.J. (1986): Volatile and precious metal geochemistry of the Mount Isa ores and their host rocks. Unpubl. PhD thesis, University of Melbourne, 236 pp.

MERCOLLI, I., SCHENKER, F., STALDER, H.A. (1984): Geochemie der Veränderung von Granit durch hydrothermale Lösungen. Schweiz. Mineral. Petrogr. Mitt. 64, 67–82.

MILLS, R.A., THOMSON, J., ELDERFIELD, H., HINTON, R.W., HYSLOP, E. (1994): Uranium enrichment in metalliferous sediments from the Mid–Atlantic Ridge. Earth Planet. Sci. Lett. 124, 35–47.

MITRA, A., ELDERFIELD, H., GREAVES, M.J. (1994): Rare earth elements in submarine hydrothermal fluids and plumes from the Mid–Atlantic Ridge. Marine Chemistry 46, 217–235.

NESBITT B., E. (1988): Gold deposit continuum: A genetic model for lode Au mineralization in the Canadian Cordillera. Geology 16, 1044–1048.

NISBETT, E.G. & FOWLER, C.M.R. (1978): The Mid–Atlantic ridge at 37 and 45°N: some geophysical and petrological constraints. Geophys. J. R. astr. Soc. 54, 631–660.

NORMAN, D.I., CONDIE, K.C., SMITH, R.W., THOMMAN, W.F. (1987): Geochemical and Sr and Nd isotopic constraints on the origin of late Proterozoic volcanics and associated tin–bearing granites from the Franklin Mountains, West Texas. Canadian J. Earth Sci. 24, 830–839.

NOWACKI, W. (1965): Ueber neue Mineralien aus dem Lengenbach. Separatdruck aus Jahrbuch des Naturhistorischen Museums Bern, 293–299.

OBERHÄNSLI R. & DIETRICH V. (1975): Geochemische Untersuchungen an Metabasalten der alpinen Ophiolite. Schweiz. Mineral. Petrogr. Mitt. 55, 574–576.

OBERHÄNSLI, R., HOFMANN, B., GRUNER, U. (1985): Ein Massivsulfidvorkommen in der Trias der Präalpen. Schweiz. Mineral. Petrogr. Mitt. 65, 95–110.

OBERLI, F., SOMMERAUER, J., STEIGER, R.H. (1981): U–(Th)–Pb systematics and mineralogy of single crystals and concentrates of accessory minerals from the Cacciola granite, central Gotthard massif, Switzerland. Schweiz. Mineral. Petrogr. Mitt. 61, 323–348.

OHMOTO, H. & LASAGA, A.C. (1982): Kinetics of reactions between aqueous sulfates and sulfides in hydrothermal systems. Cosmochim. Acta 46, 1727–1745.

OHMOTO, H. & RYE, R.O. (1979): Isotopes of sulfur and carbon. In: Barnes, H.L. (ed): Geochemistry of Hydrothermal Ore Deposits. Wiley, New York, 509–567.

O'NEIL, J.R., CLAYTON, R.N., MAYEDA, T.K. (1969): Oxygen isotope fractionation in divalent metal carbonates. J. Chem. Phys. 51, 5547–5558.

PASTORELLI, S., MARTINOTTI, G., PICCARDO, G.B., RAMPONE, E., SCAMBELLURI, M. (in prep): The Geisspfad complex and its relationships with the Monte Leone nappe (Lower Pennine, Western Alps).

PEARCE, J. A. (1980): Geochemical evidence for the genesis and eruptive setting of lavas from Tethyan Ophiolites. In: Panayiotou, A. (ed): Ophiolites. Proc. Int. Ophiol. Symp. Cyprus 1979, 261–272.

PEARCE, J. A. (1983): A «user guide» to basalt discrimination diagrams. Unpubl. report of the Open Univ. Milton Keynes, 37 pp.

PEARCE, J.A., ALLABASTER, T., SHELTON, A.W., SEARLE, M.P. (1981): The Oman ophiolite as a Cretaceous arc–basin complex: evidence and implications. Phil. Trans. R. Soc. Lond. 300, 299–317.

PEARSON, F.J., BALDERER, W., LOOSLI, H.H., LEHMANN, B.E., MATTER, A., PETERS, TJ., SCHMASSMANN, H., GAUTSCHI, A. (1991): Applied isotope hydrogeology. A case study in northern Sitzerland. Studies in Environmental Science 43, Elsevier, 439 pp.

PERETTI, A. & KÖPPEL, V. (1986): Geochemical and lead isotope evidence for a mid–ocean ridge type mineralization within a polymetamorphic ophiolite complex (Monte del Forno, North Italy/Switzerland). EPSL 80, 252–264.

PFEIFFER H.–R., COLOMBI, A., GANGUIN J. (1989): Zermatt–Saas and Antrona Zone: a geochemical comparison of polymetamorphic ophiolites from the Central Alps. Schweiz. Mineral. Petrogr. Mitt. 69, 217–236.

PIRAJNO, F. (1992): Crustal Hydrothermal Fluids and Mesothermal Mineral Deposits, Springer.

PREISWERK, H., (1907): Die Grünschiefer in Jura und Trias des Simplongebietes. Beitr. Geol. Karte der Schweiz 26.

RICKE, W. (1964): Präparation von Schwefeldioxid zur massenspektrometrischen Bestimmung des Schefelisotopenverhältnisses S^{32}/S^{34} in natürlichen Schwefelverbindungen. Z. analyt. Chem. 199, 401–413.

ROBERTSON, J.M. & CONDIE, K.C. (1989): Geology and geochemistry of early Proterozoic volcanic and subvolcanic rocks of the Pecos greenstone belt, Sangre de Cristo Mountains, New Mexico. In: Grambling, J.A. & Tewksbury, B.J. (ed): Proterozoic geology of the southern Rocky Mountains. Geol. Soc. Amer. Spec. Paper 235, Boulder, Colorado, 119–146.

ROLAND, G.W. (1968): The System Pb–As–S–Composition and Stability of Jordanite. Mineral. Deposita 3, 249–260.

RÖSCH, H. & HELLNER, E. (1959): Hydrothermale Untersuchungen am System PbS–As_2S_3. Naturwiss.46, 72.

RUSSELL M. J. & SKAULI H. (1991): A history of theoretical developments in carbonate–hosted base metal deposits an a new tri–enthalpy classification. Econ. Geol. Monogr. 8, 96–116.

RUSSELL, M.J. (1968): Structural controls of base metal mineralization in Ireland in relation to continental drift: Trans Instn. Min. Metall. (Sect.B: Appl. Earth. Sci.) 84, 128–133.

RUSSELL, M.J. (1983): Major sediment–hosted exhalative Zinc and Lead deposits: formation from hydrothermal convection cells that deepen durin crustal extension. In: Short Course in Sediment–hosted stratiform lead–zinc deposits, Min. Ass. Can., 251–282.

SANGSTER, D. F. (1983): Mississippi Valley–type deposits: a geological mélange. In: Kisvarsanyi G., Grant, S.K., Pratt, W. P. Koenig, J. W. (eds): International Conference on Mississippi Valley type lead–zinc deposits. Proc. Vol. Rolla, Univ. of Missouri Rolla, 7–19.

SANGSTER D.F. (1990): Mississippi Valley–type and sedex lead–zinc deposits: a comparative examination. Trans. Inst. Mining. Metallurg. B 99, B21–B42.

SANGSTER, D.F. & LEACH, D.L. (1995): Mississippi Valley–Type Deposits in the Spectrum of Sediment–Hosted Lead–Zinc Deposits. International Field Conference on Carbonate–Hosted Lead–Zinc Deposits, SEG–meeting, 260–263.

SAWKINS, F.J. (1990): Metal deposits in relation to plate tectonics. 2nd ed. Springer, Berlin, Heidelberg, New York, 461 pp.

SCHADE, J. CORNELL, D.H., THEAT, H.F.J. (1989): Rare Earth Element and Isotopic Evidence for the Genesis of the Prieska Massive Sulfide Deposit: South Africa. Eco. Geology 84, 49–63.

SCHALTEGGER, U. (1990): Post–magmatic resetting of Rb–Sr whole rock ages–a study in the Central Aar Granite (Central Alps, Switzerland). Geologische Rundschau 79/3, 709–724..

SCHMIDT, M.W. (1992): Amphibolite composition in tonalite as a function of pressure: an experimental calibration of the Al–in–hornblende–barometer: Contribution Mineral. Petrol. 110, 304–310.

SCHNEIDER, H. J. (1964): Facies differentiation and controlling factors for the depositional lead–zinc concentration in the Ladinian geosyncline of the Eastern Alps. In: Amstutz G.C. (ed): Sedimentology and ore genesis. Elsevier, Amsterdam, 29–45.

SCHROLL, E. (1983): Geochemical characterization of the Bleiberg type and other carbonate hosted lead–zinc–mineralizations. In: Schneider, H.–J. (ed): Deposits of the Alps and of the Alpine Epoch in Europe. Springer, Berlin Heidelberg, 189–197.

SCHROLL, E., SCHULZ, O., PAK, E. (1983): Sulphur isotope distribution in the Pb–Zn–deposit Bleiberg (Carinthia, Austria). Mineralium Depos. 18, 17–25.

SCOTT, S.D. (1983): Chemical behaviour of sphalerite and arsenopyrite in hydrothermal and metamorphic environments. Mineral. Mag. 47, 427–435.

Schütz, W., Dulski, P. & Germann, K. (1988): Geochemical Features of Magmatic Evolution and Ore Deposition in the Pyrite Belt of Southern Spain. In: Friedrich, G.H. & Herzig, P.M.(eds): Base Metal Sulfide Deposits, Springer-Verlag, Berlin. 245–247.

SEELIGER, E. (1963): Die Paragenese der Pb–Zn–Erzlagerstätte am Gänsberg bei Wiesloch (Baden) und ihre genetischen Beziehungen zu den Gängen im Odenwaldkristallin, zu Alt Wiesloch und der Vererzung der Trias des Draichgaues. Jh. Geol. Landesamt Baden–Württemberg 6, 239–299.

Shaw, D.M. (1972): The Origin of the Apsley Gneiss, Ontario. Can. J. Earth Sci. 9, 18–35.

SHERVAIS J.W. (1982): Ti–V plots and the petrogenensis of modern and ophiolitic lavas. EPSL 59, 101–118.

STACEY, J.S. & KRAMERS, J.D. (1975): Approximation of terrestrial lead isotope evolution by a two stage model. Earth Planet. Sci. Lett. 26, 107–221.

STALDER, H.A., IMHOF, J., NIGGLI, E., GRAESER, S., ARNOTH, J., NOWACKI, W. (1969): Die Mineralfundstelle Lengenbach im Binntal. Jahrb. Naturhist. Mus. Bern 1966–1968, 235–316.

STEIGER R.H. & JÄGER, E. (1977): Subcomission on geochronology: Convention on the use of decay constants in geo–and cosmochronology, Earth Planet. Sci. Lett. 36, 359–362.

STILLMAN, C.J. & WILLIAMS, C.T. (1978): Geochemistry and tectonic setting of some Upper Ordovician volcanic rocks in East and Southeast Ireland. EPSL 41, 288–310.

STRECKEISEN, A., KRAMERS, J. HUNZIKER, J.C., FRANK, E (1978): Gantergneis und Eistengneis im Simplongebiet. Schweiz. Mineral. Petrogr. Mitt. 58, 396–401.

SUNDBLAD, K., ZACHRISSON, E., SMEDS, S.A., BERGLUND, S., ALINDER, C. (1984): Sphalerite geobarometry and arsenopyrite geothermometry applied to metamorphosed sulfide ores in the Swedish Caledonides. Econ. Geol. 79, 1660–1668.

SYLVESTER, P.J., ATTOH, KODJO, SCHULZ, K.J. (1987): Tectonic setting of late Archean bimodal volcanism in the Michipicoten (Wawa) greenstone belt, Ontario. Canadian J. Earth Sci. 24, 1120–1134.

TAYLOR, S.R. & MCLENNAN, S.M. (1985): The continental crust: its composition and evolution. Blackwell, Oxford, 312 pp.

THURSTON, P.C. & FRYER, B.J. (1983): The geochemistry of repetive cyclal volcanism from basalt through rhyolite in the Uchi–Confederation greenstone belt. Canad. Contrib. Mineral. Petrol. 83, 204–226.

TRÜMPY, R. (1980): An outline of geology of Switzerland. In: Geology of Switzerland: A guide–book, Basel, Wepf, 104 pp.

TUREKIAN, K. & WEDEPOHL, H. (1961): Distribution of the Elements in some Major Units of the Earth's Crust. Bull. geol. Soc. Am. 72, 175–192.

VANCE, D. & O'NIONS, R.K. (1992): Prograde and retrograde thermal histories from the Central Swiss Alps. Earth Planet. Sci. Lett. 114, 113–129.

VEIZER, J. & HOEFS, J. (1976): The nature of O^{18}/O^{16} and C^{13}/C^{12} secular trends in sedimentary carbonate rocks: Geochim. Cosmochim. Acta 40, 1387–1395.

VOGLER, R. (1986): Spröd/Duktil–Uebergang bei der Deformation von Metadolomiten des Adamello. Schweiz. Mineral. Petrogr. Mitt. 66, 475–477.

VOKES, F.M. (1971): Some Aspects of the Regional Metamorphic Mobilization of Preexisting Sulfide Deposits. Mineral. Deposita. 6, 122–129.

WEDEPOHL, F. (1976): Handbook of Geochemistry. Springer. Berlin Heidelberg New York.

WEISSERT H.J. & BERNOULLI D. (1985): A transform margin in the Mesozoic Tethys: evidence from the Swiss Alps. Geol. Rundsch. 74 (3), 665–679.

WHITE, D.E. (1981): Active Geothermal Systems and Hydrothermal Ore Deposits. Econ. Geol. 57th Anniv. Vol., 392–423.

WINCHESTER, J. A. & FLOYD P.A. (1977): Geochemical discrimination of different magma series and their differentiation products using immobile elements. Chem. Geol. 20, 325–343.

ZEEH, S. & BECHSTÄDT, T. (1994): Carbonate–Hosted Pb–Zn Mineralization at Bleiberg–Kreuth (Austria): Compilation of Data and New Aspects. In: Fontboté, L. & Boni, M. (eds): Sediment–Hosted Zn–Pb Ores. Spec. Publ. No. 10 Soc. Geol. Applied to Min.Deposits, Springer, 271–299.

APPENDIX 1:
ANALYTICAL TECHNIQUES

A1.1 U and Pb isotopes

A1.1.1 Pb separation techniques

Mineral fractions for all isotopic analyses were obtained by selection of optically pure crystals from hand specimens, or by hand-picking from heavy mineral concentrates. Pure samples of pyrite, galena, sulfosalt, tourmaline, dolomite and feldspar were cleaned ultrasonically in water and dissolved in hot aqua regia or in a hot mixture of HCl:HF:HNO_3 = 9:1:0.01.

A1.1.1.1Plating

Up to 0.02 g of sulphosalt or galena were dissolved in an open beaker in HCl and HNO_3. The dried residue was dissolved overnight in a few drops of perchloric acid and 3 ml H_2O. The solution was treated in an ultrasonic bath. After centrifuging, the Pb was separated by electrodeposition on a Pt-Anode as PbO. The shaking of the covered teflon beakers during electroplating guaranteed a constant strength of the electric current (fig. A1.1). PbO was stripped with a 2% mixture of H_2O_2 and HNO_3. The solution was then dried at low temperature. Total blank amounted to 400–800 pg Pb.

A1.1.1.2 HBr-chemistry

The solution of whole rock samples and mineral fractions were passed twice through a preconditioned 0.5 ml quartz anion exchange column according to following procedure:

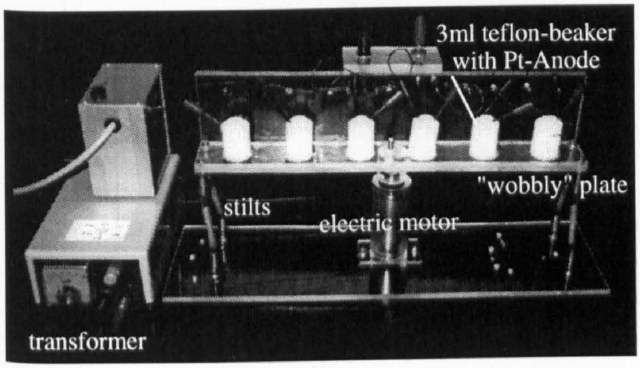

Figure A1.1: Plating equipment for the modified electrodeposition technique after CUMMING *et al. (1987). The appliance operates at 60 to 80 revolutions per minute.*

AG 1x8, 200-400 mesh DOWEX anion exchange resin

1st step: clean up	2 ml	H_2O IR
	2 ml	H_2O IR
	2 ml	HCl suprapur (9.4N)
	2 ml	H_2O IR
	2 ml	H_2O IR
	0.5 ml	HCl (6N)
	0.5 ml	HCl (6N)
	0.5 ml	HCl (6N)
	0.5 ml	HCl (6N)
2nd step: precondition	0.5 ml	HBr (1N)
3rd step: sample in	1.5 ml	HBr (1.5N):HCl (2N) (12:1) mixture
4th step: cleaning	0.75 ml	HBr (1N)
	0.75 ml	HBr (1N)
	0.5 ml	HCl (2N)
	0.1 ml	HCl (6N)
collect Pb	1.5 ml	HCl (6N)

The sample was evaporated on a hot plate at 100°C and again taken up in 0.25 ml of a HBr-HCl mixture. The quantity of the anion exchange resin was reduced by 50% for the second run and correspondingly less of reageants were used for the extraction. Total blank amounted to 300–600 pg Pb.

A1.1.2 HBr-microchemistry for uraninites

All uraninites were cleaned ultrasonically before a mixed ^{235}U-^{205}Pb spike was added. The samples were dissolved in a hot HCl-HNO_3-mixture (0.2 ml, 3:1) and afterwrds evaporated to dryness. U and Pb were separated in a teflon anion exchange column:

AG 1x8, 200-400 mesh DOWEX anion exchange resin

1st step: clean up	0.75 ml	H_2O IR
	0.75 ml	H_2O IR
	1 ml	HCl suprapur (9.4N)
	0.75 ml	H_2O IR
	0.75 ml	H_2O IR
	0.25 ml	HCl (7.5N)
	0.25 ml	HCl (7.5N)
2nd step: precondition	0.1 ml	HBr (1N)
	0.1 ml	HBr (1N)
3rd step: sample in	0.3 ml	HBr (1.5N):HCl (2N) (12:1) mixture

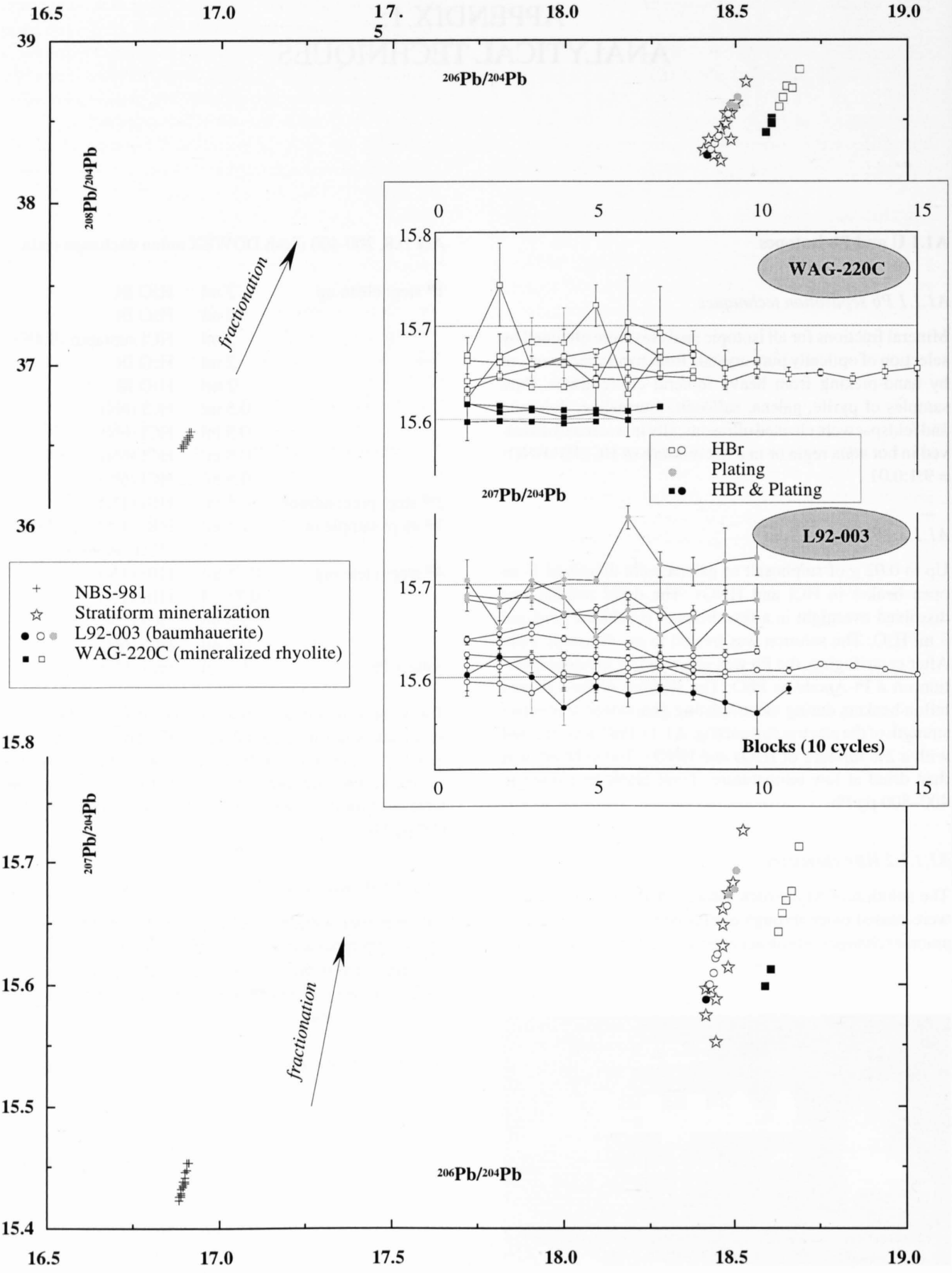

Figure A1.2: Pb isotope diagrams of mineralized whole rock sample WAG-220C and baumhauerite sample L92-003 performed by different separation techniques (plating and HBr-chemistry). The fractionation-trends recorded by 22 NBS-981 standards are shown for reference.

4th step: cleaning and collect U	0.5 ml	HBr (1N)
	0.1 ml	HCl (2N)
	0.02 ml	HCl (7.5N)
collect Pb	0.3 ml	HCl (7.5N)

U was diluted and loaded directly on the filament. Total blank amounted 150 to 170 pg Pb and 0.1 to 2 pg U.

A1.1.3 Measurement

U and Pb isotope ratios were determined using a Finnigan MAT 261 mass spectrometer at the Institute of Isotope Geology and Mineral Resources of the ETH Zürich.

10 to 50 ng of U was loaded together with silica-gel on a single Re filament with dilute H_3PO_4. A double Faraday cup method was used for these measurements.

Pb was loaded together with silica-gel on Re single filaments. Masses 204, 205, 206, 207 and 208 were measured simultaneously on Faraday cups. For U and Pb concentrations a mixed ^{235}U-^{205}Pb spike was used. During heating, the mass 203 was monitored to control ^{205}Tl. The temperature of the filaments was controlled by a pyrometer during heating and mesurement. Maximum temperature was 1270°C but normally Pb was measured at 1200°C after ^{205}Tl decayed to zero intensity at about 1150°C. Fractionation effects which amounted to 0.114% per mass unit were corrected according to measurements of the NBS SRM 981 lead. The reproducibility of 22 standards measurements is:±0.09% for $^{206}Pb/^{204}Pb$,±0.12% for $^{207}Pb/^{204}Pb$ and±0.18% for $^{208}Pb/^{204}Pb$ at a 2 sigma level.

A1.1.4 Fractionations during analytical procedure

Nine analyses of a massive sulfosalt sample (baumhauerite) from the Lengenbach deposit showed a variation of the fractionation depending on the chemical treatment. Pb separated by plating produced higher fractionation than Pb separated by the HCl-HBr anion exchange technique. The lowest $^{207}Pb/^{204}Pb$ resp. $^{208}Pb/^{204}Pb$ were measured after a combined HBr and plating technique (fig. A1.2). The reproducibility of all 9 measurements is ±0.41% for $^{207}Pb/^{204}Pb$ at a 2 sigma level. During measurements, no fractionation trends were observed. Therefore, fractionation on the filament during heating explains best the elevated μ-values of several mineralized whole rock samples and ore minerals. The data of these experiments indicate a correlation of fractionation effects with a contamination of other elements than Pb.

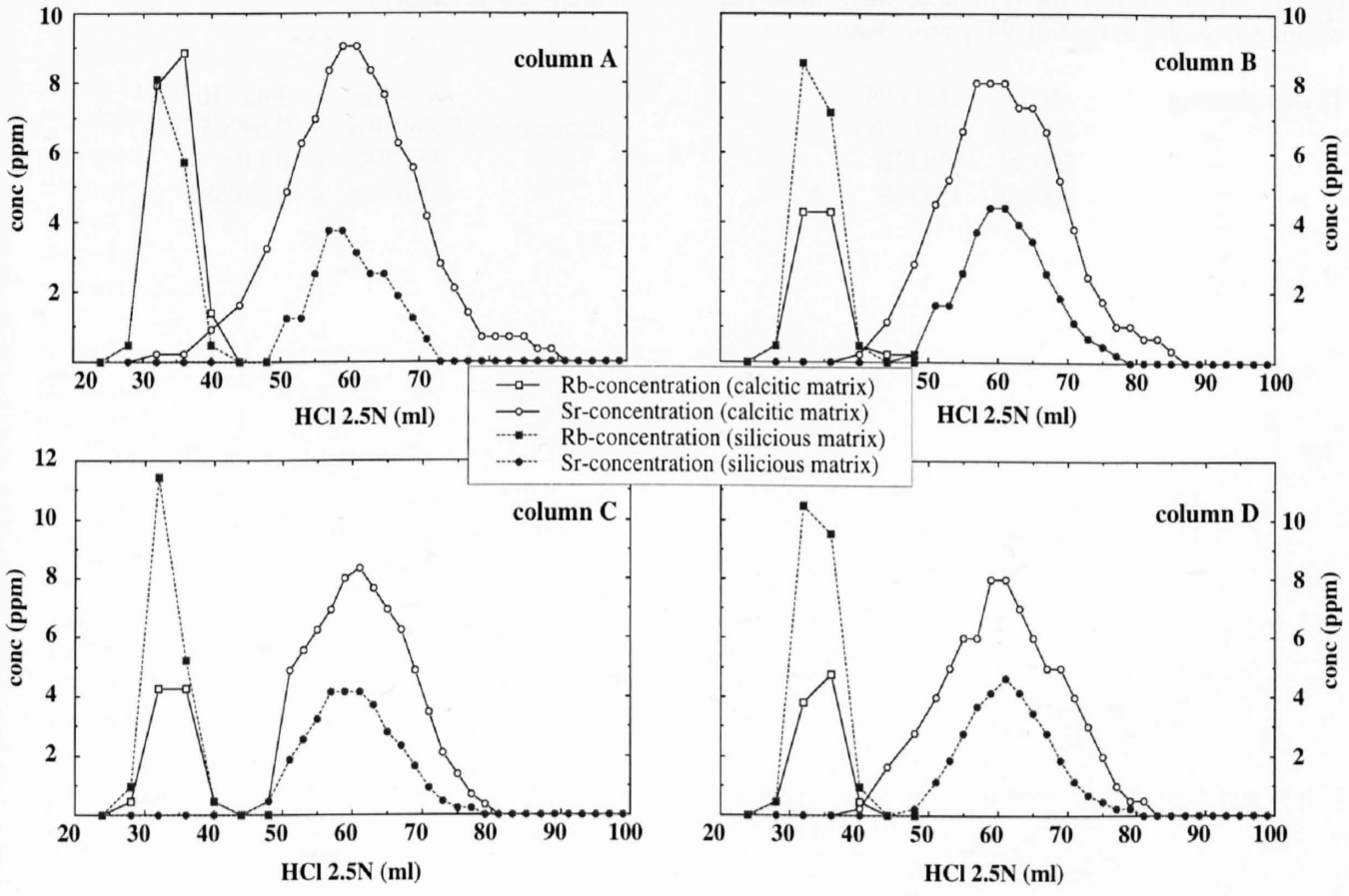

Figure A1.3: Calibration curves for Rb and Sr in four different quartz columns with 25ml AG50Wx12 cation exchange resin (200-400 mesh BIO RAD).

A1.1.5 Tracer

For determining U and Pb concentrations a mixed 531:1 = ^{235}U:^{205}Pb tracer was used, in which ^{205}Pb was enriched to 99.695% of total Pb.

A1.1.6 Decay constants

The decay constants and isotopic ratios for U-Pb were taken from STEIGER & JÄGER (1977):

$$\lambda\,(^{235}U) = 9.8485 \cdot 10^{-10}\ a^{-1}$$
$$\lambda\,(^{238}U) = 1.55125 \cdot 10^{-10}\ a^{-1}$$
$$\text{atomic ratio } ^{238}U/^{235}U = 137.88$$

A1.2 Rb and Sr isotopes

A1.2.1 Rb-Sr separation technique

Sr was separated from the solution using cation-exchange resin columns. For the separation of Rb and Sr four quartz columns with 25 ml of AG50Wx12 cation exchange resin (200–400 mesh BIO RAD) was used. All columns were calibrated with different matrix compositions by AAS (fig. A1.3). The calibration showed similar peak positions for all columns, independent of the major element composition.

Prior to sample loading, the resin underwent multi-step washing according to the following procedure:

1st step cleaning	150 ml	HCl (4N)
	100 ml	HCl (4N)
	200 ml	H_2O IR
	200 ml	H_2O IR
2nd step precondition	50 ml	HCl (2.5N)
	50 ml	HCl (2.5N)

After passing the centrifuged sample solution through the column, Rb and Sr were eluted by the following procedure:

	2 ml	HCl (2.5N) with sample
Rb-extraction	58 ml	HCl (2.5N)
Sr-extraction	22 ml	HCl (2.5N)

A1.2.2 Measurement

Sr was loaded with 0.25N HCl on a Re double-filament and analyzed by double collectors jumping mode in a Finnigan MAT 261 mass spectrometer at the Institute for Isotope Geology and Mineral Resources of the ETH Zürich. Measured $^{87}Sr/^{86}Sr$ ratios were normalized to $^{88}Sr/^{86}Sr = 8.37521$. 17 analyses of the Sr standard NBS-987 during this study yielded a mean $^{87}Sr/^{86}Sr$ ratio of 0.71025 ± 0.00002 (accepted value 0.710250, HOERNLE & TILTON, 1991). Measured ratios in samples were therefore not adjusted. Rb and Sr concentrations were determined by XRF and ICP-OES methods respectively.

A1.2.3 Decay constants

The decay constants and isotopic ratios for Rb-Sr were taken from STEIGER & JÄGER (1977):

$$\lambda\,(^{87}Rb) = 1.42 \cdot 10^{-11}\ a^{-1}$$
$$\text{atomic ratios } ^{85}Rb/^{87}Rb = 2.59265$$
$$^{86}Sr/^{88}Sr = 0.1194$$
$$^{84}Sr/^{86}Sr = 0.056584$$

APPENDIX 2:
DATA TABLES

Table A2.1: Microprobe analyses of massive sulfosalt ore from the Lengenbach deposit. The localization of analyses along profiles is shown in figure I.5.

probe	*Pb* (wt%)	*Sb* (wt%)	*S* (wt%)	*As* (wt%)	*Tl* (wt%)	*Ag* (wt%)	*Tot*	*(Pb mol%)* Pb = Pb+Tl+Ag+Sb in Pb-As-system	*assumed mineral* identification based on microprobe analyses only
massive to discordant sulfosalt (1989, 1990, 1991)									
LB-E1	51.20	0.57	24.09	24.17		0.16	100.19	60.8	rathite II
LB-E1	50.67	0.42	24.33	24.59		0.15	100.15	60.1	rathite II
LB-E1	51.49	0.50	24.30	24.86		0.17	101.32	60.3	rathite II
LB-E4	50.46	0.53	25.30	24.75		0.07	101.10	59.9	rathite II
LB-E4	50.67	0.47	24.03	24.70		0.25	100.13	60.1	rathite II
LB-E4	50.09	0.44	24.21	24.91		0.26	99.93	59.6	rathite II
LB-E5	50.39	0.59	24.54	24.59		0.11	100.20	60.0	rathite II
LB-E5	50.54	0.46	24.19	25.02		0.15	100.37	59.7	rathite II
LB-E5	50.16	0.48	24.01	24.09		0.21	98.96	60.4	rathite II
LB-E6	49.41	0.52	24.25	24.56		0.27	99.02	59.6	rathite II
LB-E6	49.57	0.46	24.21	24.38		0.18	98.81	59.8	rathite II
LB-E6	50.70	0.49	24.19	24.61		0.21	100.20	60.2	rathite II
L92-009-1	44.39	0.71	26.26	29.07	3.41	0.06	103.90	54.7	baumhauerite ?
L92-009-2	42.84	0.75	26.77	29.09	3.61	0.00	103.07	54.0	baumhauerite ?
L92-009-3	43.13	0.50	25.11	26.45	1.35	3.69	100.23	57.1	baumhauerite-2a
L92-009-4	42.85	0.51	25.27	26.68	1.93	3.81	101.05	57.1	baumhauerite-2a
L92-009-5	41.70	0.49	25.26	25.98	1.68	3.64	98.75	56.9	baumhauerite-2a
L92-009-6	39.80	0.77	26.45	29.12	3.93	0.08	100.14	52.5	baumhauerite ?
L92-009-7	40.88	0.49	25.66	26.32	0.99	3.98	98.32	56.0	baumhauerite-2a
L92-009-8	41.17	0.56	25.28	25.97	1.29	3.87	98.14	56.6	baumhauerite-2a
L92-008-1	45.58	0.54	24.97	25.24	0.45	0.17	96.94	57.3	baumhauerite
LEN-901-2	39.52	0.52	26.36	29.02	2.33	0.02	97.77	51.4	sartorite
LEN-901-3	38.85	0.64	27.02	29.05	2.59	0.12	98.26	51.2	sartorite
LEN-23a-1	41.33	1.21	25.99	28.40	1.32	0.02	98.27	52.8	sartorite
LEN-23a-2	40.67	1.01	26.19	28.53	1.75	0.15	98.29	52.5	sartorite
profiles across massive sulfosalt accumulation (sample: LEN)									
LEN-S1	0.00	0.00	28.77	63.86	0.00	0.05	92.67	0.1	realgar
LEN-S2	34.48	0.51	26.47	30.7:	7.08	0.01	99.34	49.7	sartorite
LEN-S3	35.12	0.61	26.17	30.43	6.70	0.00	99.02	50.2	sartorite
LEN-S4	0.00	0.00	30.65	13.32	0.03	1.01	45.01	5.4	tennantite
LEN-S5	38.67	0.64	25.55	27.04	2.53	3.85	98.28	55.0	baumhauerite-2a
LEN-S6	33.66	0.51	26.32	30.55	6.61	0.04	97.69	49.2	sartorite
LEN-S7	0.00	0.03	29.17	65.49	0.00	0.04	94.73	0.1	realgar
LEN-P0	37.25	0.65	25.77	28.83	4.00	0.00	96.50	51.2	sartorite
LEN-P1	37.25	0.68	26.07	29.52	4.54	0.05	98.0	51.0	sartorite
LEN-P2	39.63	0.62	26.25	29.44	3.87	0.12	99.94	52.1	sartorite
LEN-P3	39.20	0.49	25.21	26.54	1.34	3.77	96.54	55.0	baumhauerite-2a

Table A2.2: Microprobe analyses of melt inclusions in quartz from the Lengenbach deposit (from HOFMANN, 1994 and pers. comm.)

probe	*Cu* (wt%)	*S* (wt%)	*Fe* (wt%)	*Se* (wt%)	*Zn* (wt%)	*Hg* (wt%)	*Pb* (wt%)	*Sb* (wt%)	*As* (wt%)	*Tl* (wt%)	*Ag* (wt%)	*(Pb mol%)* Pb=Pb+Tl+Ag+Sb in Pb-As-system
1	0.67	33.45	0.06	0.08	0.00	0.03	6.65	0.39	49.20	2.34	0.56	12.7
2	0.61	32.94	0.00	0.19	0.17	0.20	6.86	0.41	48.80	3.78	0.62	14.7
3	1.25	31.73	0.05	0.11	0.15	0.00	14.72	0.50	43.49	3.66	0.95	24.8
4	0.98	31.68	0.00	0.19	0.09	0.17	15.23	0.54	44.06	4.69	0.77	25.8
5	1.03	31.60	0.00	0.14	0.00	0.00	15.37	0.54	43.62	4.51	0.99	26.2
6	0.24	34.93	0.05	0.16	0.03	0.00	6.93	0.36	53.05	1.93	0.06	11.2
7	0.20	36.21	0.00	0.18	0.00	0.05	5.68	0.36	52.94	2.38	0.15	10.5
8	1.58	33.41	0.00	0.16	0.12	0.09	10.94	0.45	44.42	4.45	0.79	21.3
9	1.11	33.00	0.07	0.25	0.01	0.00	5.29	0.32	49.13	5.19	0.51	14.3
10	0.33	26.49	0.02	0.09	0.01	0.00	23.98	0.76	31.78	12.51	1.50	46.9
11	0.59	34.37	0.00	0.22	0.02	0.06	8.74	0.35	48.99	2.74	0.47	15.4
12	2.66	27.37	0.05	0.06	0.10	0.12	20.41	0.61	33.43	4.96	1.52	37.3
13	0.44	33.59	0.00	0.12	0.19	0.17	13.33	0.44	45.73	2.60	0.39	21.0
14	0.06	38.74	0.07	0.25	0.09	0.07	0.24	0.25	54.40	1.21	0.20	2.5
15	1.86	28.65	0.01	0.07	0.24	0.00	21.19	0.50	39.19	5.54	1.02	34.3
16	0.43	34.02	0.06	0.23	0.00	0.04	13.14	0.29	48.64	2.31	0.31	19.3
17	0.74	32.21	0.01	0.24	0.14	0.00	14.83	0.41	46.94	2.50	0.44	21.9
18	0.50	33.73	0.01	0.16	0.10	0.00	15.30	0.40	46.34	1.97	0.21	21.8
19	0.79	32.62	0.08	0.14	0.00	0.11	13.27	0.39	48.04	2.51	0.39	20.0
20	1.00	29.01	0.12	0.00	0.48	0.00	22.79	0.45	40.44	2.71	0.58	32.2
21	0.74	32.19	0.05	0.18	0.13	0.03	15.68	0.39	44.21	2.62	0.53	23.9
22	1.30	27.23	0.02	0.07	0.21	0.00	27.17	0.58	32.27	5.39	1.25	43.5
23	2.42	28.70	0.09	0.09	0.37	0.07	24.96	0.61	34.16	6.19	1.75	41.5
24	0.32	35.50	0.04	0.16	0.07	0.14	4.35	0.47	52.19	3.57	0.20	10.6
25	4.24	23.28	0.06	0.13	0.41	0.00	32.00	0.81	24.67	10.04	0.49	56.0
26	0.20	36.09	0.00	0.23	0.01	0.12	1.84	0.29	56.91	1.92	0.09	5.0
27	0.64	36.36	0.00	0.19	0.09	0.08	2.36	0.43	52.87	3.57	0.2	8.3
28	0.44	36.84	0.00	0.18	0.27	0.00	1.80	0.28	52.15	3.66	0.29	7.7
29	0.84	27.15	0.08	0.07	0.64	0.08	18.83	0.72	34.57	7.73	7.58	42.2
30	0.73	27.62	0.04	0.18	0.38	0.09	19.60	0.70	33.48	7.39	7.08	42.9
31	1.10	27.47	0.15	0.13	0.45	0.00	18.20	0.58	33.44	6.83	7.60	41.8
32	1.23	25.71	0.00	0.13	0.69	0.00	27.90	0.85	28.80	11.30	0.40	50.4
33	1.07	25.35	0.00	0.14	0.17	0.00	29.63	0.95	28.80	10.46	0.33	51.0
34	0.22	24.94	0.00	0.07	0.00	0.19	36.81	1.23	28.18	7.95	0.03	54.2
35	0.00	24.90	0.03	0.19	0.00	0.11	34.18	1.29	28.81	8.28	0.01	52.3
36	0.02	26.14	0.00	0.04	0.05	0.00	31.60	0.93	30.78	8.36	0.00	49.0
37	0.00	26.02	0.00	0.07	0.00	0.02	31.86	0.88	30.22	7.61	0.08	49.2

Table A2.3a: Geochemical composition of whole rock samples from the Lengenbach deposit. All samples are from the Lengenbach quarry except LB32, LB-33 (Turtschi) and HB-209 (1km north of Heiligkreuz). n.d. = not determined

sample	*zone*	*remarks*	*Na* (%)	*Al* (%)	*K* (%)	*Ti* (%)	*Fe* (%)	*Li* ppm	*Be* ppm	*B* ppm	*V* ppm	*Cr* ppm	*Mn* ppm	*Co* ppm	*Ni* ppm	*Cu* ppm
LB1	As-(III)	massive Py	0.0	0.60	0.43	0.02	29.6	12	5.1	31	38	30	92	42	59	5
LB21	As-(III)	massive Py	0.0	n.d.	n.d.	n.d.	39.7	n.d.	n.d.	n.d.	n.d.	<20	n.d.	22	41	n.d.
LB2	As-(III)		0.0	0.47	0.34	0.01	1.9	14	1.2	20	20	24	452	2	12	91
LB3	As-(III)		0.0	0.45	0.29	<0.01	2.1	15	1.2	<10	20	24	508	5	11	65
LB5	As-(III)		0.0	0.58	0.11	<0.01	2.0	7	1.0	<10	13	23	474	2	13	60
LB7	As-(III)		0.3	0.50	0.29	<0.01	1.5	16	0.7	<10	16	21	588	<1	11	255
LB9	As-(III)		0.0	0.35	0.21	<0.01	3.3	11	1.2	61	22	24	394	4	12	214
LB17	As-(III)	50kg	0.3	0.27	0.26	<.01	3.1	14	1.4	17	15	21	454	<1	14	101
LB22	As-(III)		0.3	n.d.	n.d.	n.d.	17.0	n.d.	n.d.	n.d.	n.d.	<110	n.d.	20	69	n.d.
LB24	As-(III)		0.1	n.d.	n.d.	n.d.	15.0	n.d.	n.d.	n.d.	n.d.	<20	n.d.	7	39	n.d.
LB25	As-(III)		0.0	0.25	0.10	<0.01	4.1	6	1.0	10	12	15	469	4	9	192
LB26	As-(III)		0.0	0.22	0.08	<0.01	3.7	5	1.0	<10	11	15	458	5	9	299
LB8	SIL	As-rich	0.1	3.38	1.81	0.10	6.6	75	6.1	42	69	39	208	7	22	24
LB23	SIL	As-rich	0.2	n.d.	n.d.	n.d.	10.0	n.d.	n.d.	n.d.	n.d.	66	n.d.	10	54	n.d.
LB19	SIL		0.2	3.20	2.00	0.06	7.3	65	5.3	21	60	42	248	10	30	4
LB6	IR	Py, Ssa	0.3	0.15	0.19	<0.01	2.2	<1	0.7	<10	13	19	629	<1	7	263
LB10	IR		0.3	0.10	0.19	<0.01	1.0	11	0.6	<10	7	18	567	<1	18	66
LB16	IR	Py	0.0	0.12	0.08	<0.01	8.2	3	3.6	<10	18	27	530	2	16	1
LB14	IR	Py, Ssa	0.0	0.13	0.08	<0.01	7.1	9	2.0	<10	22	24	539	7	20	51
LB18	IR		0.3	0.80	0.75	0.02	0.5	30	1.5	26	24	26	472	<1	3	11
LB20	IR		0.0	n.d.	n.d.	n.d.	6.6	n.d.	n.d.	n.d.	n.d.	47	n.d.	12	<44	n.d.
LB27	IR		0.1	1.39	0.75	0.03	4.2	35	2.4	19	46	19	621	15	17	10
LB28	IR		0.1	1.10	0.66	0.03	1.4	25	2.1	31	26	20	408	4	8	9
LB29	IR	fuchsitic	0.0	0.44	0.14	<0.01	1.3	11	0.9	<10	91	76	677	5	6	2
LB4	RED	Apy, Po	0.0	0.31	0.27	<0.01	7.9	9	2.5	<10	54	23	229	3	14	491
LB11	RED	Mag	0.0	0.31	0.25	<0.01	24.4	27	4.7	<10	64	30	304	2	27	4
LB12	RED	Mag	0.0	0.39	0.32	0.02	46.1	29	9.2	10	141	36	240	<1	29	6
LB13	RED	Apy	0.3	0.48	0.48	0.01	2.0	36	0.8	<10	42	29	613	<1	12	10
LB15	RED	Mag	0.0	0.29	0.28	0.01	25.6	10	5.4	<10	143	28	250	2	13	213
LB30	UM		0.2	0.74	0.78	<0.01	0.4	39	1.0	11	19	16	282	4	5	5
LB31	UM	graphitic	0.2	0.63	0.73	<0.01	0.4	34	<0.5	<10	21	14	328	13	4	2
LB32	UM		0.2	0.60	0.69	0.02	0.5	36	1.0	<10	11	16	380	<1	11	<1
LB33	UM	graphitic	0.2	0.82	0.62	<0.01	0.5	28	1.0	<10	18	14	592	2	1	11
HB-209	UM		n.d.	0.44	0.32	0.02	0.3	6	n.d.	n.d.	5	14	n.d.	5	11	<1

Table A2.3b: Geochemical composition of whole rock samples from the Lengenbach deposit.

sample	*Zn* ppm	*Ga* ppm	*As* ppm	*Rb* ppm	*Sr* ppm	*Mo* ppm	*Ag* ppm	*Cd* ppm	*Sn* ppm	*Sb* ppm	*Cs* ppm	*Ba* ppm	*Hg* ppm	*Tl* ppm	*Au* ppb	*Pb* ppm	*Bi* ppm	*Th* ppm	*U* ppm
LB1	74000	<3	177	20	1880	8	2.8	87.0	<5	20	1.2	67000	1.95	10.8	<3	383	<5	<0.2	1.1
LB21	<100	n.d.	222	<5	n.d.	8	<2	<5	n.d.	0.3	<.5	7760	n.d.	n.d.	<3	n.d.	n.d.	<0.2	1.4
LB2	6290	18	4420	12	422	2	126.2	26.8	13	103	<.5	9650	3.15	221	<5	9383	<5	0.5	6.9
LB3	781	22	8680	12	722	3	178.3	14.3	<5	144	<.5	27700	3.63	277	<5	11800	<5	1.1	6.6
LB5	2493	22	8160	9	350	3	176.6	16.7	6	145	<.5	6800	6.41	357	<5	14100	<5	<0.2	5.5
LB7	961	14	2246	6	313	4	71.3	10.8	<5	47.0	<.5	3800	4.00	144	<5	3948	94	0.5	7.7
LB9	2568	36	9400	<5	369	4	186.8	21.8	5	225	<.5	5900	5.26	284	<10	26700	<5	0.6	10.0
LB17	428	17	4420	7	362	5	68.9	8.9	<5	84	<.5	4300	2.26	197	<5	5528	82	<0.2	8.1
LB22	<100	n.d.	4790	86	n.d.	12	46.0	<14	n.d.	62.7	3.9	54900	n.d.	n.d.	4	n.d.	n.d.	9.3	35.9
LB24	160	n.d.	2930	<14	n.d.	9	28.0	<5	n.d.	41.2	<.5	690	n.d.	n.d.	<3	n.d.	n.d.	<.6	3.3
LB25	272	24	8700	<17	629	<1	155.0	<.5	2	177	<0.5	11300	3.03	355	<15	11250	<5	<1.3	6.8
LB26	325	71	27400	<48	627	<1	426.0	<.5	6	642	<2.5	12700	6.71	961	<44	59300	<5	<3.9	7.7
LB8	72	29	5090	86	673	9	93.6	7.2	6	97	2.9	25300	0.96	325	<5	5795	6	7.3	124.0
LB23	<100	n.d.	2230	130	n.d.	7	30.0	<5	n.d.	24	2.7	36800	n.d.	n.d.	<3	n.d.	n.d.	8.0	80.6
LB19	108	19	37	82	645	4	1.4	1.1	<5	1.9	2.4	28700	0.04	51.2	<2	86	<5	6.1	32.0
LB6	140	27	5960	<5	123	<1	137.9	22.8	10	277	<.5	192	3.78	64.3	<5	15700	87	<.2	7.2
LB10	91	15	1217	<5	182	2	29.1	9.4	<5	94	<.5	83	1.48	30.4	<5	4552	90	<.2	5.2
LB16	242	13	53	<5	260	<1	<.2	<.5	<5	0.6	<.5	3600	0.02	2	<2	124	<5	<.2	1.6
LB14	140	17	2260	<5	384	3	34.6	5.6	<5	85	<.5	11100	1.26	21.1	<5	3934	<5	<.2	2.7
LB18	48400	<3	39	27	249	4	0.5	21.2	<5	8.1	5300	0.11	12.5	<2	511	93	1.3	4.2	
LB20	>90000	n.d.	79.3	<17	n.d.	12	227	1190.0	n.d.	270	<1.3	>90000	n.d.	n.d.	4	n.d.	n.d.	<1	<.5
LB27	41900	<3	150	37	751	6	75.0	47.0	<2	63	3.2	20800	1.90	23	<2	24200	<5	1.1	5.9
LB28	11802	6	195	32	156	3	5.0	5.0	<2	34	1.5	2100	0.11	7	<2	1927	<5	<2	4.7
LB29	1372	11	50	10	608	<1	7.0	3.0	<2	1.7	<0.5	15700	0.08	7	4	124	<5	<0.2	2.5
LB4	225	13	5720	31	99	2	3.1	7.6	<5	<0.5	5.4	161	0.02	6.7	<5	138	<5	0.7	7.6
LB11	380	14	47	16	406	<1	0.6	2.9	<5	0.4	4.0	6400	0.01	12.3	<2	101	<5	<0.2	6.1
LB12	474	19	44	25	255	2	0.6	4.0	8	1.9	5.6	5600	0.02	19.4	<2	118	<5	0.7	13.0
LB13	84	13	552	21	166	5	1.4	5.9	<5	0.3	1.9	110	<0.005	4.3	<2	172	90	0.9	6.2
LB15	986	13	127	21	100	<1	2.1	1.9	<5	1.0	4.6	149	0.09	8.6	<2	101	<5	0.6	15.0
LB30	58	14	1.4	25	129	<1	<0.2	<0.5	n.d.	<0.1	1.2	93	<0.005	0.5	2	8.6	n.d.	1.5	0.8
LB31	78	14	3.9	26	105	<1	<0.2	<0.5	n.d.	0.2	1.5	48	0.01	0.9	<2	6.5	n.d.	1.1	2.0
LB32	12	14	0.5	20	127	<1	<0.2	<0.5	n.d.	0.2	1.2	94	0.01	0.2	<2	5.1	n.d.	1.0	1.4
LB33	31	14	3.3	18	128	<1	<0.2	<0.5	n.d.	0.7	0.8	58	0.01	0.2	<2	4.8	n.d.	1.6	4.2
HB-209	84	<2	<0.5	5	85	<1	<0.2	<0.5	<5	0.3	<0.5	16	n.d.	<0.1	<2	92	n.d.	<0.2	1.0

Table A2.3c: Isotopic composition (fractionation corrected) of whole rock samples from the Lengenbach deposit. All within run statistical errors are given at a 2 sigma level. The errors of the $^{87}Rb/^{86}Sr$ were calculated assuming an uncertainty of 4% for Rb (ICP-ES) and 2% for Sr (XRF). The μ and W values as well as the model ages were calculated according the evolution model of STACEY & KRAMERS (1975).

sample	$^{206}Pb/^{204}Pb$	$^{207}Pb/^{204}Pb$	$^{208}Pb/^{204}Pb$	μ	*W*	*t (Ma)*	$^{87}Sr/^{86}Sr$	$^{87}Rb/^{86}Sr$
LB1	18.440±18	15.630±15	38.432±36	9.8	37.74	202	0.70824±1	0.030±2
LB21	n.d.	n.d.	n.d.	n.d.	n.d.	n.d.	n.d.	n.d.
LB2	n.d.	n.d.	n.d.	n.d.	n.d.	n.d.	n.d.	n.d.
LB3	18.488±6	15.660±7	38.515±20	9.92	38.42	226	0.70821±1	0.047±3
LB5	n.d.	n.d.	n.d.	n.d.	n.d.	n.d.	n.d.	n.d.
LB7	18.511±10	15.696±8	38.644±22	10.07	39.68	282	0.70838±1	0.054±3
LB9	n.d.	n.d.	n.d.	n.d.	n.d.	n.d.	n.d.	n.d.
LB17	18.498±1	15.663±1	38.533±2	9.93	38.51	226	0.70837±1	0.055±3
LB22	n.d.	n.d.	n.d.	n.d.	n.d.	n.d.	n.d.	n.d.
LB24	n.d.	n.d.	n.d.	n.d.	n.d.	n.d.	n.d.	n.d.
LB25	n.d.	n.d.	n.d.	n.d.	n.d.	n.d.	n.d.	n.d.
LB26	n.d.	n.d.	n.d.	n.d.	n.d.	n.d.	n.d.	n.d.
LB8	18.472±4	15.640±3	38.460±7	9.84	37.84	198	0.70822±1	0.361±21
LB23	n.d.	n.d.	n.d.	n.d.	n.d.	n.d.	n.d.	n.d.
LB19	n.d.	n.d.	n.d.	n.d.	n.d.	n.d.	n.d.	n.d.
LB6	n.d.	n.d.	n.d.	n.d.	n.d.	n.d.	n.d.	n.d.
LB10	n.d.	n.d.	n.d.	n.d.	n.d.	n.d.	n.d.	n.d.
LB16	n.d.	n.d.	n.d.	n.d.	n.d.	n.d.	n.d.	n.d.
LB14	n.d.	n.d.	n.d.	n.d.	n.d.	n.d.	n.d.	n.d.
LB18	18.440±7	15.645±6	38.479±14	9.87	38.3	233	0.70929±1	0.306±18
LB20	n.d.	n.d.	n.d.	n.d.	n.d.	n.d.	n.d.	n.d.
LB27	18.475±21	15.679±19	38.570±48	10.01	39.22	276	0.70826±3	0.139±8
LB28	18.474±1	15.693±1	38.627±3	10.07	39.83	304	0.70993±1	0.579±34
LB29	18.530±4	15.633±4	38.418±9	9.79	37.06	140	0.70801±2	0.046±3
LB4	18.575±17	15.661±15	38.496±37	9.9	37.7	164	0.70931±1	0.884±52
LB11	n.d.	n.d.	n.d.	n.d.	n.d.	n.d.	n.d.	n.d.
LB12	18.743±4	15.659±4	38.488±9	9.86	36.45	36	0.70848±1	0.277±16
LB13	18.532±20	15.641±17	38.446±41	9.83	37.36	155	n.d.	n.d.
LB15	18.657±10	15.674±8	38.527±21	9.94	37.54	131	0.70947±2	0.593±35
LB30	n.d.	n.d.	n.d.	n.d.	n.d.	n.d.	0.70988±2	0.547±32
LB31	19.075±9	15.660±9	38.511±25	9.8	34.43	-215	0.71018±4	0.699±41
LB32	19.094±2	15.679±1	38.577±4	9.88	34.98	-186	0.70968±2	0.444±26
LB33	n.d.	n.d.	n.d.	n.d.	n.d.	n.d.	0.70955±2	0.397±23
HB-209	n.d.	n.d.	n.d.	n.d.	n.d.	n.d.	0.70888±1	0.166±10

Table A2.4: REE-data for selected Lengenbach samples and Feldbach magnetite ore (FEL). Values determined by ICP-MS (slight differences with table A2.3 possible). Ti was determined by XRF.
- geometric type of mineralization: S = stratiform, MS = massive to interstitial sulfosalt accumulation, DISC = discordant sulfosalt veinlets, D = idiomorphic minerals in druses and fissures, m.i. = melt inclusions
- paragenetic zone: As(III)-rich zone, IR = intermediate redox zone, RED = reduced zone, SIL = silicate-rich zone, UM = unmineralized zone
- minerals: Gn = galena, Py = pyrite, Sl = sphalerite, Bar = barite, Tur = tourmaline, Adu = adularia, Hya = hyalophane, Dol = dolomite, Ssa = sulphosalt (not specified) Sar = sartorite, Te = tennantite, Ori = orpiment, Bau = baumhauerite, Duf = dufrenoisite, Apy = arsenopyrite, Li = Liveingite, Jo = jordanite, Re = realgar and L = HCl-leach.

probe	**LB8**	**LB17**	**LB11**	**LB12**	**LB15**	**FEL**	**LB30**	**LB31**
zone	As(III)	As(III)	RED	RED	RED		UM	UM
remarks	*silicate-rich*	*50 kg*	*magnetite*	*magnetite*	*magnetite*	*magnetite*		
La	2.80	1.60	2.10	1.10	2.30	0.80	2.80	2.80
Ce	5.50	3.00	4.40	2.60	4.50	2.20	5.80	5.80
Pr	0.70	0.30	0.50	0.30	0.50	0.30	0.70	0.70
Nd	3.00	1.30	2.00	1.20	1.90	1.40	2.60	2.50
Sm	0.90	0.40	0.60	0.30	0.50	0.50	0.60	0.60
Eu	0.19	0.10	0.18	0.08	0.10	0.09	0.09	0.10
Gd	1.00	0.40	0.50	0.40	0.50	0.70	0.50	0.50
Dy	0.80	0.30	0.40	0.30	0.40	0.60	0.40	0.40
Ho	0.14	0.05	0.09	0.06	0.08	0.13	0.07	0.07
Er	0.40	0.20	0.30	0.20	0.20	0.30	0.20	0.20
Yb	0.30	0.10	0.30	0.20	0.20	0.20	0.20	0.20
Th	6.30	0.50	0.40	0.60	0.40	0.30	1.30	0.80
U	119.00	7.10	5.10	12.80	10.90	1.10	0.70	1.60
Al	33800	2700					7400	6300
Ti	1740	180					200	360
total REE	15.73	7.75	11.37	6.74	11.18	7.22	13.96	13.87
La/Yb	9.33	16.00	7.00	5.50	11.50	4.00	14.00	14.00
Eu/Eu*	1.14	1.44	1.89	1.30	1.15	0.85	0.95	1.05
	Eu* = (Sm/Sm(UM) + Gd/Gd(UM))/2							
$^{Al}/_{total}$ ***REE***	2149	348					530	454
$^{Ti}/_{total}$ ***REE***	111	23					14	26
$^{Th}/_{total}$ ***REE***	0.40	0.06					0.09	0.06

Table A2.5: Pb isotopic composition (fractionation corrected) of minerals from the Lengenbach deposit. The μ and W values as well as the model ages were calculated according the evolution model of STACEY & KRAMERS, 1975. All within run statistical errors are given at a 2 s level. All samples are from the Lengenbach quarry except MEK-301 which is from a druse close (1m) to the stratigraphic contact to the gneisses. Abbreviations are explained in table A2.4.

sample	*mineral*	*type*	*zone*	$^{206}Pb/^{204}Pb$	$^{207}Pb/^{204}Pb$	$^{208}Pb/^{204}Pb$	μ	*W*	*t (Ma)*
PbS-85.2	Gn	S	IR	18.462 ± 6	15.629 ± 8	38.540 ± 16	9.79	38.12	183
PbS-85.1	Gn	S	IR	18.517 ± 6	15.667 ± 2.5	38.548 ± 12	9.95	38.54	221
L16832 A	Gn	S	IR	18.445 ± 5	15.647 ± 4	38.493 ± 10	9.88	38.37	233
BH23	Py	S	As(III)	18.504 ± 13	15.716 ± 11	38.730 ± 26	10.17	40.65	328
BH22	Py	S	As(III)	18.487 ± 1	15.606 ± 2	38.454 ± 4	9.69	37.01	115
LEN-T	Tur	S	As(III)	18.477 ± 1	15.639 ± 1	38.459 ± 2	9.83	37.79	193
LEM-201	Py	S	As(III)	18.461 ± 2	15.647 ± 1	38.491 ± 3	9.87	38.24	221
BH24 PBS	Gn	S	SIL	18.493 ± 4	15.685 ± 3	38.612 ± 9	10.03	39.43	275
BH21 PY	Py	S	IR	18.519 ± 4	15.725 ± 3	38.729 ± 9	10.20	40.70	334
B6281 DSS	Ssa	MS	As(III)	18.509 ± 3	15.699 ± 3	38.662 ± 7	10.09	39.87	291
B6281	Sar,Te&Ori	MS (m.i.)	As(III)	18.482 ± 8	15.681 ± 7	38.565 ± 17	10.02	39.18	275
L92-002	Bau	MS	As(III)	18.616 ± 2	15.657 ± 2	38.503 ± 4	9.88	37.37	126
L92-001	Bau	MS	As(III)	18.639 ± 1	15.645 ± 1	38.465 ± 3	9.82	36.77	83
L92-003 SS1	Bau	MS	As(III)	18.523 ± 4	15.726 ± 4	38.773 ± 9	10.21	40.94	333
BH24 SS	Ssa	MS	As(III)	18.517 ± 2	15.682 ± 3.4	38.597 ± 9	10.01	39.10	250
A1293 SS	Ssa	MS	As(III)	18.519 ± 5	15.715 ± 4	38.708 ± 11	10.16	40.39	315
LEN-91A	Bau	MS	As(III)	18.483 ± 2	15.672 ± 2	38.572 ± 5	9.98	39.02	256
L22012	Bau	DISC	As(III)	18.512 ± 5	15.712 ± 5	38.698 ± 13	10.15	40.32	314
L92-004	Bau	DISC	As(III)	18.467 ± 2	15.653 ± 4	38.503 ± 4	9.90	38.38	229
L92-009	Sar	DISC	As(III)	18.474 ± 1	15.660 ± 1	38.523 ± 4	9.93	38.58	238
L92-007	Bau	DISC	As(III)	18.461 ± 1	15.641 ± 1	38.465 ± 3	9.84	37.98	209
L23462	Duf	D	As(III)	18.560 ± 8	15.749 ± 6	38.819 ± 16	10.30	41.39	352
LEN23A	Sar	D	As(III)	18.585 ± 3	15.661 ± 2	38.524 ± 6	9.90	37.78	158
L23186	Duf	D	As(III)	18.675 ± 5	15.665 ± 4	38.531 ± 10	9.90	37.25	99
L23224	Gn	D	IR	18.674 ± 12	15.711 ± 10	38.673 ± 26	10.10	38.93	195
L16832 C	Gn	D	IR	18.482 ± 11	15.697 ± 9	38.664 ± 23	10.09	40.05	307
L16832 B	Gn	D	IR	18.497 ± 6	15.707 ± 5	38.688 ± 12	10.13	40.28	315
L92-005	Gn	D	IR	18.693 ± 2	15.678 ± 2	38.574 ± 4	9.95	37.60	112
L92-004 Py	Py	D	As(III)	18.777 ± 2	15.663 ± 2	38.502 ± 4	9.87	36.36	18
L23470.1	Apy	D	IR	18.547 ± 2	15.667 ± 2	38.543 ± 5	9.94	38.29	198
L14643	Li	D	As(III)	18.652 ± 2	15.671 ± 3	38.534 ± 8	9.93	37.55	129
L10767	Li	D	As(III)	18.663 ± 1	15.679 ± 1	38.559 ± 4	9.96	37.76	137
L22744	Sar	D	As(III)	18.560 ± 5	15.697 ± 4	38.640 ± 10	10.07	39.32	250
JOR-72	Jo	D	As(III)	18.486 ± 9	15.683 ± 8	38.600 ± 17	10.02	39.38	276
L21068	Jo	D	As(III)	18.605 ± 4	15.695 ± 4	38.628 ± 12	10.05	38.87	213
A2195.K	Py	D	As(III)	18.612 ± 1	15.676 ± 1	38.557 ± 2	9.96	38.06	169
L23186	Duf	D	As(III)	18.685 ± 1	15.679 ± 1	38.566 ± 4	9.96	37.64	121
L23468	Py	D	As(III)	18.587 ± 4	15.673 ± 3	38.569 ± 8	9.96	38.24	181
LER 201	Re	D	As(III)	18.536 ± 1	15.673 ± 1	38.566 ± 5	9.97	38.60	218
L 16763	Hya	D	SIL	18.501 ± 1	15.673 ± 1	38.569 ± 2	9.98	38.89	245
L16763 L2	Hya (L)	D	SIL	18.474 ± 3	15.638 ± 3	38.456 ± 7	9.83	37.77	193
L-12675	Adu	D	As(III)	18.470 ± 1	15.664 ± 1	38.495 ± 3	9.94	38.55	249
L12675 L2	Adu (L)	D	As(III)	18.476 ± 2	15.641 ± 1	38.463 ± 4	9.84	37.86	198
SG 657 L	Adu	D	As(III)	18.527 ± 14	15.717 ± 12	38.643 ± 29	10.17	40.02	314
P 59 A	Py	D		18.467 ± 11	15.657 ± 10	38.489 ± 23	9.92	38.39	238
LEK-X	Dol	D		19.098 ± 2	15.676 ± 2	38.521 ± 4	9.87	34.63	-196
SG 657	Adu	D		18.579 ± 1	15.694 ± 1	38.627 ± 3	10.05	39.04	229
LAD	Adu	D		18.492 ± 1	15.674 ± 1	38.574 ± 3	9.98	39.01	253
MEK-301	Dol	D	UM	18.913 ± 5	15.654 ± 4	38.499 ± 11	9.81	35.28	-104
L21068.K	Dol	D		18.645 ± 3	15.654 ± 2	38.489 ± 5	9.86	37.03	98
B3760	Py	S	RED	19.305 ± 9	15.703 ± 7	38.581 ± 18	9.95	34.16	-291
B3760 L	Py (L)	S	RED	22.326 ± 9	15.830 ± 7	38.710 ± 16	10.24	23.74	-2452
B7153 PY	Py	S	RED	21.449 ± 6	15.788 ± 4	38.458 ± 11	10.10	25.26	-1801
B7153 PY.L	Py (L)	S	RED	20.638 ± 4	15.772 ± 3	38.547 ± 7	10.08	28.48	-1165
BH24 PY	Py	S	RED	18.583 ± 2	15.669 ± 1	38.551 ± 3	9.94	38.10	175
BH-24 Py L	Py (L)	S	RED	18.655 ± 6	15.676 ± 5	38.585 ± 13	9.96	37.90	138
B3760 PY	Py	S	RED	18.835 ± 10	15.690 ± 8	38.598 ± 21	9.97	36.97	32
B3760 PY L	Py (L)	S	RED	18.481 ± 6	15.670 ± 5	38.411 ± 12	9.97	38.14	253
A7471 PY	Py	S	RED	19.321 ± 3	15.694 ± 2	38.502 ± 6	9.91	33.54	-325
L21068.Z	Dol		As(III)	18.626 ± 4	15.650 ± 3	38.471 ± 8	9.85	36.99	104
LEZ-112	Dol		As(III)	18.519 ± 3	15.650 ± 2	38.494 ± 5	9.87	37.90	185
LEZ-103	Dol		UM	18.592 ± 1	15.651 ± 1	38.499 ± 2	9.86	37.40	131
B 3760 D2	Dol		RED	18.630 ± 2	15.702 ± 1	38.657 ± 3	10.07	38.98	208
LED-123	Dol		UM	18.645 ± 2	15.654 ± 1	38.481 ± 3	9.86	36.98	97

Table A2.6: Sr- isotopic composition of mineral separates from the Lengenbach deposit. a to d indicate pairs of druse and host rock minerals.

sample	*pairs*	*mineral*	*type*	$^{87}Sr/^{86}Sr$	*2S (M)*
		poorly or unmineralized zone			
LEZ-101		dolomite	sugary	0.710516	0.000009
LEG-002	a	dolomite	sugary	0.710064	0.000038
LEZ-103		dolomite	sugary	0.709612	0.000012
LEZ-107		dolomite	sugary	0.709430	0.000010
LEZ-107L		dolomite	sugary	0.709472	0.000021
L-17905 DOL		dolomite	sugary	0.709604	0.000007
L-17905	a	goyazite	druse	0.710176	0.000047
L-16459		goyazite	druse	0.708748	0.000051
L-16223		goyazite	druse	0.708630	0.000009
LEK-123 D	b	dolomite	druse	0.709036	0.000028
LED-123	b	dolomite	porphyroclast	0.708876	0.000027
LED-23B	b	dolomite	porphyroclast	0.709033	0.000013
		mineralized zone			
LEZ-112	c	dolomite	sugary	0.708505	0.000044
LEZ-115	d	dolomite	sugary	0.708425	0.000020
LEK-X	c	dolomite	druse	0.708290	0.000042
LEK-X02	d	dolomite	druse	0.708302	0.000018
L-17762		goyazite	druse	0.708413	0.000015
B-8034B		barite	massive	0.708512	0.000012
LEZ-2GA		dolomite	sugary	0.708688	0.000014
LEZ-2GB		dolomite	sugary	0.708611	0.000013
B-3760 D2		dolomite	sugary	0.708705	0.000018

Table A2.7 (right): Sulfur isotope data of minerals from the Lengenbach deposit.

sample	*mineral*	*type*	*zone*	$\delta^{34}S$
B9130	Bar	D	As(III)	-1.45
A1293	Bar	D	As(III)	6.04
B9145	Re	D	As(III)	-17.60
B9146	Re	D	As(III)	-16.98
B9145	Sar	D	As(III)	-18.08
B9146	Sar	D	As(III)	-18.34
B9147	Duf	DISC	As(III)	-25.66
B9147	Re	DISC	As(III)	-24.59
B9152	Re	DISC	As(III)	-17.86
B9152	Sar	DISC	As(III)	-19.44
B5347	Bau	MASS	As(III)	-18.47
B9131	Bar	S	As(III)	-9.80
B9148	Bar	S	As(III)	-8.61
B9150	Bar	S	As(III)	-6.77
B9151	Bar	S	As(III)	-6.24
B9152	Bar	S	As(III)	-6.62
B9127	Bau	S	As(III)	-20.11
B9128	Py	S	As(III)	-24.46
B9129	Py	S	As(III)	-23.22
B9131	Py	S	As(III)	-21.19
B9148	Py	S	As(III)	-22.52
B9152	Py	S	As(III)	-18.52
B9127	Py	S	As(III)	-21.19
B9129	Sl	S	As(III)	-23.75
B9136	Bar	D	IR	8.47
B9137	Bar	D	IR	5.93
A7924	Bar	D	IR	12.41
B9141	Gn	D	IR	-24.72
B432	Py	D	IR	-7.61
B432	Py	D	IR	-7.00
B9141	Sl	D	IR	-23.37
B9144	Sl	D	IR	-20.80
B9135	Bar	S	IR	1.27
B9138	Bar	S	IR	3.65
B9139	Bar	S	IR	5.26
B8034	Bar	S	IR	0.68
B9153	Gn	S	IR	-19.66
B9126	Py	S	IR	-11.34
B9133	Py	S	IR	-15.86
B9139	Py	S	IR	-10.03
B9140	Py	S	IR	-21.14
A2195	Py	S	IR	-23.16
A2195	Py	S	IR	-23.11
B9149	Py	S	IR	-24.01
B9153	Py	S	IR	-16.83
B9154	Py	S	IR	-12.20
B9126	Sl	S	IR	-11.94
B9142	Sl	S	IR	-20.88
B9140	Sl	S	IR	-21.24
B9153	Sl	S	IR	-15.44
B9149	Sl	S	IR	-24.34
B9134	Py	DISC	R	-5.43
B9143	Py	DISC	R	-5.64
B9134	Sl	DISC	R	-5.03
B9143	Sl	DISC	R	-4.78
B9132	Apy	S	R	1.26
5311	Apy	S	R	-1.22
B7153	Py	S	R	-0.99
B3760	Py	S	R	2.09
B9132	Py	S	R	3.44

Table A2.8: O and C isotopic composition of dolomites from the Binn Valley. a to e indicate pairs of druse and host rock minerals. C = central zone, S = southern zone, N = northern zone.

sample	*pairs*	*type*	*zone/ locality*	$\delta^{13}C$ (PDB)%	$\delta^{18}O$ (SMOW)%
LEK-X01	a	druse	C	1.320	26.790
LEK-X04		druse	C	1.547	26.498
LEK-111	b	druse	C	1.410	26.840
LEK-1TA	c	druse	C	0.950	25.920
LEK-150	d	druse	S	2.150	25.520
LEK-123		druse	S	1.920	24.900
LEK-115	e	druse	S	1.027	23.484
LEK-001		druse	S	1.790	25.971
LEK-002		druse	S	1.786	25.491
LEK-100	f	druse	N	-0.539	25.057
LEZ-100	f	sugary	N	0.260	25.790
LEZ-101		sugary	N	0.210	26.369
LEZ-102		sugary	N	0.265	25.601
LEZ-103		sugary	C	1.090	26.770
LEZ-104	a	sugary	C	0.962	26.756
LEZ-105		sugary	C	0.580	26.790
LEZ-105 (WW)		sugary	C	0.653	26.304
LEZ-106(W)		sugary	C	0.787	26.709
LEZ-107		sugary	C	0.974	26.306
LEZ-108		sugary	C	1.600	27.210
LEZ-109	c	sugary	C	1.180	26.450
LEZ-109(W)		sugary	C	1.006	26.169
LEZ-110		sugary	C	0.975	27.184
LEZ-111	b	sugary	C	1.048	26.834
LEZ-112		sugary	C	1.230	26.840
LEZ-113		sugary	C	1.470	26.640
LEZ-114		sugary	S	1.749	25.309
LEZ-115		sugary	S	1.980	26.020
LEZ-115(W)	e	sugary	S	0.918	23.496
L92-003B		sugary	C	1.066	26.382
L92-004B		sugary	C	1.134	26.509
L92-004C		sugary	C	1.152	26.737
L92-004D		sugary	C	1.158	26.716
LEZ-154		sugary	S	1.130	24.010
LEZ-154(W)		sugary	S	1.619	25.032
LEZ-155		sugary	S	2.027	25.924
LEZ-156		sugary	S	1.898	24.963
LEZ-157		sugary	S	1.753	24.828
LEZ-158		sugary	S	1.110	23.425
LEZ-159		sugary	S	1.658	24.724
LED-151	d	porphyroclast	S	2.080	25.710
LED-152	d	porphyroclast	S	2.120	25.750
LED-153	d	porphyroclast	S	2.110	25.730
L92-003A		porphyroclast	C	1.052	26.514
	dolomite separates from other localities of the Binn Valley				
MER-101		vein	Messerbach	1.630	23.380
WEZ-101		sugary	Weisse Fluh	2.180	26.100
MIZ-101		sugary	Mischibach	1.466	27.510
MEZ-101		sugary	Messerbach	1.917	24.616
MEK-XO2		porphyroclast	Messerbach	2.220	27.210
LEK-X02		porphyroclast	close to gneisses	-0.500	21.650
LEK-X02(W)		porphyroclast	close to gneisses	-0.410	22.023
LEK-X03		porphyroclast	close to gneisses	0.544	23.010

Table A2.9: Geochemical and isotopic composition (fractionation corrected) of pre-Mesozoic gneisses and Mesozoic amphibolites from the Monte Leone nappe. All within run statistical errors are given at a 2 sigma level.

sample	*rock type*	*coordination*	*ρ (g/cm³)*	*SiO_2*	*TiO_2*	*Al_2O_3*	*Fe_2O_3*	*MnO*	*MgO*	*CaO*	*Na_2O*	*K_2O*	*P_2O_5*	*H_2O*	*Tot*
BIA-202	coarse grained amphibolite	659.000/135.800		47.08	1.52	17.46	10.22	0.11	8.08	8.76	2.64	1.59	0.21	1.61	99.28
BIA-207	fine grained amphibolite	658.700/135.700		49.17	1.24	16.16	9.79	0.14	7.26	10.00	2.81	0.32	0.11	1.92	98.92
BIA-210	quarzitic Bündnerschiefer	658.850/135.750		75.63	0.11	8.26	0.75	0.00	2.03	2.31	0.00	2.88	0.44	4.07	96.48
HB-201	Bündnerschiefer	656.300/133.800		47.81	0.47	10.58	3.26	0.08	1.69	16.65	0.03	2.20	0.07	15.02	97.86
WAO-301	augengneiss	658.750/130.500		71.98	0.24	14.08	1.87	0.07	0.70	1.37	2.80	5.19	0.09	1.18	99.57
WAO-302	augengneiss	658.750/130.650		75.20	0.16	12.64	1.44	0.05	0.33	0.85	3.43	4.48	0.05	0.70	99.33
FUG-202	augengneiss	659.900/133.500		74.46	0.07	12.98	0.62	0.03	0.26	0.16	3.12	5.02	0.03	1.48	98.23
WAG-307	two-mica-gneiss	660.150/130.750		75.21	0.17	12.37	1.37	0.01	0.64	0.89	2.90	5.50	0.04	0.61	99.71
WAG-311	two-mica-gneiss	660.350/131.000		74.01	0.19	12.97	1.63	0.00	0.74	0.25	2.36	5.79	0.05	1.21	99.20
WAG-316	two-mica-gneiss	659.900/130.250		75.14	0.19	12.84	1.73	0.02	0.78	0.39	2.91	5.36	0.05	0.56	99.97
WAG-324	two-mica-gneiss	660.300/131.250	2.72	76.33	0.06	12.59	1.06	0.00	0.58	0.79	5.38	2.07	0.02	0.76	99.64
WAG-332	two-mica-gneiss	659.850/131.250	2.72	72.22	0.24	13.91	2.19	0.03	1.14	0.39	3.27	5.16	0.06	1.07	99.68
WAG-220B	two-mica-gneiss	659.700/130.850		75.05	0.23	12.34	1.54	0.01	0.88	0.90	2.62	4.36	0.07	1.32	99.32
WAG-220C	two-mica-gneiss	659.700/130.850		75.13	0.21	12.13	1.16	0.01	0.87	0.53	1.87	5.75	0.06	1.13	98.85
WAG-308	biotite-epidote-rock	660.150/130.850		54.82	1.04	13.92	8.40	0.13	6.83	7.08	0.59	4.59	0.11	1.23	98.74
WAG-317	biotite-epidote-rock	659.750/130.900	2.94	49.59	0.97	14.54	9.56	0.17	8.80	5.94	0.71	5.64	0.09	2.49	98.50
WAG-220A	biotite-epidote-rock (mineralized)	659.700/130.850		45.45	0.99	19.10	9.61	0.06	9.43	0.74	5.27	7.01	0.25	2.09	100.00
WAN-14	biotite-epidote-rock (mineralized)	659.700/130.450	2.93	49.93	1.26	15.61	9.89	0.25	8.51	2.78	2.56	5.52	0.03	2.14	98.48
WAG-304	biotite-epidote-rock (mineralized)	159.850/130.850	2.94	60.36	0.54	13.99	5.36	0.11	5.31	4.14	1.70	4.98	0.03	2.41	98.93
WAG-310	biotite-epidote-rock (mineralized)	159.850/130.850		69.54	0.21	14.09	1.51	0.00	1.36	0.64	5.69	5.79	0.10	1.08	100.01

Table A2.9 (continued)

sample	*F*	*Ba*	*Rb*	*Sr*	*U*	*Th*	*Pb*	*Cu*	*Zn*	*Sb*	*Au*	*Ag*	*Zr*	*V*	*Mo*	*Nb*	*Cd*	*Y*	*Li*	*Ga*	*Cr*
BIA-202	1312	103	61	710	0.4	1.2	44	46	186	0.7	<2	0.9	109	160	2	11	<0.5	28	140	13	246
BIA-207	348	52	<5	252	<0.2	<0.2	19	51	76	0.8	<2	0.6	88	180	<1	9	<0.5	22	130	9	388
BIA-210	605	830	82	65	0.7	4.6	10	6	20	<0.1	<2	<0.2	32	14	<1	<5	<0.5	<3	82	10	14
HB-201	2091	321	90	570	2.4	8.9	40	5	83	<0.1	<2	0.5	99	120	<1	7	<0.5	12	50	7	71
WAO-301	933	508	207	179	8.1	20.8	28	23	47	<0.1	4	0.2	92	51	2	16	0.7	11	27	25	7
WAO-302	868	227	237	84	11.0	27.2	31	2	33	<0.1	<2	<0.2	101	15	2	12	<0.5	32	24	23	6
FUG-202	430	60	311	52	12.0	33.1	36	<1	18	<0.1	4	<0.2	61	2	<1	11	<0.5	43	8	15	9
WAG-307	783	283	128	71	7.6	22.3	26	25	31	<0.1	<2	<0.2	162	15	2	11	0.9	34	6	24	8
WAG-311	889	227	183	76	5.5	22.5	30	10	33	<0.1	3	0.4	181	16	2	10	<0.5	30	15	25	6
WAG-316	1404	214	225	48	7.3	21.0	45	44	62	<0.1	<2	0.3	160	17	4	10	1	34	26	23	13
WAG-324	1192	25	273	39	23.5	46.7	36	5	26	<0.1	6	0.2	91	5	2	17	1.4	98	28	28	12
WAG-332	2437	226	237	43	5.5	21.6	34	61	87	0.4	<2		210	20	2	12	1.4	34	58	28	10
WAG-220B	2097	237	203	66	7.0	21.6	70	520	79	1.3	<2	1.0	202	24	4	12	1.1	33	50	26	10
WAG-220C	2187	306	250	55	6.6	20.8	76	105	78	0.2	<2	0.2	196	19	2	11	<0.5	28	55	24	8
WAG-308	1483	220	239	48	2.4	1.0	24	69	70	0.3	4	0.4	64	186	2	9	<0.5	46	30	24	334
WAG-317	2338	113	439	71	2.7	1.8	29	30	137	<0.1	<2	0.2	65	206	3	17	1.9	17	103	30	317
WAG-220A	20295	185	441	36	6.4	18.0	63	18585	802	1.1	<2	0.7	<10	53	5	17	5.9	30	277	35	432
WAN-14	10703	192	337	46	2.6	3.4	31	8641	503	1.3	7	0.6	<10	242	2	36	7.2	29	171	19	313
WAG-304	5516	208	256	72	4.9	12.0	76	1245	181	2.4	<2	0.6	56	68	2	19	4.3	28	90	30	228
WAG-310	2644	164	172	70	14.0	25.4	73	2384	274	0.5	<2	1.2	100	8	2	14	1.7	33	50	29	24

Table A2.9 (continued)

sample	*Co*	*Ni*	*Cs*	*Sc*	*Hf*	*Ta*	*Tl*	*Br*	*As*	*S*	*La*	*Ce*	*Pr*	*Nd*	*Sm*	*Eu*	*Gd*	*Tb*	*Dy*	*Ho*	*Er*	*Tm*	*Yb*	*Lu*
BIA-202	30	142	23	47.4	2	0.9	0.2	<0.5	5.6	5290	12	28	•	•	3.6	2	•	0.8	•	•	•	•	4	0.6
BIA-207	44	179	2.3	50.1	2	<0.5	<0.1	0.8	<0.5	<50	5	<0.5	•	•	3.2	2	•	0.8	•	•	•	•	5	0.7
BIA-210	9	8	2.2	2.4	<1	0.8	0.6	<0.5	<0.5	976	11	20	•	•	1.6	<1	•	<0.5	•	•	•	•	<2	<0.2
HB-201	14	32	9	11	3	0.9	0.2	<0.5	<0.5	<50	32	61	•	•	4.8	1	•	0.6	•	•	•	•	2	0.3
WAO-301	10	6	7.2	5.1	6	3.2	1.1	<0.5	1.4	<50	29	47	•	•	4.3	<1	•	0.5	•	•	•	•	3	<0.2
WAO-302	16	3	5.9	4.6	8	4.5	1.6	1.3	<0.5	<50	25	40	•	•	5.4	<1	•	1.2	•	•	•	•	6	<0.2
FUG-202	6	5	4.1	3.7	2	7.1	1	1	<0.5	<50	15	36	•	•	5	<1	•	1.1	•	•	•	•	7	0.7
WAG-307	19	4	4.8	4.6	8	2.9	1.2	1.4	5.1	433	42	90.6	10.5	39.5	8.7	0.46	6.9	1.05	6.5	1.32	3.8	0.56	3.3	0.5
WAG-311	14	3	4.2	4.5	8	2.1	1.3	1	<0.5	<50	65	120	•	•	10	•	•	1.2	•	•	•	•	5	•
WAG-316	15	4	9.2	4.4	7	3.1	1.6	1.3	42	70	52.2	111	13.3	47.8	9.8	0.58	7.6	1.21	6.9	1.38	3.8	0.57	3.3	0.5
WAG-324	12	6	10	8	7	6	2.7	1.2	15	<50	•	•	•	•	•	•	•	•	•	•	•	•	•	•
WAG-332	14	4	17	4.6	9	2.4	3	1.4	66	<50	58.3	120	14.2	50.8	10.5	0.69	7.8	1.21	7	1.39	3.8	0.54	3.3	0.5
WAG-220B	23	5	22	6.2	6	2.7	3.9	2.2	104	134	65	110	•	•	10	•	•	1	•	•	•	•	5	•
WAG-220C	28	5	21	5	10	2.9	<0.1	2.1	64.3	<50	62	120	•	•	10	•	•	1.3	•	•	•	•	4	0.53
WAG-308	51	176	23	36.3	<1	0.7	2.5	<0.5	23	1863	•	•	•	•	•	•	•	•	•	•	•	•	•	•
WAG-317	59	168	67.4	37.1	<1	1.1	3.5	0.5	51.8	<50	•	•	•	•	•	•	•	•	•	•	•	•	•	•
WAG-220A	108	189	138	26.6	<1	2.5	2.6	0.9	122	<50	22	37	•	•	7.2	•	•	1.5	•	•	•	•	8	•
WAN-14	42	124	72.2	24.4	<1	1.7	2.5	0.6	107	<50	18.5	43.7	5.22	20.3	4.73	1.14	5.72	0.87	6.35	1.37	4.05	0.663	4.44	0.675
WAG-304	52	104	79.8	21.6	<1	2.1	4.3	2.3	142	<50	25.5	54	6.71	25.7	6.1	0.68	5.9	0.97	6	1.3	3.8	0.58	3.8	0.6
WAG-310	44	16	19	6.1	7	3.2	3.4	1.4	68	<50	•	•	•	•	•	•	•	•	•	•	•	•	•	•

Table A2.9 (continued)

sample	$^{87}Rb/^{86}Sr$	$^{87}Sr/^{86}Sr$	$^{206}Pb/^{204}Pb$	$^{207}Pb/^{204}Pb$	$^{208}Pb/^{204}Pb$	*Model-t (Ma)*	μ
BIA-202							
BIA-207			18.774 ±0.004	15.678 ±0.003	38.793 ±0.007	53	9.94
BIA-210			18.773 ±0.002	15.571 ±0.002	38.405 ±0.006	-97	9.70
HB-201			18.778 ±0.001	15.648 ±0.001	38.769 ±0.001	-16	9.81
WAO-301	3.27 ±0.31	.72089 ±0.00001	19.462 ±0.002	15.715 ±0.002	39.231 ±0.005	-384	9.97
WAO-302	7.99 ±0.76	.73980 ±0.00002	19.487 ±0.001	15.716 ±0.001	39.132 ±0.004	-402	9.97
FUG-202	17.01 ±1.62	.78568 ±0.00005					
WAG-307	5.10 ±0.49	.72681 ±0.00001					
WAG-311	6.81 ±0.65	.73187 ±0.00010	18.887 ±0.001	15.677 ±0.001	39.023 ±0.002	-35	9.91
WAG-316	13.29 ±1.27	.74773 ±0.00002	18.702 ±0.002	15.682 ±0.002	38.792 ±0.005	114	9.97
WAG-324	19.87 ±1.89	.76863 ±0.00002	19.984 ±0.001	15.731 ±0.001	39.311 ±0.002	-750	9.98
WAG-332	15.62 ±1.49	.75218 ±0.00001	18.793 ±0.001	15.684 ±0.001	38.851 ±0.003	52	9.96
WAG-220B	8.71 ±0.83	.74479 ±0.00001	18.710 ±0.005	15.738 ±0.005	38.901 ±0.013	222	10.21
WAG-220C	12.88 ±1.23	.74571 ±0.00001	18.668 ±0.001	15.696 ±0.001	38.762 ±0.004	167	10.03
WAG-308			18.817 ±0.002	15.655 ±0.002	38.787 ±0.004	-30	9.83
WAG-317	17.51 ±1.67	.74141 ±0.00003	18.800 ±0.001	15.658 ±0.001	38.773 ±0.002	-10	9.84
WAG-220A			18.695 ±0.014	15.744 ±0.012	38.938 ±0.030	244	10.24
WAN-14	20.78 ±1.98	.75912 ±0.00001	18.700 ±0.001	15.670 ±0.001	38.753 ±0.003	90	9.92
WAG-304			18.698 ±0.001	15.662 ±0.001	38.704 ±0.002	75	9.88
WAG-310			18.710 ±0.001	15.699 ±0.001	38.782 ±0.003	143	10.04

APPENDIX 3:
MAPS AND PROFILES

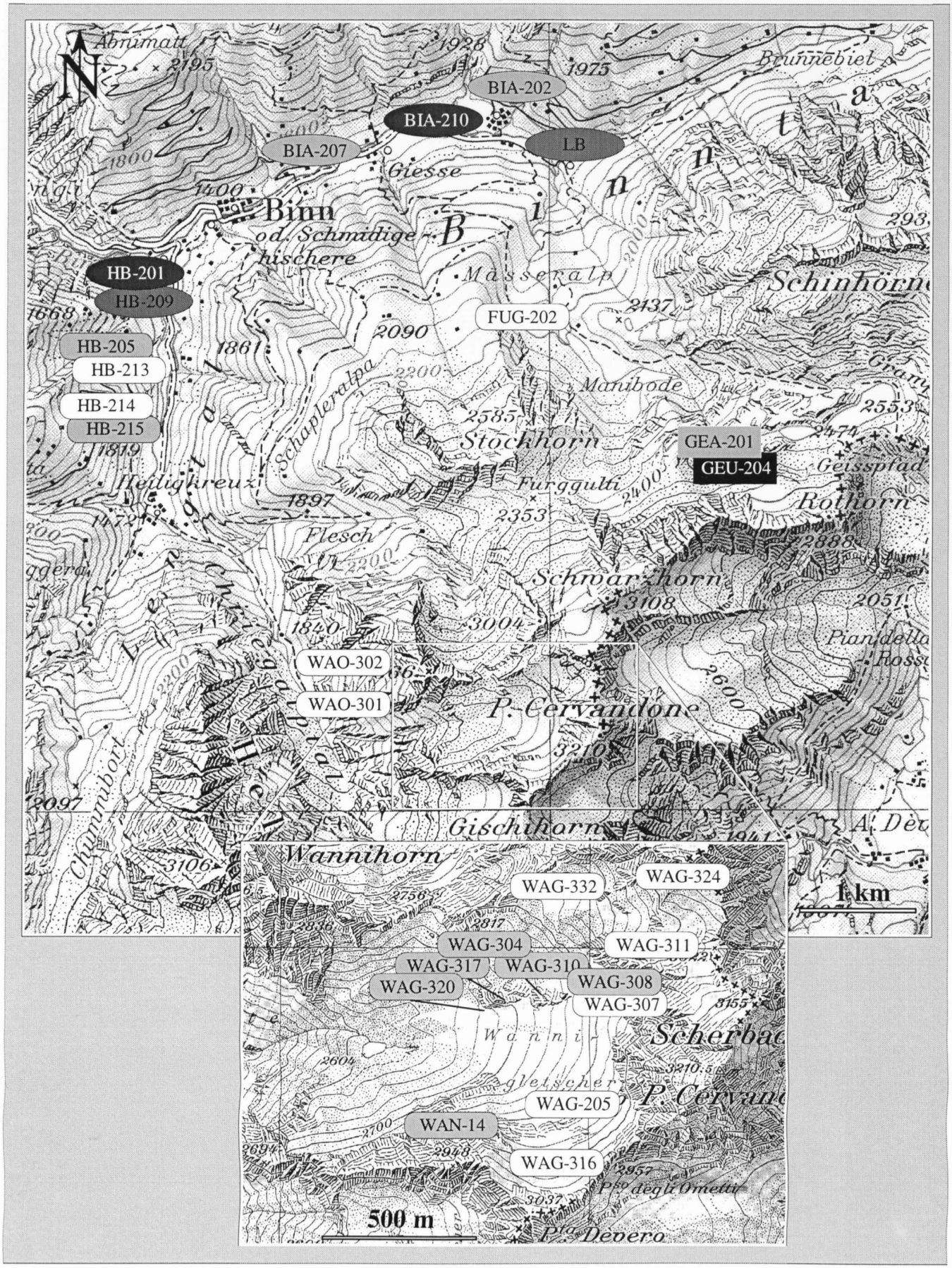

Figure A3.1: Topographical map of the Monte Leone-terrain with the localization of the whole rock samples. Enlargements of sheets 42 (1:100000) and 1290 (1:25000). Reproduced by permission of the Swiss Federal Office of Topography, October 30, 1996.

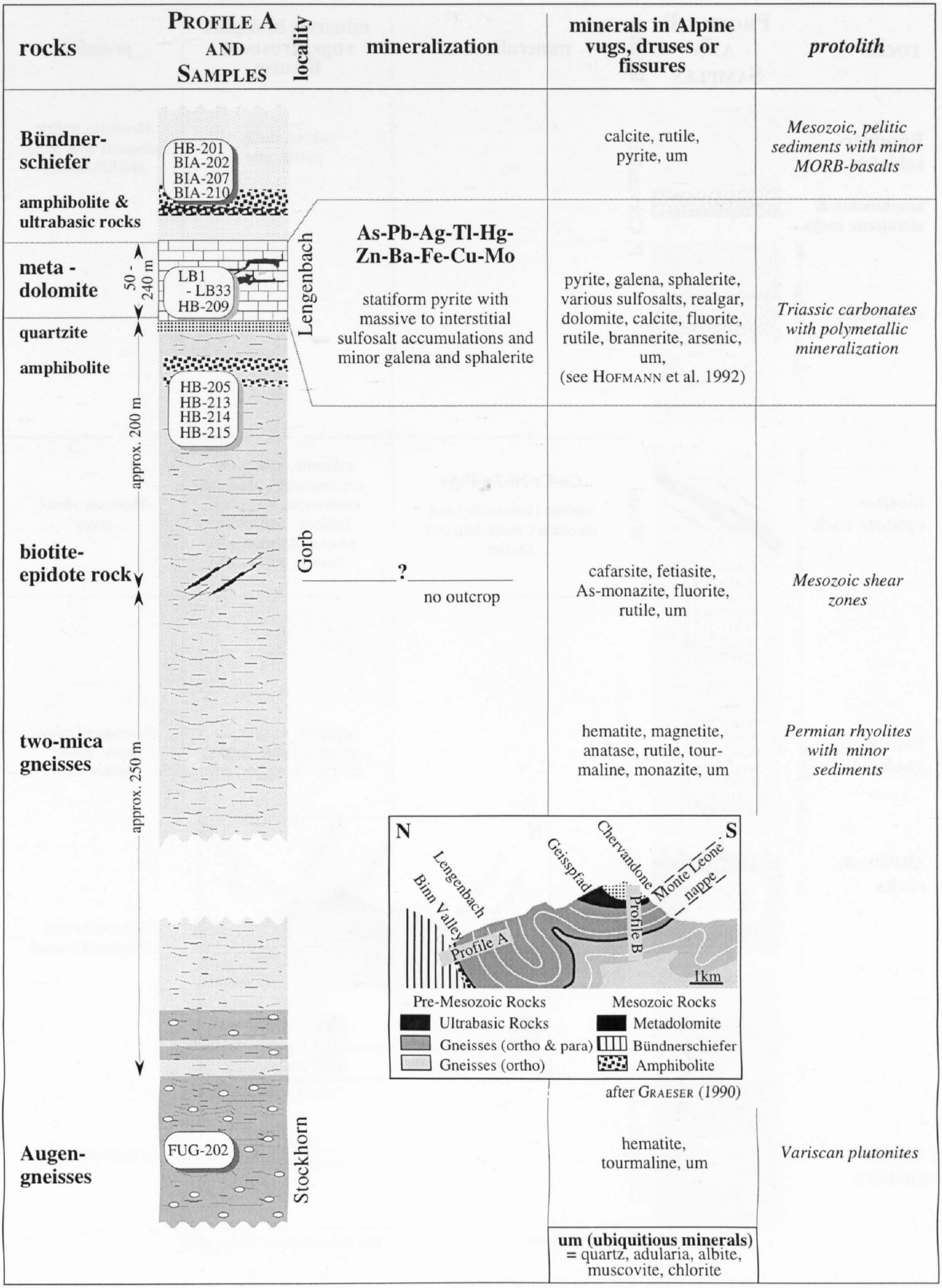

Figure A3.2: Schematic stratigraphic profiles of the Monte Leone nappe in the region of the Binn Valley with the localization of the whole rock samples.

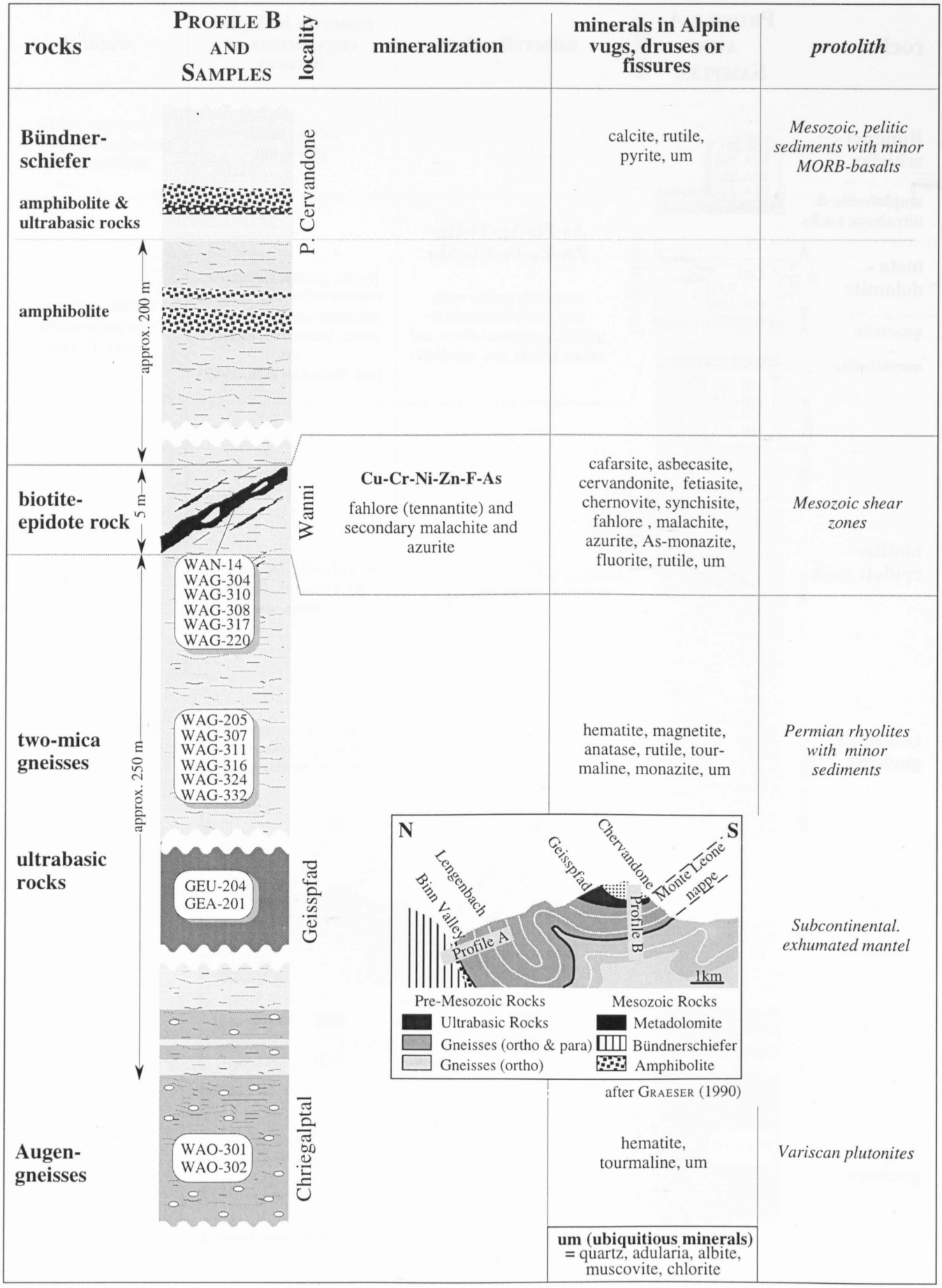

Figure A3.3: Schematic stratigraphic profiles of the Monte Leone nappe in the region of the Monte Chervandone with the localization of the whole rock samples.